Toward an Improved Chronic Myelogenous Leukemia Treatment: Blocking the Stem Cell Factor–Mediated Innate Resistance With Anti–c-Kit Synthetic-Antibody Inhibitors

A Thesis Submitted

to the College of Graduate Studies and Research

in Partial Fulfillment of the Requirements

for the Degree of Master of Science

in the Department of Pathology and Laboratory Medicine

University of Saskatchewan

by

Avy An Bui

Saskatoon, Saskatchewan, Canada

Permission to Use

In presenting this thesis in partial fulfillment of the requirements for a Postgraduate degree from the University of Saskatchewan, it is agreed that the Libraries of this University may make it freely available for inspection. Permission for copying of this thesis in any manner, in whole or in part, for scholarly purposes may be granted by the professors who supervised this thesis work or, in their absence, by the Head of the Department of Pathology and Laboratory Medicine or the Dean of the College of Graduate Studies and Research at the University of Saskatchewan. Any copying, publication, or use of this thesis, or parts thereof, for financial gain without the written permission of the author is strictly prohibited. Proper recognition shall be given to the author and to the University of Saskatchewan in any scholarly use which may be made of any material in this thesis.

Request for permission to copy or to make any other use of material in this thesis in whole or in part should be addressed to:

Head of the Department of Pathology and Laboratory Medicine
107 Wiggins Road
University of Saskatchewan
Saskatoon, Saskatchewan, Canada
S7N 5E5

Abstract

Chronic Myelogenous Leukemia (CML) is a blood cancer that arises when hematopoietic cells acquire an abnormal protein known as BCR-ABL. Current therapies for CML include drugs that inhibit BCR-ABL. However, these drugs only suppress the disease and do not cure it. One reason is that BCR-ABL drugs fail to kill the primitive population of CML cells, referred to as leukemia stem cells (LSCs), which are responsible for initiating and propagating CML. Since LSCs are not killed, the cancer is not cured and many affected patients eventually relapse. Recent studies suggest that LSCs are protected from current therapies by the bone marrow micro-environment where they reside. There, cytokine signaling molecules are present, which mediate processes that protect LSCs from BCR-ABL drugs. The stem cell factor (SCF) is one of these signaling molecules. It activates the receptor c-Kit located on the surface of LSCs, and this activation in turn allows proliferating LSCs to resist BCR-ABL drugs, even without prior exposure to these drugs, i.e., innate resistance is observed.

In this thesis, the mechanism of this innate resistance is investigated, so that a suitable treatment strategy can be developed. To this end, a co-agent approach based on synthetic antibodies (sABs) is proposed to inhibit the receptor c-Kit, with the goal of disrupting its activation by the ligand SCF. This disruption should in turn block the SCF-mediated innate resistance, thus potentially restoring BCR-ABL drug apoptotic activity. The method for this disruption involves targeting the c-Kit structural susceptibility. Specifically, the sABs are designed via antibody phage display technology to target the D1–D2–D3 domains representing the SCF binding sites, hence preventing downstream pathway activation. The hypothesis is that, by blocking the SCF-mediated innate resistance, a suitable combination of such an sAB co-agent and a BCR-ABL drug should be conducive to suppressing LSCs, thereby providing a potential means to improve CML treatment.

In addition, to assess the performance of the proposed treatment strategy, a set of *in vitro* tests is conducted, focusing on performance behaviors such as cell binding, cell death, and the progenitor inhibition. The experimental results support the hypothesis that the proposed combinatorial strategy is indeed a promising approach to mitigate the innate resistance, thus restoring BCR-ABL drug apoptotic activity.

Acknowledgments

First and foremost, I thank my advisor, Professor C. Ronald Geyer, for his guidance, patience, and financial support throughout my M.Sc. studies. His advice, expertise, and encouragement inspired me to pursue an intellectually stimulating thesis topic on synthetic antibody research for cancer therapy. I would like to also acknowledge my thesis committee members, Professor John DeCoteau, Professor Andrew Freywald, and Professor Franco Vizeacoumar for their insightful feedback on this research.

My gratitude also goes to all the special members of the Geyer and DeCoteau Lab for nurturing a collegial and uplifting research environment.

Last but not least, I would like to thank my family members for their unswerving love and understanding.

Dedication

To my beloved husband and family.

Table of Contents

List of Tables

List of Figures

List of Abbreviations and Symbols

APC	Allophycocyanin Conjugate
AR2G	Amine Reactive 2nd Generation
Arg	Abelson-Related Gene
BC	Blast Crisis
BCR-ABL	Breakpoint Cluster Region–Abelson
BLI	Bio-Layer Interferometry
BM	Bone Marrow
CD	Cluster of Differentiation
CDR	Complementarity Determining Region
CFC	Colony Forming Cell
CML	Chronic Myelogenous Leukemia
CP	Chronic Phase
EDC	1-Ethyl-3-(3-Dimethylaminopropyl)Carbodiimide
Fab	Antigen Binding Fragment
FBS	Fetal Bovine Serum
FITC	Fluorescein Isothiocyanate
GIST	Gastrointestinal Stromal Tumor
HEK	Human Embryonic Kidney
IC_{50}	Half Maximal Inhibitory Concentration
IgG	Immunoglobulin

k_a	Association Constant
k_d	Dissociation Constant
K_D	Equilibrium Dissociation Constant
LSC	Leukemia Stem Cell
μg/mL	Microgram per Milliliter
MRD	Minimal Residual Disease
ng/mL	Nanogram per Milliliter
NGS	Next-Generation Sequencing
nM	Nanomolar
NHS	N-Hydroxysuccinimide
NSB	Non-Specific Binding
PAP	2-Phenylamino-pyrimidine
PBS	Phosphate Buffered Saline
PCR	Polymerase Chain Reaction
PDGF-R	Platelet-Derived Growth Factor–Receptor
PE	Phycoerythrin
PEI	Polyethylenimine
PI	Propidium Iodide
RPMI	Roswell Park Memorial Institute
sAB	Synthetic Antibody
SB	Specific Binding

SCF	Stem Cell Factor
TKI	Tyrosine Kinase Inhibitor
V_H	Variable Heavy Domain
V_L	Variable Light Domain
v/v	volume per volume

1. Introduction

The overarching objective of this thesis is to explore the challenge of innate resistance in chronic myelogenous leukemia (CML), so that a novel treatment based on synthetic antibodies (sABs) can be developed accordingly.

1.1 Thesis Background

CML is a cancer of the hematopoietic system that is initiated by an abnormal breakpoint cluster region–Abelson (BCR-ABL) fusion gene [1–4]. Because of its highly consistent genetic abnormality and qualitatively different fusion gene product, CML remains a prime example for the development of selective treatment, even promisingly as a paradigm of curative strategies [5, 6]. In fact, exploiting the consistent genetic characterization of CML, the first generation BCR-ABL inhibitor imatinib has achieved notable success. In clinical applications, imatinib has been the mainstay of first-line therapy, even though later-generation drugs have been developed to address known shortcomings, including potency and drug resistance, of imatinib [7, 8]. For instance, the second-generation nilotinib should only be contemplated once imatinib resistance is observed. However, recent evidence suggests that second-generation drugs may in fact be considered for first-line defense, effectively supplanting imatinib completely [9–12]. The rationale is that the initial treatment is highly indicative of the overall therapeutic effectiveness. Specifically, patients not achieving a complete cytogenetic response by 12 months have an increased risk of disease progression, while those achieving an early major molecular response have a very low probability of disease progression [9]. The results suggest that CML treatments may be improved with more potent BCR-ABL inhibition, e.g., using second-generation drugs, during initial therapy. In either case, whether used as a second-line or first-line defense therapy, second-generation drugs such as nilotinib are clearly

becoming important research focus for improving CML treatments.

While more potent than first-generation drugs and effective against various imatinib-resistant CMLs, second-generation drugs also have fundamental challenges, including the problem of drug resistance and relapse. In particular, the drugs may suffer from an innate resistance challenge, which means that the drugs have reduced activity against CML with no prior exposure [13, 14]. Furthermore, most existing drugs do not address this challenge, which may lead to treatment failure. Therefore, this thesis investigates strategies to overcome the innate resistance challenge, in order to improve CML treatment.

To this end, the focus of this thesis is mainly on the drug nilotinib. Compared to imatinib, this second-generation drug offers a number of advantages. Specifically, imatinib is characterized by low potency (requiring micromolar range), as well as by the inability to completely eradicate BCR-ABL+ hematopoietic stem cells. Therefore, imatinib suffers from drug resistance, leading to disease relapse. Resistance to imatinib in CML may be due to innate resistance, or to acquired resistance, where the tumor initially responds to imatinib but becomes resistant over time [15–17]. In response to these shortcomings of imatinib, nilotinib was developed [1, 14]. Nilotinib offers higher potency relative to imatinib, and is active against most imatinib-resistant BCR-ABL mutants. In other words, nilotinib is a promising drug in effectively addressing acquired imatinib resistance. However, nilotinib still does not overcome the problem of innate resistance. As such, nilotinib may also be ineffective for patients exhibiting imatinib resistance without prior exposure to this drug, since the mechanism of this innate resistance may not be dependent on BCR-ABL. It is this type of resistance that the thesis seeks to mitigate.

1.2 Combinatorial Strategy to Reduce Innate Resistance

One significant class of mechanism responsible for innate resistance is due to cytokine mediated signaling, which is implicated in the protection of leukemia stem cells (LSCs) against BCR-ABL inhibitors [13, 18, 19]. LSCs, a primitive population of cancer stem cells that reside and survive long term in the bone marrow (BM) endosteal niche, are known to be important target for leukemia treatment, and eliminating the quiescent LSCs should be critical for developing potential curative strategies [20, 21]. One promising direction for suppressing LSCs is to block the cytokine

signaling pathways so as to induce apoptosis, since these pathways provide protection mechanisms for these proliferating LSCs [22, 23]. Specifically in CML, a pathway protecting LSCs is mediated by the stem cell factor (SCF), which activates its receptor c-Kit present on LSCs [24, 25]. Therefore, to restore the apoptotic activities of BCR-ABL inhibitors, the c-Kit pathway must be inhibited [26, 27].

To this end, the strategy to be proposed should achieve the following properties to be an efficient solution. First, it should specifically target the c-Kit pathway with high affinity sABs in order to enhance potency and minimize possible side effects. Moreover, the synthetic antibody design process should flexibly allow for incorporation of c-Kit configuration information. Lastly, the antibody production process should be cost effective, allowing for efficient mass production and rapid optimization to derive the suitable candidates, since a massive number of receptor molecules may need to be inhibited to block the pathway. An emerging design paradigm immensely conducive to achieving these desired properties is based on the antibody display technology to generate sABs [28–30]. It should be noted that, in the context of CML therapy, it is not sufficient to solve the innate resistance alone — the original CML disease still needs to be addressed. In other words, these sABs need to be applied as co-agents in a combination with a suitable BCR-ABL drug. Therefore, the solution to be developed in this thesis involves an investigation of both sAB production and combinatorial therapy strategy.

1.3 Thesis Organization

The remainder of this thesis is organized as follows. Chapter 2 provides a focused literature survey on CML and existing therapies, in order to formulate the research problem and hypothesis in Chapter 3. Chapter 4 describes experimental materials, equipment, and protocols utilized for all preparation steps and tissue culture assays in this work. The proposed research methodology is described in Chapters 5 and 6, respectively on the combinatorial strategy, and the corresponding test strategy with experimental findings. Lastly, Chapter 7 summarizes the thesis and outlines directions for future research.

2. Literature Survey: CML Overview and Existing Therapies

This chapter reviews the CML literature with a focus on existing therapies and the problem of innate resistance.

2.1 CML Overview

CML is a cancer disease of hematopoietic stem cells with hyperproliferation of often immature cells of the myeloid, megakaryocytic and erythroid lineages. It exhibits a mainly biphasic characterization: an initially chronic phase (CP) progressing to a treatment-resistant blast crisis (BC). Symptoms of CML patients include night sweats, fatigue, abdominal fullness, gout, leukocytosis, and splenomegaly. Most often, the disease occurs in adults, where the median age at diagnosis is 50 to 55 years [14, 31]. The exact causes are generally indeterminate, but it may be found after exposure to high doses of ionizing radiation. CML may initially linger with unspecific symptoms over three to five years (i.e., CP of the disease), but without proper therapy, the disease likely progresses to an accelerated phase, characterized by an increase in disease burden and the occurrence of leukemic stem cells (LSCs). Finally, if still unchecked, the disease progress exacerbates, rapidly leading into blast crisis with highly aberrant leukemic cells and lethality within months [14,32,33].

Epidemiologically, CML is actually not a pervasive cancer, with a modest annual incidence of $1.5/10^5$ [1]. Nevertheless, it is a clinically significant disease, due to its profound impact on the development of evidence-based medicine, as well as on cancer cytogenetics and therapy [34, 35]. In fact, historically, CML was the first human cancer to be consistently associated with a genetic abnormality, namely the Philadelphia (Ph) chromosome t(9;22) (q34;q11). Furthermore, the fusion protein BCR-ABL, encoded by the Ph chromosome, illustrated in Figure 2.1, was discovered to be

the etiological determinant of CML. Subsequently, detailed knowledge of BCR-ABL structure was unraveled as a subset of the tyrosine kinase family, thus facilitating suitable therapy development. In other words, this discovery in CML disease characterization changed the landscape of general cancer research, and laid the foundation for the field of targeted anticancer therapy [36, 37].

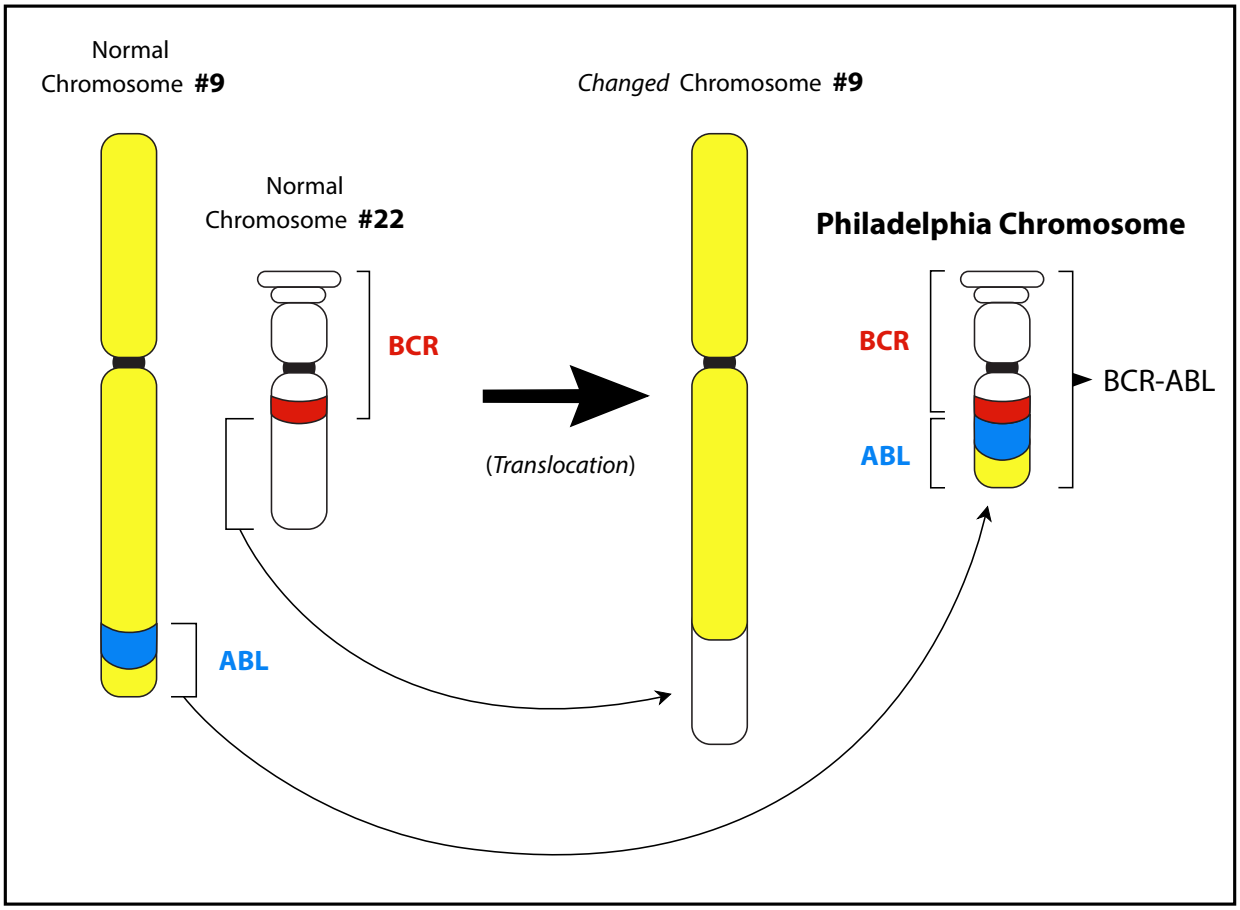

Figure 2.1: Schematic Diagram of the Philadelphia Chromosome as a Result of Reciprocal Translocation. The ABL and BCR genes locate on the long arms of the chromosome 9 and 22, respectively. As a result of the reciprocal translocation, the Philadelphia chromosome forms, which involves the ABL proto-oncogene on the chromosome 9 and BCR on the chromosome 22, thus creating the BCR-ABL fusion gene.

2.2 Early CML Therapies

The early therapeutics include spleen irradiation, hydroxycarbamide, and busulfan or interferon-alpha. These solutions are generally undesirable, since the involved cytotoxic agents target malignant cells by modifying their DNA to inhibit the mechanics of cell division [6, 38, 39]. While this approach achieved a notable degree of success in treating leukemias, lymphomas, and other malignancies, it is also fundamentally flawed: these cytotoxic agents destroyed both malignant and benign cells, often with adverse side-effects. Moreover, among the early therapeutics, only interferon-alpha induced cytogenetic responses in around 20% of patients, and actually with only partial responses ($\leq$35% Ph-positive metaphases) [40–42]. In other words, even the most successful solution of this era offered limited therapy, temporally prolonging survival, but only for selected patients.

Instead, by exploiting biochemical knowledge of the cancer pathways, molecularly targeted agents were developed, with the noteworthy advent of the BCR-ABL inhibitor imatinib mesylate for CML treatment. Imatinib has revolutionized CP-CML treatment, by improving the 5-year survival rates of CML patients from approximately 30% to 90–95% [1, 17, 36].

Imatinib mesylate is the first tyrosine kinase inhibitor (TKI), belonging to the 2-phenylaminopyrimidine (PAP) class of pharmacological compounds, approved for the treatment of multiple cancers, most notably CML and gastrointestinal stromal tumor (GIST) [43–45]. Imatinib functions as a specific competitive inhibitor that blocks the ATP binding of the ABL kinase domain in its inactive conformation, thereby inhibiting the tyrosine kinase activity. Besides selectively inhibiting all the ABL tyrosine kinases, including BCR-ABL and Abelson-related gene (Arg), imatinib is also found to partially inhibit the kinase activity against the α- and β-platelet-derived growth factor–receptors (PDGF-Rs) and SCF receptor [46–50].

2.3 Resistance Challenges with Existing CML Therapies

While the targeted small-molecule chemotherapeutics exhibit tremendous improvements compared to the early therapeutics, they are still far from a panacea. Specifically, imatinib is characterized by low potency (requiring micromolar range), as well as by the inability to completely

eliminate proliferating LSCs. Therefore, relapse and drug resistance can be observed [51,52]. Resistance to imatinib in CML may be due to innate resistance, i.e., without prior exposure to the drug, or to acquired resistance, where the tumor initially responds to therapy but becomes resistant over time. Multiple mechanisms of resistance to imatinib in CML have been defined [15–17, 44]. Importantly, it is found that bone marrow cytokine signaling is responsible for the mechanism of innate resistance. And perhaps more startlingly, whether intrinsic or acquired, resistance is believed to cause treatment failure in over 90% of patients treated with CML drugs [53, 54]. Examples of imatinib resistance mechanisms include BCR-ABL–dependent mutations [43, 45, 48, 55, 56]:

1. Point mutations in the ABL kinase domain that directly impede imatinib binding;
2. BCR-ABL gene amplification and protein overexpression that allow for residual kinase activity during or after imatinib therapy.

Despite the known challenge with resistance, imatinib currently remains a preferred solution in treating many CML cases, at 400 mg daily as the initial treatment. Only when resistance occurs at this dose, defined as either no response even at onset (i.e., innate resistance), or an eventual loss of effectiveness (i.e., acquired resistance), then the clinician may adopt three possible options [40,57]:

1. dose increase to 600 or 800 mg daily;
2. replacement with another TKI;
3. allogeneic stem cell transplant if suitable conditions are met, e.g., young patients and an availability of suitable stem cell donor.

However, these options have practical limitations and in fact, may not always be viable. For instance, a response may not occur even with acceptable dose increase, i.e., a response only occurs at a cytotoxic level of TKI, with unacceptable risk and adverse side effects [14]. This is particularly relevant if innate resistance due to BCR-ABL–independent factors is the underlying cause, e.g., with the SCF-mediated resistance thwarting TKI effectiveness [58].

In response to the shortcomings of imatinib, several second-generation TKIs, including nilotinib and dasatinib [1, 14, 59], were developed with improved affinity and specificity against the

BCR-ABL kinase domain and most of the clinically relevant BCR-ABL mutants, except the T315I gatekeeper mutant (which is addressed by the developing drug ponatinib [60,61]). While dasatinib exhibits increased potency, it suffers from reduced selectivity with respect to certain BCR-ABL mutations and also has a relatively short circulating half-life, thus limiting its applicability [62,63]. Structurally similar to imatinib, nilotinib is also a selective TKI that inhibits the activity of certain tyrosine kinases, particularly with high potency against ABL as well as robustness against many kinase domain mutations responsible for imatinib acquired resistance. This means that nilotinib can be effective in treating CML cases with BCR-ABL-dependent imatinib resistance. However, compared to imatinib, nilotinib demonstrates much lower potency in inhibiting the kinase activity of the α- and β-PDGF-Rs and SCF receptor [64–67]. And as will be seen in the sequel, this SCF receptor is implicated in innate resistance and also needs to be inhibited to effectively treat CML. In other words, in cases with innate resistance due to BCR-ABL–independent mutations, nilotinib may actually be less effective compared to imatinib, unless a co-agent is used to block the SCF pathway, in turn restoring the nilotinib apoptotic activity.

Nevertheless, at least with respect to acquired imatinib resistance in treating CML, nilotinib represents a promising replacement. However, nilotinib does not overcome the problem of innate resistance due BCR-ABL-independent mechanisms, including those sustained by cytokine signaling [65, 67]. In other words, for such cases, nilotinib may be incapable of completely eradicating the minimal residual disease (MRD) due to the ineffectiveness against the primitive population of quiescent LSCs, which reside in the bone marrow (BM) micro-environment to evade TKI treatment [68–70]. This evasion is possible since the BM micro-environment provides a protective sanctuary — via cytokine signaling — in which proliferating LSCs are resistant to the TKI-induced apoptosis — prolonging their survival and acquiring other advantageous mutations — and thus sustaining MRD in CML patients [66, 71–73]. One such cytokine signaling pathway responsible for protecting LSCs against BCR-ABL inhibitors is mediated by the SCF growth factor. Released by the BM niche, this growth factor is a signaling molecule, which orchestrates the biological activities of cells through intercellular communication, and its receptor is the c-Kit molecule, also known as cluster of differentiation (CD) 117, located on the LSCs [25, 74–76].

Biochemically c-Kit belongs to the tyrosine kinase family, and knowledge about its structure can be found in the existing literature. In particular, specific epitopes related to susceptibility in the c-Kit configuration have been identified [25, 77, 78]. As will be elaborated subsequently in Chapter 5, treatment strategies will specifically target these epitopes located on the c-Kit molecule in order to block the SCF-mediated pathway. In other words, the co-agents targeting these epitopes will help mitigate innate resistance and, together with a BCR-ABL inhibitor such as nilotinib, provide a suitable overall treatment against CML. This is a combinatorial approach which offers synergistic potential for selectively targeting and suppressing proliferating LSCs, which are a cause of innate resistance and a reservoir for CML relapse [5, 21].

3. Hypothesis and Objectives

In this chapter, a recapitulation of limitations with existing CML therapies will first be presented, in order to formally define the problem addressed by this thesis. Then an overview of the methodology for developing strategies to overcome innate resistance will be provided.

3.1 Limitations with Existing CML Therapies

As explored in Chapter 2, the challenge of interest is innate resistance, particularly as caused by cytokine signaling. Most existing CML drugs focus on inhibiting the BCR-ABL oncogene pathway. New drugs offer improvements with respect to potency and resistance of older drugs. However, the resistance types addressed are mainly limited to those dependent on BCR-ABL mutations. For example, most recently approved CML drugs, viz. bosutinib and ponatinib, still do not have specific provisions against innate resistance to eradicate LSCs, and thus remain susceptible to treatment failure [60, 79].

Furthermore, recent research findings indicate that innate resistance is best characterized as multifactorial, which means that a combinatory approach is suitable for simultaneously addressing the different aspects involved [14]. In other words, a singleton solution with only one drug is likely unable to simultaneously treat the causative factor of CML disease, as well as to mitigate innate resistance. On the other hand, to be efficient in treating innate resistance in CML, a combinatory treatment needs to be strategically designed to fulfill suitable objectives, including complementarity of the involved co-agents for overall synergy.

In brief, with respect to the innate resistance problem in CML, limitations with existing therapies mainly involve:

1. a deficiency in solutions targeting innate resistance, specifically with respect to cytokine signaling mechanisms;

2. a lack of assessment results and research findings on combinatorial strategies especially with novel co-agents such as sABs, to target the multifactorial problem described above.

Addressing the first limitation is tantamount to designing suitable co-agents, whereas tackling the second limitation consists of selection and testing strategies to ensure efficiency and complementary properties of the constituents in the combinatorial therapy. These factors will be taken into account in this research.

3.2 Hypothesis

In light of requirements established in the previous section, the following hypothesis is formulated: a strategically designed combination of a nilotinib and a co-agent inhibiting the SCF/c-Kit pathway should be effective in suppressing proliferating LSCs with innate resistance, thus providing a potential means to improve CML treatment.

As will be elaborated in Chapter 5, candidates for inhibitors will be designed based on sABs to inhibit the c-Kit pathway responsible for innate resistance.

Visually, Figure 3.1 depicts a schematic representation of the proposed strategy in order to simultaneously target both aspects: (a) the BCR-ABL pathway; and (b) the SCF-mediated innate resistance.

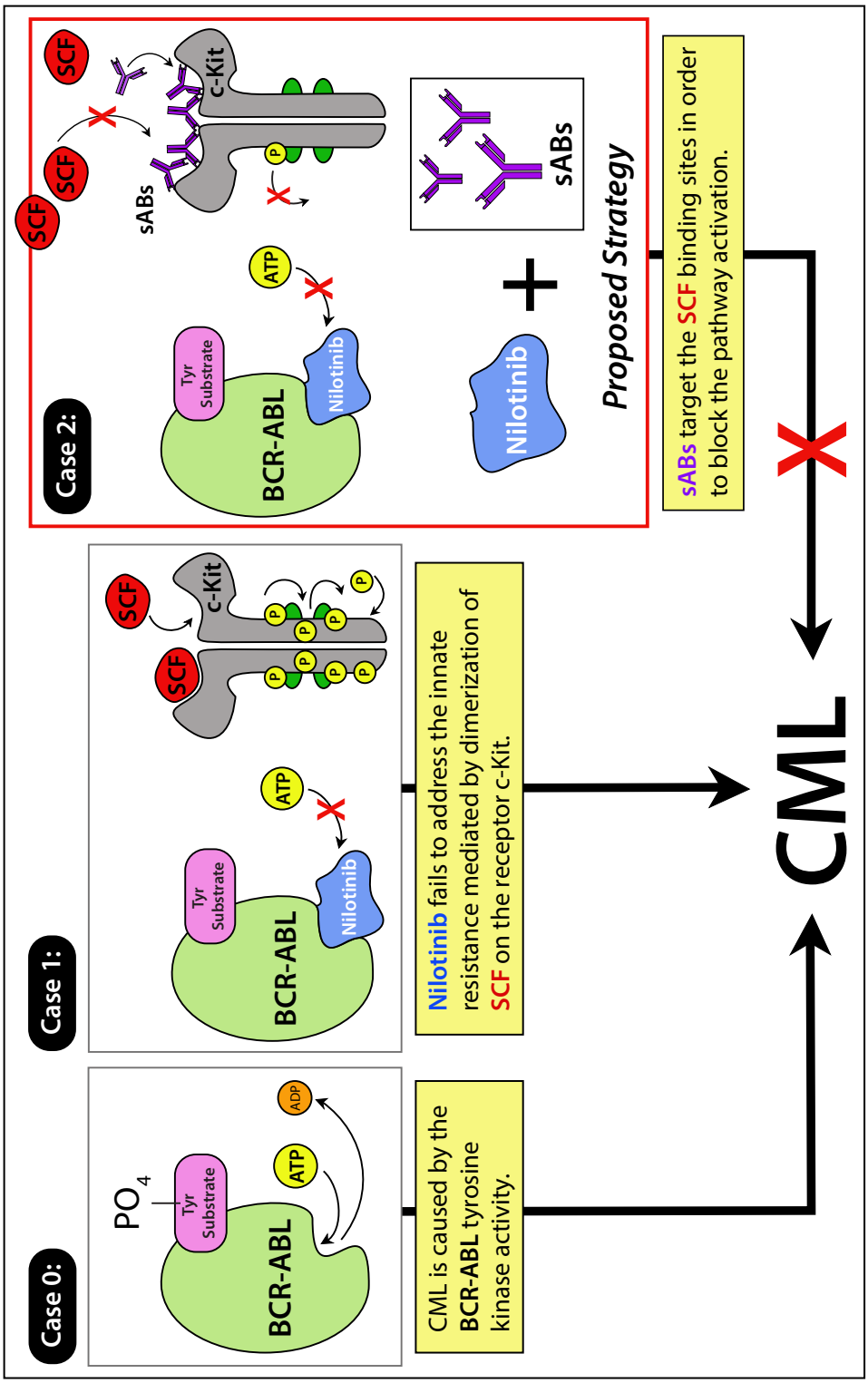

Figure 3.1: A Suitable Combinatorial Approach to Target Both the Origin of CML and Innate Resistance. A proposed strategy to block the SCF-mediated innate resistance, in order to efficiently treat CML involving: (1) targeted drug (e.g., nilotinib) to inhibit the BCR-ABL aspect; (2) pathway receptor inhibitors (e.g., sAB co-agents) to block the innate resistance mediated by dimerization of SCF on the receptor c-Kit.

3.3 Objectives

In order to validate the hypothesis posed above, the following two broad objectives are developed:

- **Objective 1**: Propose a combinatorial approach to derive candidate treatments, that simultaneously target BCR-ABL and block the SCF-mediated innate resistance, respectively consisting of: (a) targeted drug (e.g., nilotinib); and (b) and pathway receptor inhibitors (e.g., c-Kit antibodies).
- **Objective 2**: Assess the treatment performance of the proposed candidate combinations, to achieve high potency and specificity, using a set of *in vitro* tests on suitable CML cell lines.

Overall, these broad objectives aim to deliver combinatorial treatment solutions that have the potential to block the SCF-mediated innate resistance.

3.4 Methodology Overview

To achieve the stated objectives, the corresponding methodology and supporting experiments will be designed as follows:

- **The proposed combinatorial strategy**: corresponding to Objective 1, this first stage of the methodology endeavors to generate treatment candidates with desirable properties.
  - Combinatorial approach: as discussed in the above Sec. 3.1, a single-drug solution is inefficient to both treat the origin of CML and block the SCF-mediated innate resistance. Therefore, a combination of appropriately designed agents will be considered to target both aspects.
  - sABs: to generate effective combinations, the design process should provide agents exhibiting complementary properties, with multiple possibilities of these agents for consideration. In this case, to complement the main drug, multiple co-agent candidates

with the ability to block innate resistance need to be generated. Given these requirements, sAB technology is a suitable solution since it is able to:

  * exploit given structural knowledge on c-Kit susceptibility, e.g., specific epitopes, in generating candidates;
  * as a versatile design process, synthetically provide a large pool of candidates with the required complementary properties.

- **Assessment of proposed strategy**: corresponding to Objective 2, this subsequent stage of the methodology seeks to quantify the performance of the proposed candidates, in their capacity to effectively and efficiently treat CML and its innate resistance.

  – In particular, three aspects will be considered to assess cell behaviors: cell binding, cell death, and progenitor inhibition.

  – Logistically, as shown in Figure 3.2, the following six *in vitro* tests will be experimentally conducted to sequentially screen the candidates and derive suitable solutions: (a) kinetic test; (b) cell binding test; (c) specific binding test; (d) cell viability assay; (e) apoptosis assay; (f) colony forming cell assay.

In terms of organization, Chapter 4 describes materials, equipment, and protocols utilized for all experiments in order to support the proposed strategy in Chapter 5. Then, Chapter 6 describes the assessment methods, and reports corresponding findings.

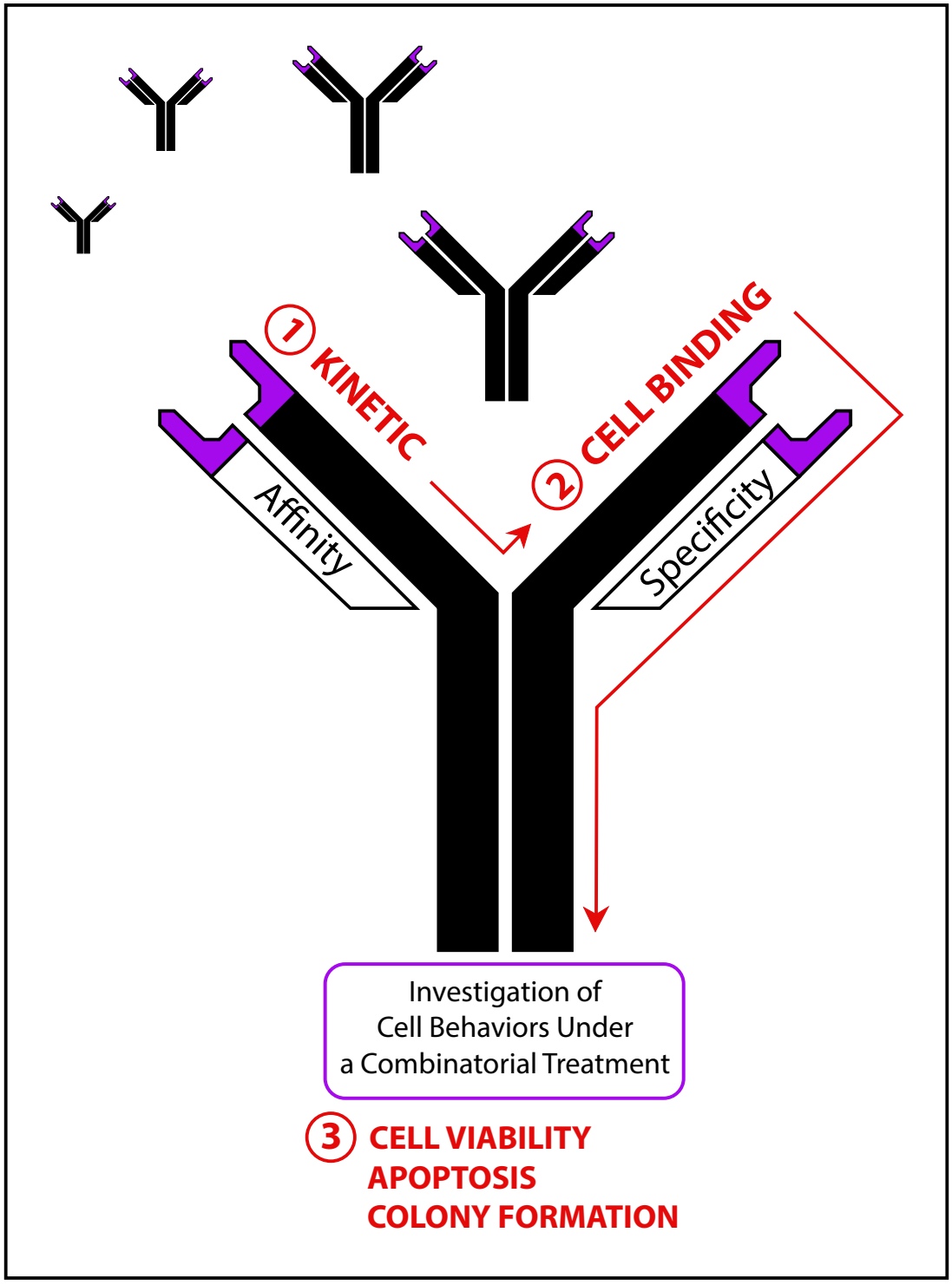

Figure 3.2: Schematic Overview of the Assessment Methods. In order to investigate cell behaviors, the assessment cycle begins with an initial screening test based on sAB affinity. Once the affinity requirement has been met, cell binding and specificity assay are performed. These first two test stages establish the minimum qualification requirements, focusing only on the sAB candidates. Last but not least, with the addition of BCR-ABL drug, further tests on cell viability, apoptosis, and colony formation can be conducted.

4. Experimental Materials and Methods

In order to propose a suitable treatment strategy (to be developed in Chapter 5), various materials and methods will be needed. The goal of this chapter is to describe these supporting components. In particular, to effectively target the c-Kit pathway responsible for the SCF-mediated innate resistance, materials and protocols germane to designing and producing c-Kit sABs (i.e., Fab generation, affinity maturation, IgG antibody expression, and optimization) are described in Section 4.2.

In addition, to assess the proposed treatment strategy (subsequently presented in Chapter 6), a number of tissue culture assays will be performed to test binding criteria of sABs and investigate cell behaviors under a combinatorial treatment. These materials, protocols, and data analytic software applications are described in the following Sections 4.1, 4.3, and 4.4 to complement Chapter 6, where the rationale of each test and resulting data will be discussed and analyzed with respect to the experimental performance.

4.1 Materials

In the context of Chapter 6, materials such as chemical reagents, experimental equipment, and various cell lines and tissue culture conditions will be necessary to conduct all preparation steps and tissue culture assays in order to obtain meaningful data. This section describes these relevant materials.

4.1.1 Chemical Reagents

The experimental reagents used to prepare and conduct all tests are listed in Table 4.1 with their corresponding supplier names. For instance, as described in Section 4.2.1, to perform kinetic test for each sAB with the goal of quantifying antibody-protein binding interactions, the reagents used in preparation and setup steps before operating the *forte*Bio Octet $^{\text{Red}}$ 384 system include:

- protein A (biosensor package);
- regeneration buffer;
- reconstituted c-Kit (Recombinant Human CD 117) reagent;
- phosphate-buffered saline (PBS).

Experimental Reagent	Supplier
Annexin V: FITC Apoptosis Detection Kit I	BD Pharmingen
APC Annexin V Reagent	BD Pharmingen
Goat F(ab')2 Anti-Human IgG (H+L)-FITC	Beckman Coulter
Goat F(ab')2 Anti-Human IgG (H+L)-PE	Beckman Coulter
Nilotinib (100 mg)	BioVision Inc.
PerfectPrep™ EndoFree Maxi Kit Manual	Fisher Scientific
Protein A (Biosensor Package)	*forte*BIO
Amine Reactive Second-Generation (AR2G) (Biosensor Package)	*forte*BIO
Regeneration Buffer	*forte*BIO
N-hydroxysulfosuccinimide (Sulfo-NHS)	*forte*BIO
Ethanolamine (ETA) Reagent	*forte*BIO
Sodium Acetate Buffer	*forte*BIO
1-ethyl-3-(3-dimethylaminopropyl)carbodiimide (EDC)	*forte*BIO
293fectin™ Transfection Reagent	Invitrogen Life Technologies
Blasticidin S HCl (powder)	Invitrogen Life Technologies
Fetal Bovine Serum (FBS)	Invitrogen Life Technologies
FreeStyle™ 293 Expression Medium	Invitrogen Life Technologies
Opti-MEM® Reduced Serum Medium (powder)	Invitrogen Life Technologies
Phosphate-Buffered Saline (PBS) (powder)	Invitrogen Life Technologies
Penicillin-Streptomycin Solution (10,000 U/mL)	Invitrogen Life Technologies
Roswell Park Memorial Institute (RPMI) 1640 Medium, phenol red (powder)	Invitrogen Life Technologies
Dulbecco's Modified Eagle Medium (DMEM), high glucose, phenol red (powder)	Invitrogen Life Technologies
SYTOX® Blue Dead Cell Stain	Invitrogen Life Technologies
Trypan Blue Solution (0.4%)	Invitrogen Life Technologies
Trypsin-EDTA (0.05%), phenol red	Invitrogen Life Technologies
Zeocin™ Selection Reagent	Invitrogen Life Technologies
G418 Sulfate	InvivoGen
Recombinant Human CD 117/c-kit, CF (50 μg)	R&D Systems
Recombinant Human SCF/c-kit Ligand (10 μg)	R&D Systems
Recombinant Mouse SCF/c-kit Ligand (10 μg)	R&D Systems
MethoCult™ GF M3434 Methylcellulose (Mouse Cells)	StemCell Technologies
MethoCult™ H4434 Classic Methylcellulose (Human Cells)	StemCell Technologies

Table 4.1: List of Reagents and Suppliers

4.1.2 Experimental Equipment

Table 4.2 lists experimental equipment necessary to perform the corresponding tissue culture assays. For instance, MACSQuant Analyzer is the flow cytometry system used to conduct the following experiments: cell binding test, non-specific and specific binding test, and apoptosis assay.

Experimental Equipment	Method
AKTA Prime System	sAB Purification and Elution
*forte*Bio Octet ^{Red} 384 System	sAB Quantification; Kinetic Test
NanoDrop 2000/2000c Spectrophotometer	sAB Concentration Measurement
MACSQuant Analyzer	Cell Binding Test; Non-specific and Specific Binding Test; Apoptosis Assay
Light Microscope	Cell Viability Assay
Inverted Microscope	Colony Forming Cell Assay

Table 4.2: List of Experimental Equipment

4.1.3 Cell Lines and Tissue Culture Environments

Table 4.3 lists different cell lines, which are utilized in tissue culture assays, to investigate the effectiveness and repeatability of proposed combinatorial CML treatments.

Cell Line	Description
CJ	Murine blast-crisis CML cell line, obtained from the Craig Jordan Research Lab, with the BCR-ABL and Nup98/HoxA9 translocation products, and c-Kit expression [80].
JURL-MK1	Human blast-crisis CML cell line, obtained from the DSMZ Bioresource Center in Braunschweig, Germany, with one t(9;22) translocation, b3-a2 BCR-ABL fusion, and c-Kit expression.
KU-812	Human blast-crisis CML cell line, obtained from the DSMZ Bioresource Center in Braunschweig, Germany, with two t(9;22) translocations, b3-a2 BCR-ABL fusion, and c-Kit expression.
HEK 293F	A specific mammalian cell line, obtained from Life Technologies, is originally derived from the human embryonic kidney cells grown in tissue culture.

Table 4.3: List of Cell Lines

The cells are maintained according to manufacturer's guidelines as follows.

All CML cell lines are utilized for tissue culture assays and maintained in a humidified incubator containing 5% CO_2 at 37º C:

- Murine CML cells – CJ – are cultured in Roswell Park Memorial Institute (RPMI) 1640 medium supplemented with 20% volume per volume (v/v) fetal bovine serum (FBS);
- Human CML cells – JURL-MK1 and KU-812 – are cultured in RPMI 1640 medium supplemented with 10% v/v FBS and 1% v/v penicillin-streptomycin solution.

Suspension cells are utilized for co-transfection and maintained in a humidified incubator containing 8% CO_2 at 37º C:

- Human embryonic kidney (HEK) 293F cells are cultured in FreeStyle™ 293 Expression medium.

4.2 Protocols for Generation of Anti–c-Kit Synthetic Antibodies (sABs)

The protocols necessary for generating anti–c-Kit sABs are described. Specifically, Sections 4.2.1–4.2.3 sequentially summarize the three main stages involved. These steps demonstrate how the generated anti–c-Kit sABs should serve as suitable starting points for developing combinatorial treatment candidates, as elaborated later in Chapter 5.

4.2.1 Production of c-Kit Antigen Binding Fragments (Fabs)

The **first stage** to generate Fabs is described in the following:

With phage display technology, c-Kit Fabs, designed to specifically target the c-Kit D1–D3 region, are generated from *in vitro* screening and selection strategy. As presented in Figure 4.1, for a specific Fab designated as Apo A, the screening and selection strategy starts with:

- Immobilized antigens of the purified human c-Kit ectodomain, supplied by the Schlessinger Lab (Yale University);
- The phage-displayed Fab library known as "Library F", designed and constructed by the Sidhu Lab (University of Toronto), which contains more than 10^{10} unique members that vary in the amino acid composition of variable heavy domain (V_H) complementarity determining regions (CDRs) 1–3 and variable light domain (V_L) CDR 3.

The generation process of Apo A Fab was performed by the Sidhu Lab.

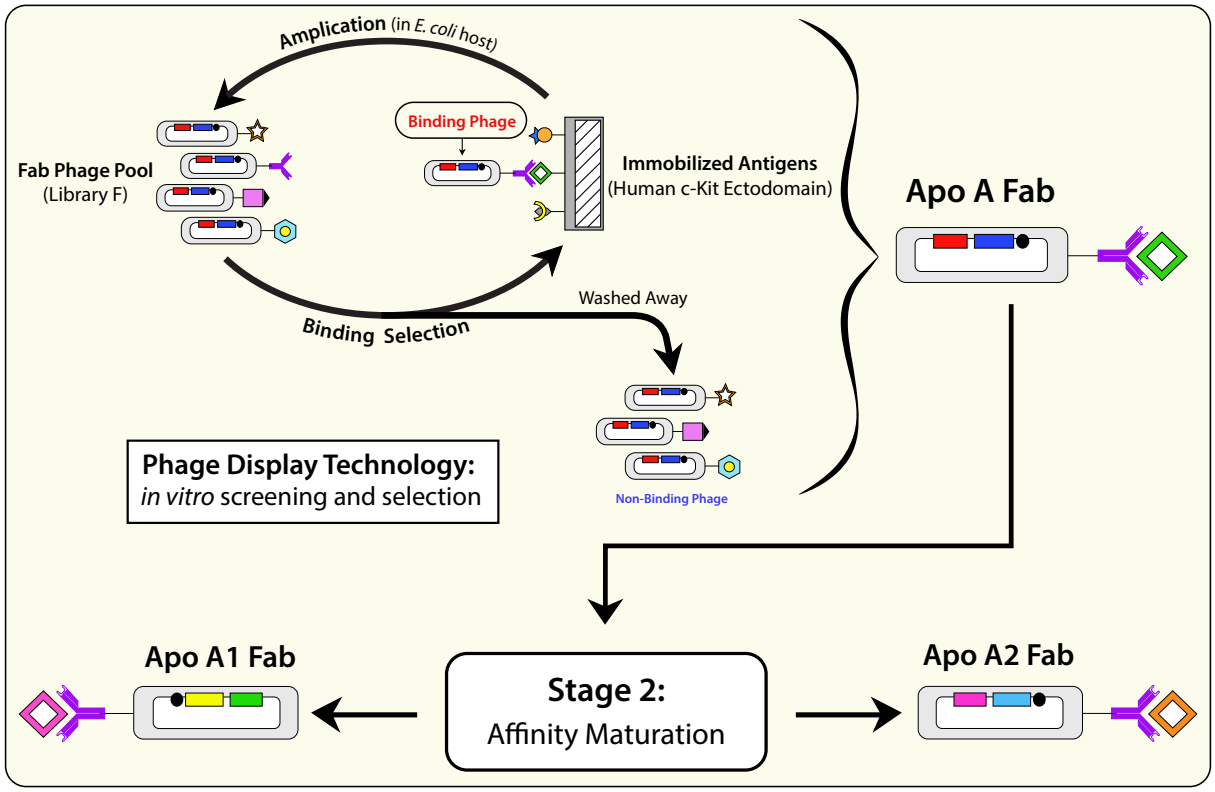

Figure 4.1: Schematic Diagram of Stage 1 – Generation of Synthetic c-Kit Fabs. In this case, a c-Kit Fab designated as Apo A is specifically illustrated, with phage display technology allowing for *in vitro* screening and selection strategies to select specific binders, using the Library F and immobilized antigens of the human c-Kit ectodomain.

4.2.2 Affinity Maturation

The **second stage** to produce alternative c-Kit Fabs with a potentially improved binding affinity is described in the following:

1. As illustrated in Figure 4.2, using a soft randomization process, a new oligonucleotide primer is created based on the parental nucleotide sequence of Apo A to introduce moderated mutations at random positions in the CDR-H1–H3, L3 segments.

2. With the new primer, Kunkel mutagenesis is performed to construct a secondary mutagenic phage library (i.e., library Apo A) that comprises several mutants of the nucleotide sequence.

3. This new phage library is used in consecutive rounds of biopanning to select specific c-Kit Fabs with improved binding properties.

4. Once the biopanning is finished, the nucleotide sequence of new c-Kit phagemids is analyzed using the next-generation sequencing (NGS).

With the goal of fine-tuning the binding affinity and specificity, new c-Kit Fabs (i.e., Apo A1 Fab and Apo A2 Fab) are generated from an affinity selection, using the mutagenic phage library and immobilized antigens of the human c-Kit ectodomain. Table 4.4 illustrates the resulting CDR sequences of Apo A1 Fab and Apo A2 Fab. This affinity maturation process was performed by Dr. Patricia Cano during her postdoctoral fellowship in the Geyer and DeCoteau Lab.

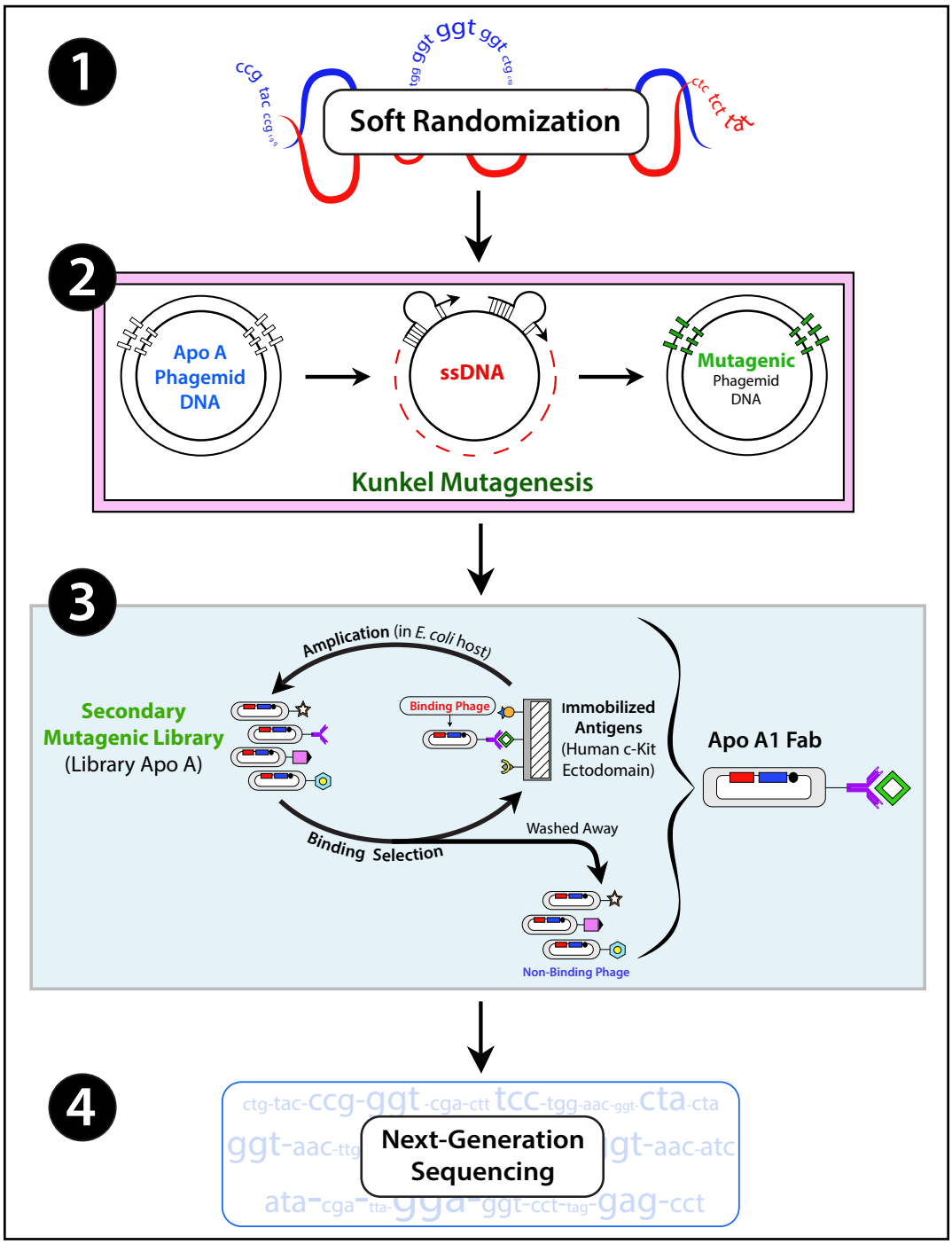

Figure 4.2: Schematic Diagram of Stage 2 – Affinity Maturation Process to Produce Alternative c-Kit Fabs: 1) A soft randomization process is applied to create a new oligonucleotide primer with moderated mutations at random positions in the CDR-H1–H3, L3 segments of Apo A; 2) Using the new primer, Kunkel mutagenesis is utilized to construct a secondary mutagenic phage library (i.e., library Apo A) for affinity selection; 3) To generate new c-Kit Fabs with improved binding affinity, biopanning is performed using the new mutagenic phage library to select c-Kit Fabs with desirable properties; and 4) The nucleotide sequence of new c-Kit phagemids is analyzed using the next-generation sequencing (NGS).

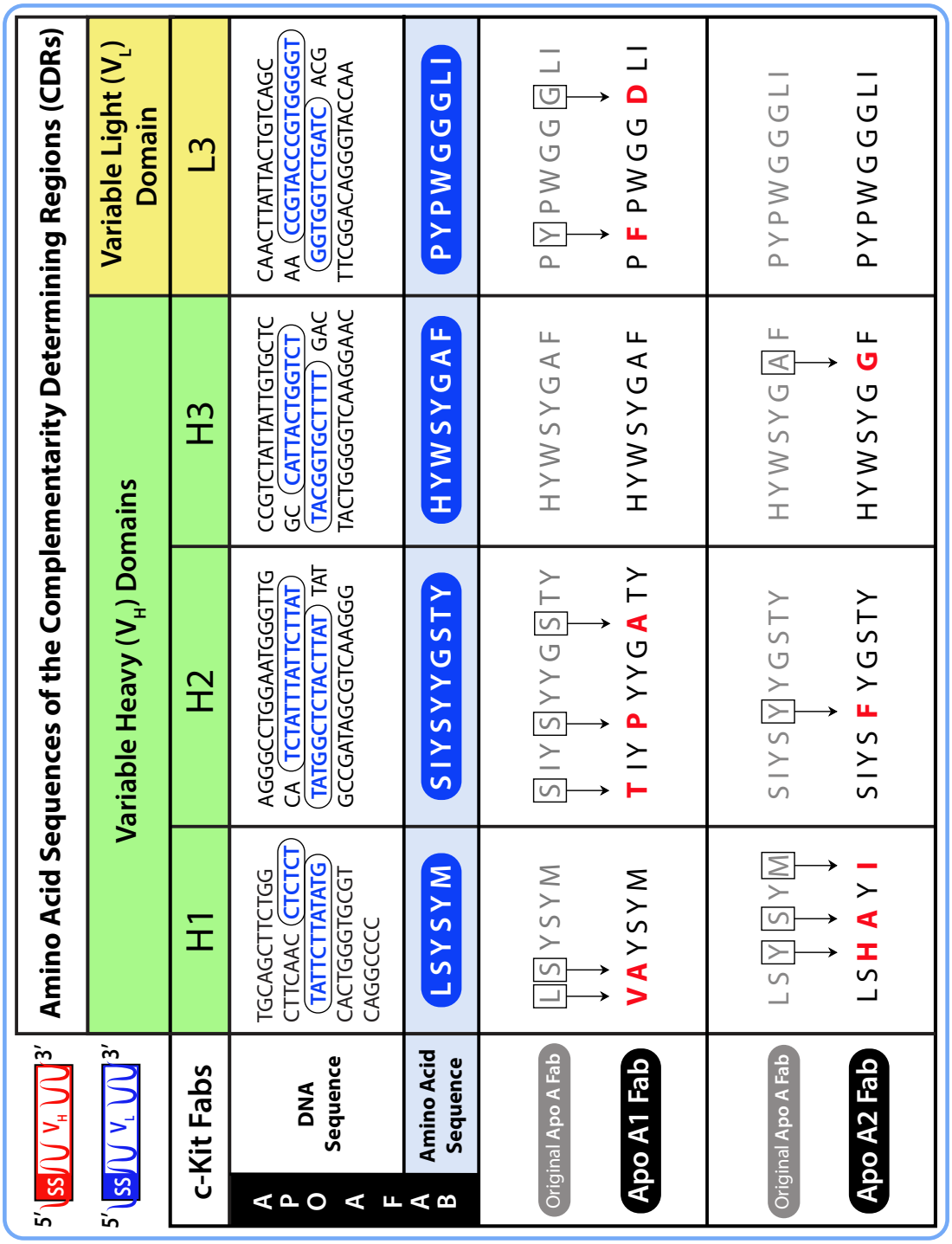

Table 4.4: Variant CDR Sequences of the New Affinity-Matured Fabs: **Apo A Fab** - For the affinity maturation stage, a soft randomization process is applied to the DNA segments of interest (marked in blue), to introduce moderated mutations at random positions in the CDR-H1–H3, L3 sequences. The corresponding amino acid sequences of the CDR-H1–3, L3 are shown in the next row; **Apo A1 Fab** - The new amino acid sequence has several substitutions in the CDR-H1–2, L3 segments from a successful affinity maturation process; **Apo A2 Fab** - The new amino acid sequence has several substitutions in the CDR-H1–3 segments.

As a result, when compared to the original amino acid sequence of Apo A Fab, the new sequence of the **Apo A1 Fab** has substitutions in the following CDR segments:

1. Valine (V) and arginine (A) for leucine (L) and serine (S), respectively in the amino acid sequence of CDR-H1;
2. Threonine (T), proline (P), and arginine (A), respectively for serine (S) on locations 1, 4, 8 in CDR-H2;
3. Phenylalanine (F) and aspartic acid (D) for tyrosine (Y) and glycine (G), respectively in CDR-L3.

Similarly, for the **Apo A2 Fab**, the new sequence has the following substitutions:

1. Histidine (H), arginine (A), and isoleucine (I) for tyrosine (Y), serine (S), and methionine (M), respectively in CDR-H1;
2. Phenylalanine (F) for tyrosine (Y) in the CDR-H2;
3. Glycine (G) for arginine (A) in the CDR-H3.

4.2.3 Conversion of c-Kit Fabs Into Complete IgG Antibodies

The **third stage** to convert the c-Kit Fabs into complete sABs consists of the following steps:

1. V_H and V_L domains are isolated from the Fab phagemid and amplified by polymerase chain reaction (PCR).
2. DNA encoding V_H and V_L domains are cloned into the recombinant pFUSE-CHIg and pFUSE2-CLIg plasmids.
3. The PerfectPrep^{TM} Endofree Maxi Kit facilitates purifying and extracting the recombinant pFUSE-CHIg and pFUSE2-CLIg plasmids in an advanced transfection-grade condition.

4. As illustrated in Figure 4.3, using the purified pFUSE-CHIg and pFUSE2-CLIg plasmids, a transient-plasmid-DNA transfection is performed in accordance with the manufacturer's instructions, in order to produce the candidate human IgG sABs. The materials for this step include 293fectin^{MT} transfection reagent, and the human embryonic kidney (HEK) 293F cells which should be cultured in the FreeStyle^{TM} 293 Expression medium containing GlutaMAX™ supplement for an adequate incubation duration, i.e., 5 days.

5. After incubation, the sABs are purified and extracted from the supernatant, using the ÄKTA-prime system with the IgG purification and IgG elution buffers.

6. Last, using the *forte*Bio Octet ^{Red} 384 system with protein A biosensors, quantification is performed to measure the antibody concentration for each sAB, in order to select the candidates with antibody concentration sufficiently high, i.e., possessing promising properties, for subsequent assays. In addition, to double check the result accuracy and consistency, the NanoDrop 2000/2000c Spectrophotometer Version 1.0 software is also used to provide an independent set of measurements for cross-comparison.

It can be seen that the experiments in this third stage are relevant for validating additional performance properties. In other words, they serve as criteria for further short-listing of candidates sABs with desirable properties.

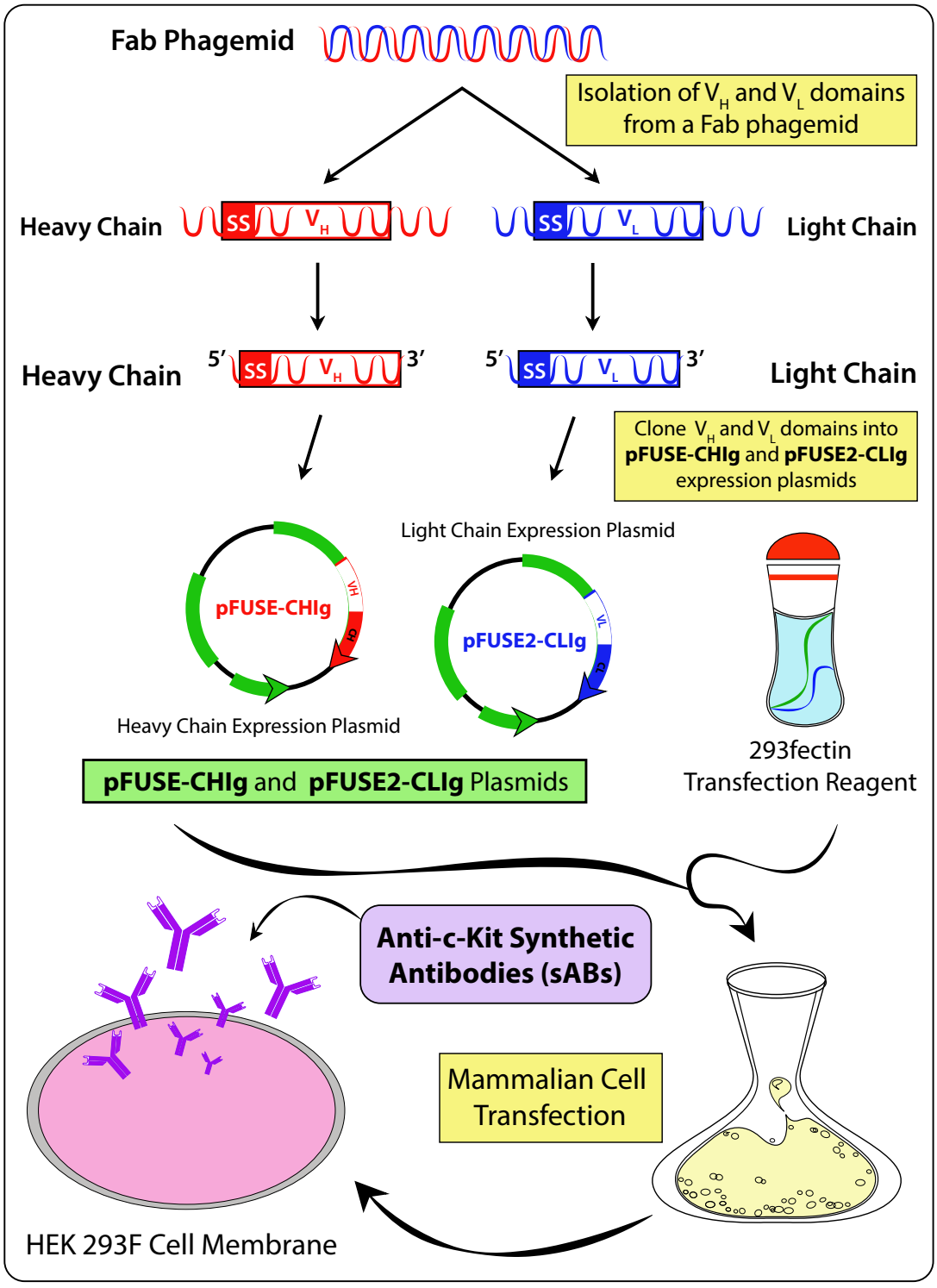

Figure 4.3: Schematic Diagram of Stage 3 – Converting the c-Kit Fabs Into Complete Synthetic Antibodies. First, V_H and V_L domains are isolated from the Fab phagemid, amplified by the PCR, and cloned into the recombinant pFUSE-CHIg and pFUSE2-CLIg expression plasmids. Through an antibody expression system, using the purified pFUSE-CHIg and pFUSE2-CLIg plasmids and a 293fectin reagent, a transient plasmid DNA transfection is applied with the mammalian cells (e.g., HEK 293F) in order to produce the human IgG sABs.

4.3 Protocols for Tissue Culture Assays

Various tissue culture assays will be performed to assess the proposed strategy, as presented later in Chapter 6. This section describes the experimental protocols for these assays.

4.3.1 Kinetic Test

To screen binding tightness and obtain affinity measurements including association constant (k_a), dissociation constant (k_d), and equilibrium dissociation constant (K_D), kinetic test is performed using the *forte*Bio Octet $^{\text{Red}}$ 384 system with bio-layer interferometry (BLI) biosensors, which uses an optical technique to quantify and analyze biomolecular interactions between sABs and c-Kit.

The kinetic experimental setup is described and illustrated in Figures 4.4, 4.5, and 4.6 respectively for Apo A IgG, Apo A1 IgG, and Apo A2 IgG.

For each sAB, a microplate is used to prepare the test samples, with 50 μL per each well. The specific configurations are as follows for the three candidate sABs.

- Apo A IgG with a titration series of 50, 100, 200 and 400 nM of c-Kit concentrations diluted with phosphate-buffered saline (PBS), using protein A biosensors;
- Apo A1 IgG with a titration series of 25, 50, 100, and 200 nM of c-Kit concentrations diluted with PBS, using protein A biosensors;
- Apo A2 IgG with a titration series of 50, 100, 200, and 400 nM of c-Kit concentrations diluted with sodium acetate buffer at pH 4, using Amine reactive second-generationo (AR2G) biosensors.

Then, the prepared microplates are individually loaded on the Octet system for kinetic analysis.

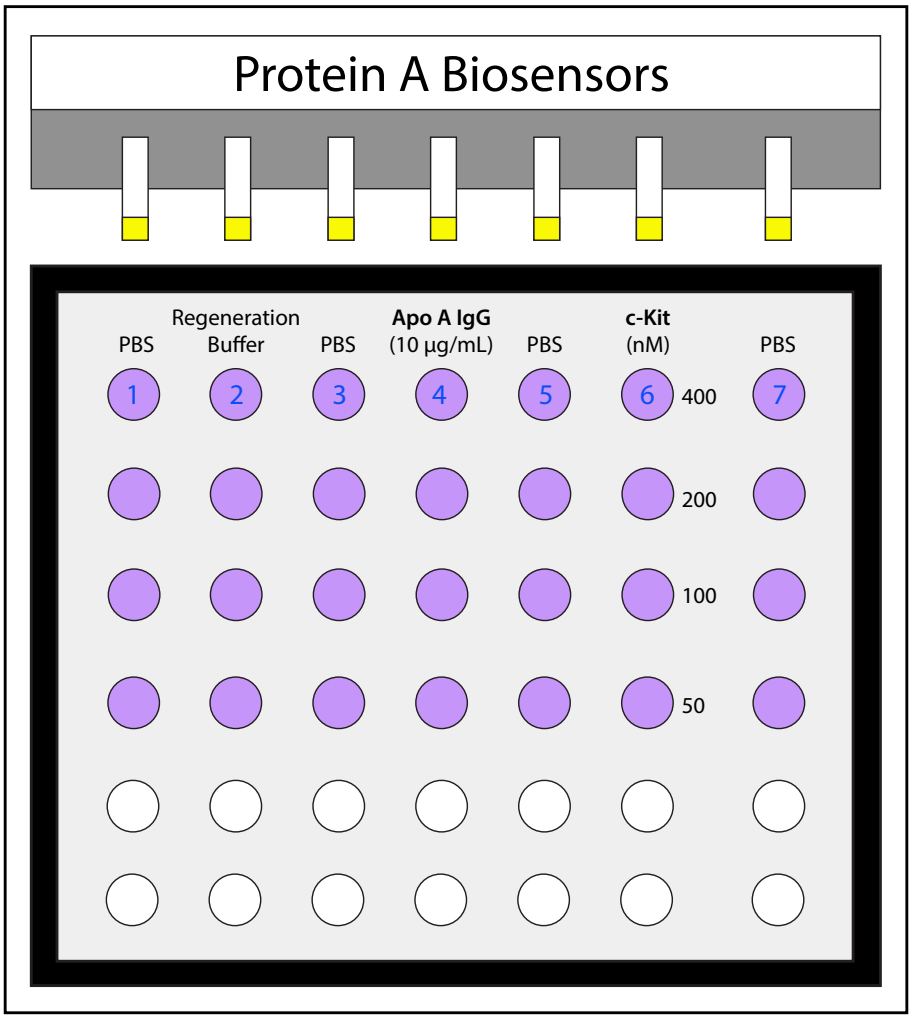

Figure 4.4: The Kinetic Experimental Setup for Apo A IgG Using Protein A Biosensors. The microplate was prepared with 50 µL of sample per each well (purple) in the respective test conditions: 1) phosphate-buffered saline (PBS); 2) regeneration buffer; 3) PBS; 4) Apo A IgG with a concentration of 10 µg/mL diluted with PBS; 5) PBS; 6) a titration series of 400, 200, 100, and 50 nanomolar (nM) of c-Kit concentrations diluted with PBS; and 7) PBS.

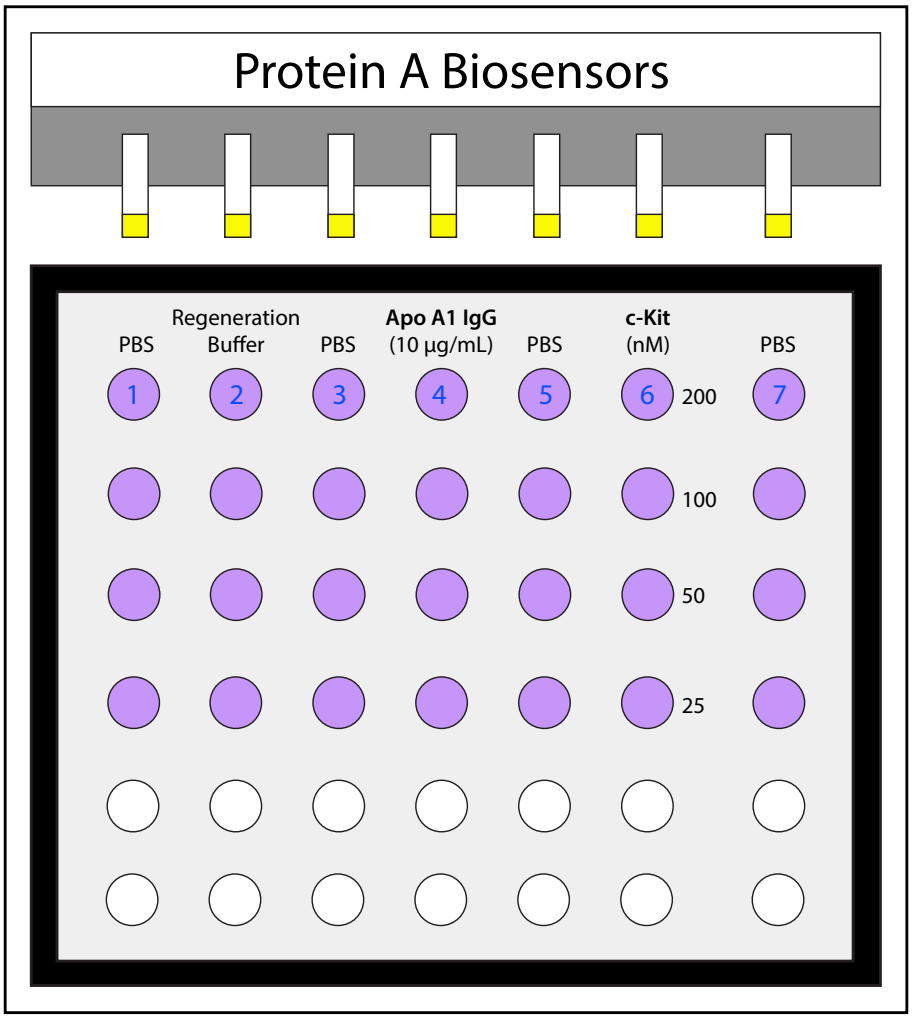

Figure 4.5: The Kinetic Experimental Setup for Apo A1 IgG Using Protein A Biosensors. The microplate was prepared with 50 µL of sample per each well (purple) in the respective test conditions: 1) phosphate-buffered saline (PBS); 2) regeneration buffer; 3) PBS; 4) Apo A1 IgG with a concentration of 10 µg/mL diluted with PBS; 5) PBS; 6) a titration series of 200, 100, 50, and 25 nanomolar (nM) of c-Kit concentrations diluted with PBS; and 7) PBS.

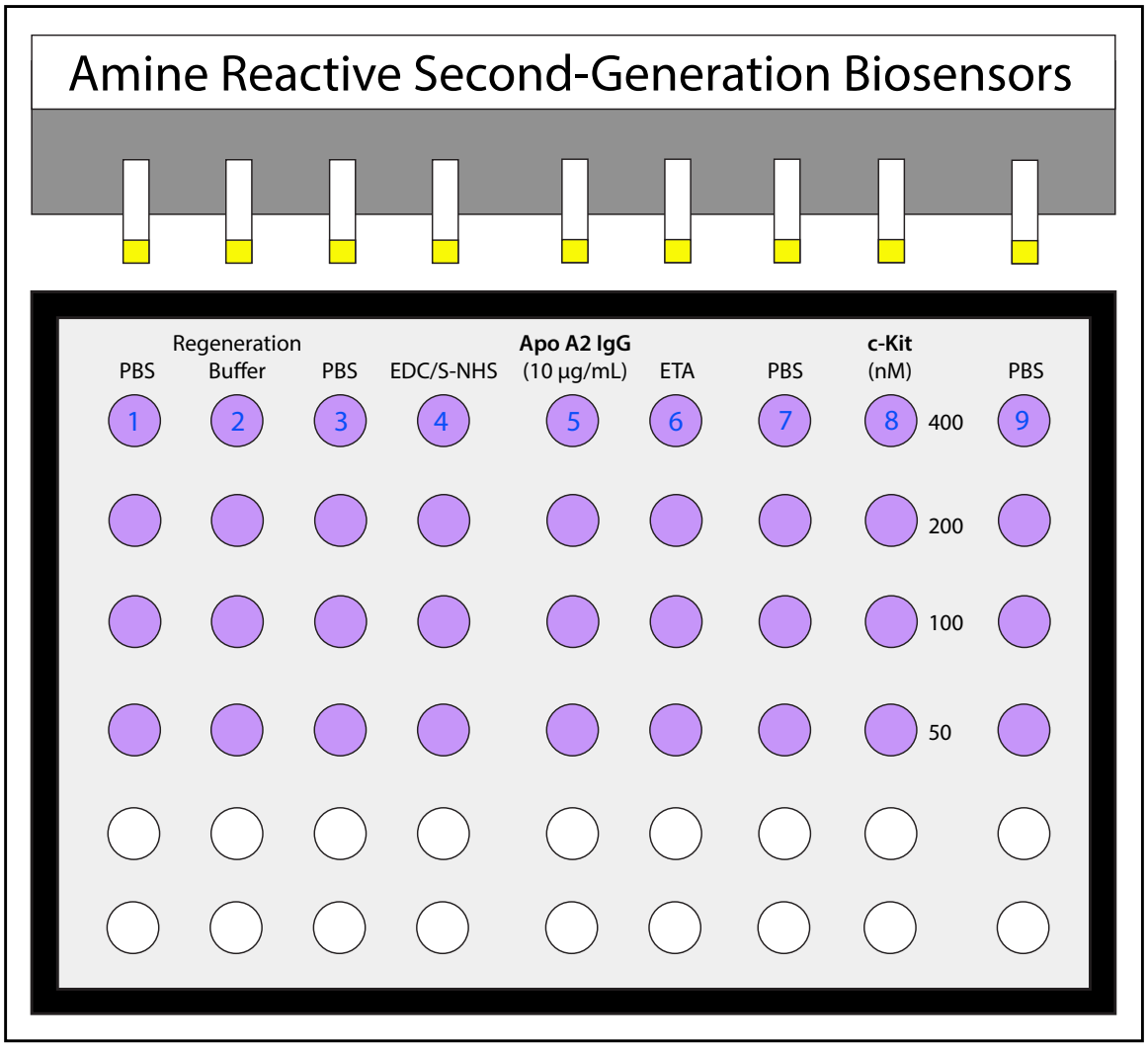

Figure 4.6: The Kinetic Experimental Setup for Apo A2 IgG Using Amine Reactive Second-Generation (AR2G) Biosensors. The microplate was prepared with 50 µL of sample per each well (purple) in the respective test conditions: 1) phosphate-buffered saline (PBS); 2) regeneration buffer; 3) PBS; 4) 1-ethyl-3-(3-dimethylaminopropyl)carbodiimide (EDC) and N-hydroxysulfosuccinimide (sulfo-NHS); 5) Apo A2 IgG with a concentration of 50 µg/mL diluted with sodium acetate buffer; 6) ethanolamine (ETA); 7) PBS; 8) a titration series of 400, 200, 100, and 50 nanomolar (nM) of c-Kit concentrations diluted with sodium acetate buffer; and 9) PBS.

4.3.2 Cell Binding Test

This test allows for assessing the quantity of sABs binding to the cell surface on various CML cells. The experimental procedure involves immunofluorescence staining and flow cytometry to optically estimate the level of c-Kit fluorescence.

1. Cells are initially prepared with approximately 300, 000 cells per flow tube, for a set of 3 tubes:
   (a) cells;
   (b) cells + secondary antibody;
   (c) cells + primary antibody (i.e., anti–c-Kit sAB) + secondary antibody.
2. Next, immunofluorescence staining is performed in accordance with the manufacturer's instructions.
3. Then, the prepared test samples are loaded on the flow cytometry system for cell binding analysis.

It should be noted that, the antibody staining step facilitates the estimation of the cell population of interest using a secondary antibody conjugated to a fluorochrome, e.g., phycoerythrin (PE) for murine CML cells or fluorescein isothiocyanate (FITC) for human CML cells. This fact, along with its rationale, will be further elaborated and utilized later in Section 6.2.

4.3.3 Specific Binding (SB) and Non-Specific Binding (NSB) Tests

For specific binding and non-specific binding tests, the human embryonic kidney (HEK) 293F cells are utilized to investigate the different binding activities occurring on different cell surface types: surface with c-Kit molecules (i.e., specific case of interest) versus surface without c-Kit, but with other surface proteins. The protocol is as follows:

1. To control the presence of c-Kit domain on the cell membrane, a polyethylenimine (PEI) transfection with c-Kit plasmid DNA is performed in accordance with the manufacturer's instructions.

2. Once transfection is finished, the cell preparation procedure is similar to that in the cell binding test described above in Section 4.3.2.

3. With the prepared cell samples, the SB and NSB tests proceed as follows:

   (a) For SB, the HEK 293F cell line (transfected with c-Kit plasmid DNA) is stained with primary antibody (i.e., anti–c-Kit sAB) and secondary antibody (conjugated to FITC);

   (b) For NSB, the HEK 293F cell line is also stained with both primary and secondary antibodies.

4. Immunofluorescence staining is performed, also following the same procedure as that described above in Section 4.3.2.

5. Then, the prepared test samples are loaded on the flow cytometry system for SB and NSB analysis.

4.3.4 Cell Viability Assay

To investigate cell behaviors in response to a combinatorial effect on various CML cell lines, cell viability assay is performed to estimate cell number, using a trypan blue dye to differentiate viable and non-viable cells.

The protocol for this assay is as follows.

1. First, all CML lines are prepared in triplicate with a cell concentration of 0.5×10^6 cells/mL, cultured as described previously in Section 4.1.3, and treated with the combinatorial treatment consisting of c-Kit antibody and nilotinib, applied with stem cell factor (SCF).

2. The following test scenarios are considered:

   - [1] - Cells (untreated)
   - [2] - Cells + stem cell factor (SCF)
   - [3] - Cells + nilotinib (Nil)
   - [4] - Cells + SCF + Nil

- [5] - Cells + antibody (Ab)
- [6] - Cells + Ab + SCF
- [7] - Cells + Ab + Nil
- [8] - Cells + Ab + SCF + Nil

3. The corresponding nilotinib, sAB (including Apo A, Apo A1, and Apo A2 IgG's), and SCF concentrations are configured according to Table 4.5.

4. After 40–48 hours of incubation, a culture sample of 10 µLs is then diluted with 10 µLs of 0.4% Trypan Blue dye, and cell counting (i.e., cell density and cell viability in percentage) is determined using a hemocytometer under a light microscope.

Experimental Setup for Nilotinib, sABs, and SCF			
CML Cell Line	**IC_{50} Nilotinib** (nM)	**sABs** [Apo A, Apo A1, and Apo A2 IgG's] (µg/mL)	**SCF** (ng/mL)
CJ	50	3	200
KU-812	10	3	200
JURL-MK1	30	3	200

Table 4.5: Experimental Setup for CML Cell Lines. The table lists half maximal inhibitory concentration (IC_{50}) nilotinib, sAB, and SCF concentrations for all three CML cell lines.

4.3.5 Apoptosis Assay

To identify and measure the apoptotic effect on CML cells, apoptosis assay needs to be performed in order to confirm whether a majority of the cell deaths is caused by a combinatorial treatment versus a single drug alone.

1. The initial preparation steps of this experimental setup are similar to those in the cell viability assay.

2. After 40–48 hours of incubation, Annexin V staining is performed in accordance with the manufacturer's instructions.

3. Then, the prepared test samples are loaded on the flow cytometry system for apoptosis analysis.

4.3.6 Colony Forming Cells (CFC) Assay

To investigate the progenitor ability of CML cells after a combinatorial treatment, CFC assay needs to be performed to ensure that c-Kit sAB could restore nilotinib effect.

1. The initial preparation steps are similar to those in the cell viability assay.
2. After 40–48 hours of incubation, CFC assay is set up using MethoCult™ methylcellulose-based medium in accordance with the manufacturer's instructions. Cells are plated in triplicate at a density of 100–300 cells per 150 μL methylcellulose reagent.
3. Colony formation is quantified under an inverted microscope after 7–14 days of incubation in a humidified atmosphere.

4.4 Statistical Analyses and Data Presentation

All data analyses including statistical tests are to be performed using IBM SPSS Statistics Version 20 software for subsequent interpretation and visual presentation. P-values for cell viability, apoptosis, and colony formation assay data are calculated using one-tailed Student's t-test to compare a combinatorial treatment versus one drug solution. FlowJo Version 8.8.7 is utilized to:

1) generate histogram graphs for cell binding and specific binding tests;

2) process analytical data for apoptosis assay.

Furthermore, all figures, illustrations, and tables are produced using Adobe® Illustrator CC 2014 and Microsoft® Excel 2011.

5. Proposed Strategy: A Combinatorial Treatment Using Nilotinib and Anti–c-Kit Synthetic Antibodies

In this chapter, a strategy is provided to potentially reduce the SCF-mediated innate resistance. Here the rationale for designing a suitable combinatorial strategy to improve CML therapy is presented. More specifically, a targeted therapy approach is possible due to the biochemical knowledge of the c-Kit pathway, which is responsible in part for innate resistance.

5.1 c-Kit Pathway Revisited for Targeted CML Treatment

The receptor c-Kit (also known as CD117), activated by its ligand SCF, is a member of type III receptor tyrosine kinase family. It was first identified and characterized in 1987 as the cellular homologue, encoded by the viral oncogene v-kit, of Hardy-Zuckerman IV feline sarcoma virus [81, 82].

As previously described in Chapter 2, the SCF/c-Kit pathway is intimately implicated in the innate resistance mechanism [76, 83]. Even in normal cells, this pathway plays a pivotal role in maintaining and stimulating diverse biological functions in hematopoiesis, which in mutated cells are conducive to supporting tumorigenesis, including: cell growth and survival; proliferation and differentiation, and adhesion and migration [75, 76, 84]. For instance, mutations in the c-Kit transduction pathway are actively linked to the occurrence of various human cancers, including gastrointestinal stromal tumors (GISTs) and leukemias [76, 85–87]. In the context of CML, from a signaling perspective, the c-Kit pathway is responsible for stimulating innate resistance, and this mechanism is in turn mediated by SCF, one of the crucial hematopoietic cytokines [25, 58, 77, 88]. Stromal SCFs are released by the bone marrow (BM) endosteal niche, where the population of quiescent LSCs reside and receive protection from these growth factors, in order to activate tyrosine

kinase inhibitor (TKI) innate resistance [89–91].

Clearly, to reduce innate nilotinib resistance, it is vital to block the c-Kit pathway. In this thesis, the receptor c-Kit will be targeted to inhibit SCF-mediated signal transduction initialization. To this end, identifying the structural susceptibility of c-Kit is relevant. The receptor c-Kit is a type I transmembrane glycoprotein composed of 976 amino acids, with a relative molecular mass of 145 kDa [77, 92]. The extra-cellular fragment consists of five immunoglobulin-like domains (D1–D5), which are categorized into two separate functional units: (1) D1–D2–D3 domains are the essential binding sites of SCF; and (2) D4–D5 domains are the region for homodimerization of the two receptor c-Kit monomers. The ligand SCF homodimer binds to domains (D1–D2–D3) of the receptor c-Kit, which results in homodimerization in order to activate the intrinsic tyrosine kinase activity and drive downstream signal transduction pathways [25, 77, 92–94]. Since successful interaction between the receptor c-Kit and its ligand SCF is important for activating the pathway, disrupting this initial interaction is a judicious strategy to disable this pathway, which can be achieved by targeting the epitopes involved. The integration sites D1–D2–D3 are therefore precisely the epitopes sought for targeted treatment, since these epitopes are implicated in the activation of the c-Kit/SCF pathway. Therefore, blocking this SCF signaling should reduce the protection mechanisms of the LSCs by targeting the binding sites of a SCF homodimer on the receptor c-Kit with some inhibiting co-agents. The described c-Kit structure and its ligand SCF, with specific sites as potential targets to block the downstream activation of many intracellular pathways for therapeutic strategies, are illustrated in Figures 5.1 and 5.2.

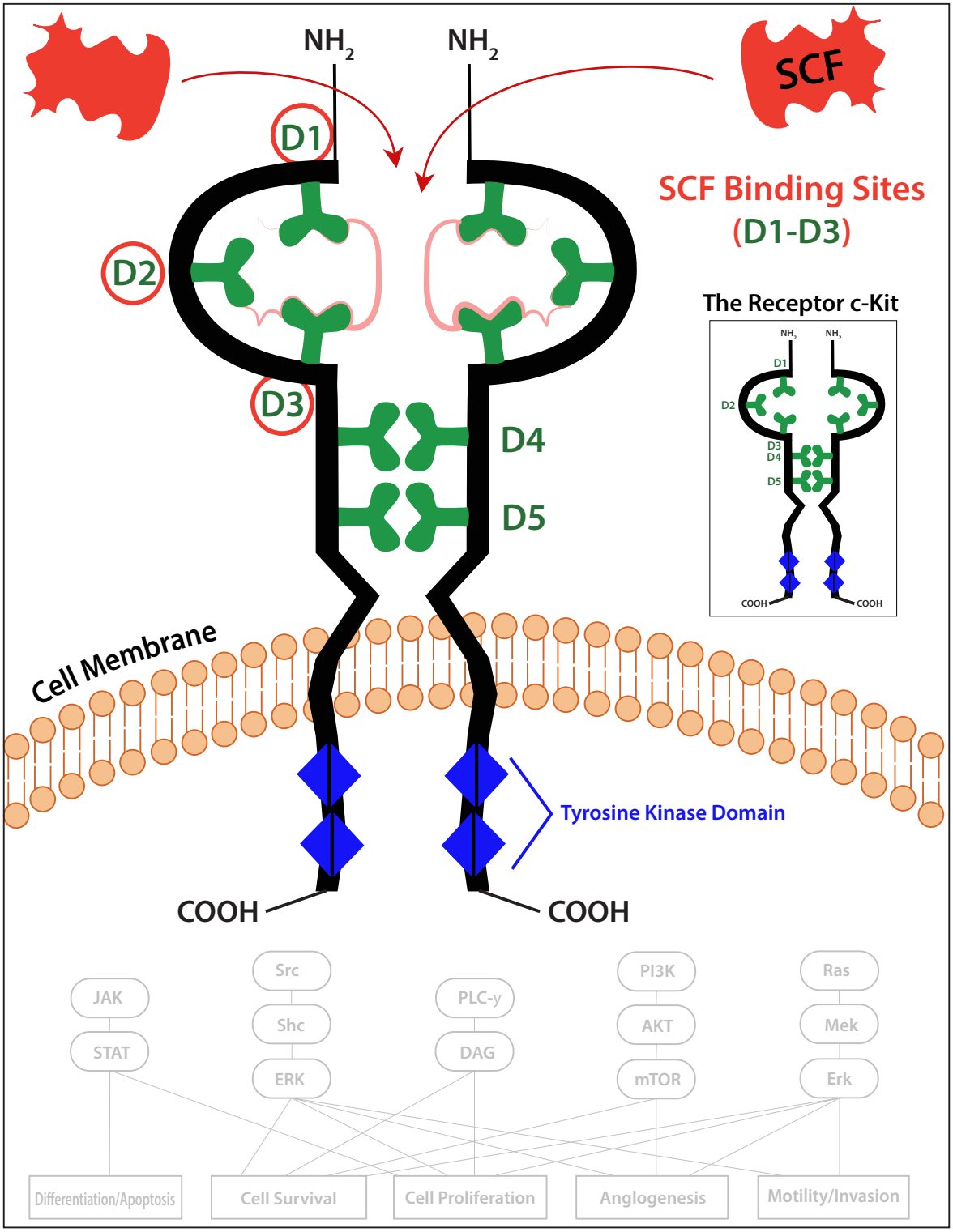

Figure 5.1: Schematic Diagram of c-Kit Structure with Its Ligand SCF. The extra-cellular fragment consists of five immunoglobulin-like domains (D1–D5). In particular, D1–D2–D3 domains are the essential binding locations for SCF (red), whereas D4–D5 domains are the region for homodimerization of the receptor c-Kit. The intra-cellular portion contains the tyrosine kinase domain (blue).

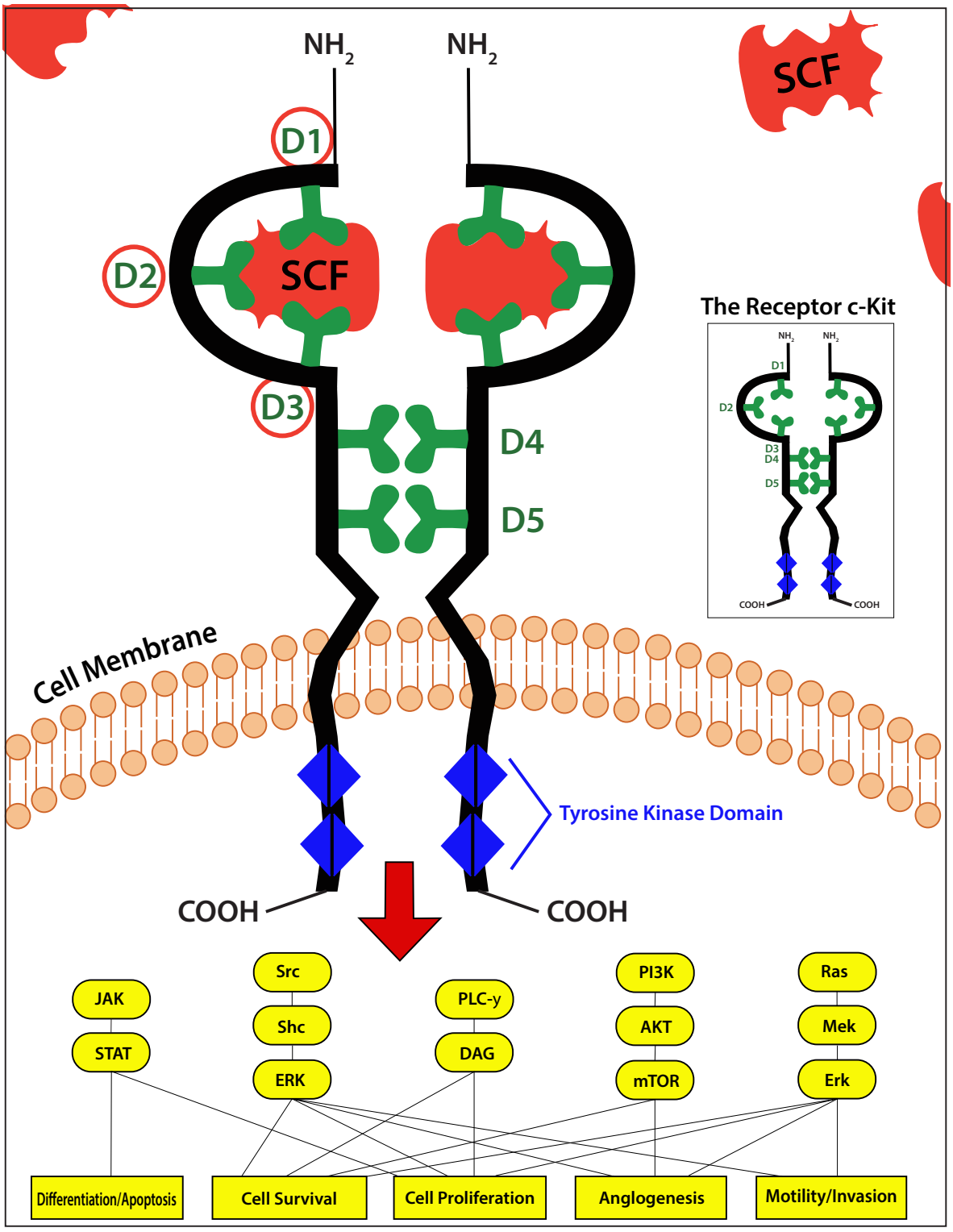

Figure 5.2: Schematic Diagram of an Activated c-Kit Molecule. Once the ligand SCF homodimer binds to specific domains (D1–D3) on the receptor, the SCF/c-Kit complex results in homodimerization to activate the intrinsic tyrosine kinase activity, thus driving downstream signal transduction pathways.

5.2 sAB Technology: A Versatile Platform for Targeted and Combinatorial Treatment

The previous section highlights the necessity of targeted treatment to specifically target D1–D2–D3 domains, which are intimately involved in the pathway activation, and thus represent vulnerable sites on the c-Kit molecule [77,92]. Moreover, as a one-drug solution can typically achieve only limited objectives, a combination of treatments is desired to simultaneously inhibit the BCR-ABL problem and block the innate resistance. In other words, a suitable solution should involve a treatment platform that can be flexibly configured to fulfill two perspectives: (1) incorporate specific structural information in design; (2) amenable to development of combinatorial therapy. For precisely these reasons, the emerging sAB technology represents a versatile and compelling solution to be considered. In particular, combinatorial treatments based on sABs have the potential to achieve high affinity and strong specificity to the selective targets [95].

Antibodies have emerged as a potent molecularly-targeted therapy for human cancer, especially when combined with other chemotherapy drugs [96]. The combinatorial advantage is also realized by converting two antibodies into a single bi-specific antibody, to increase the effective concentration of antigen binding sites and potency [97]. Compared to small-molecule therapeutics, the virtues of antibodies include the ability to simultaneously inhibit the activity of their target, and also stimulate the immune response to induce cellular cytotoxicity. This characteristic is strategically important in targeting LSCs, since inhibition of a specific signaling pathway may be compensated by bone marrow cytokine stimulation of alternative pathways. The antibody therapeutic approach is further facilitated and enhanced by the phage display methodology, in which sABs can be effectively generated for targeting specific c-Kit domains.

With the state-of-the-art phage display technology, it is possible to screen antigen binding fragment (Fab) libraries, thus isolating individual Fabs that bind specific targets. Furthermore, recombinant DNA techniques make it possible to generate fully synthetic libraries of Fabs, with diverse and customizable properties [98–101]. This synthetic flexibility is a major advantage, since antibodies with unique and specific characteristics can be generated, which would be otherwise unattainable if antibodies are limited to the natural repertoires derived from immune cells or present within hybridoma libraries [30, 102, 103]. In fact, since it is known that the SCF/c-Kit signaling

is required for hematopoietic cell development [83, 94], Fabs can be generated to target multiple signaling sites on the c-Kit ectodomain (i.e., D1–D3 as explained previously).

The illustrations of sABs targeting the D1–D3 domains on the c-Kit receptor are shown in Figures 5.3 and 5.4. Furthermore, the resulting combinatorial treatment strategy, simultaneously targeting the c-Kit structure (with sABs) and BCR-ABL (with nilotinib), is as previously shown in Figure 3.1 from Chapter 3. In this manner, the generated antibodies can inhibit the SCF/c-Kit pathway in order to restore nilotinib activity for treatments against CML, with high affinity and specificity. These properties will be validated in the following Chapter 6, describing a comprehensive set of tissue culture assays.

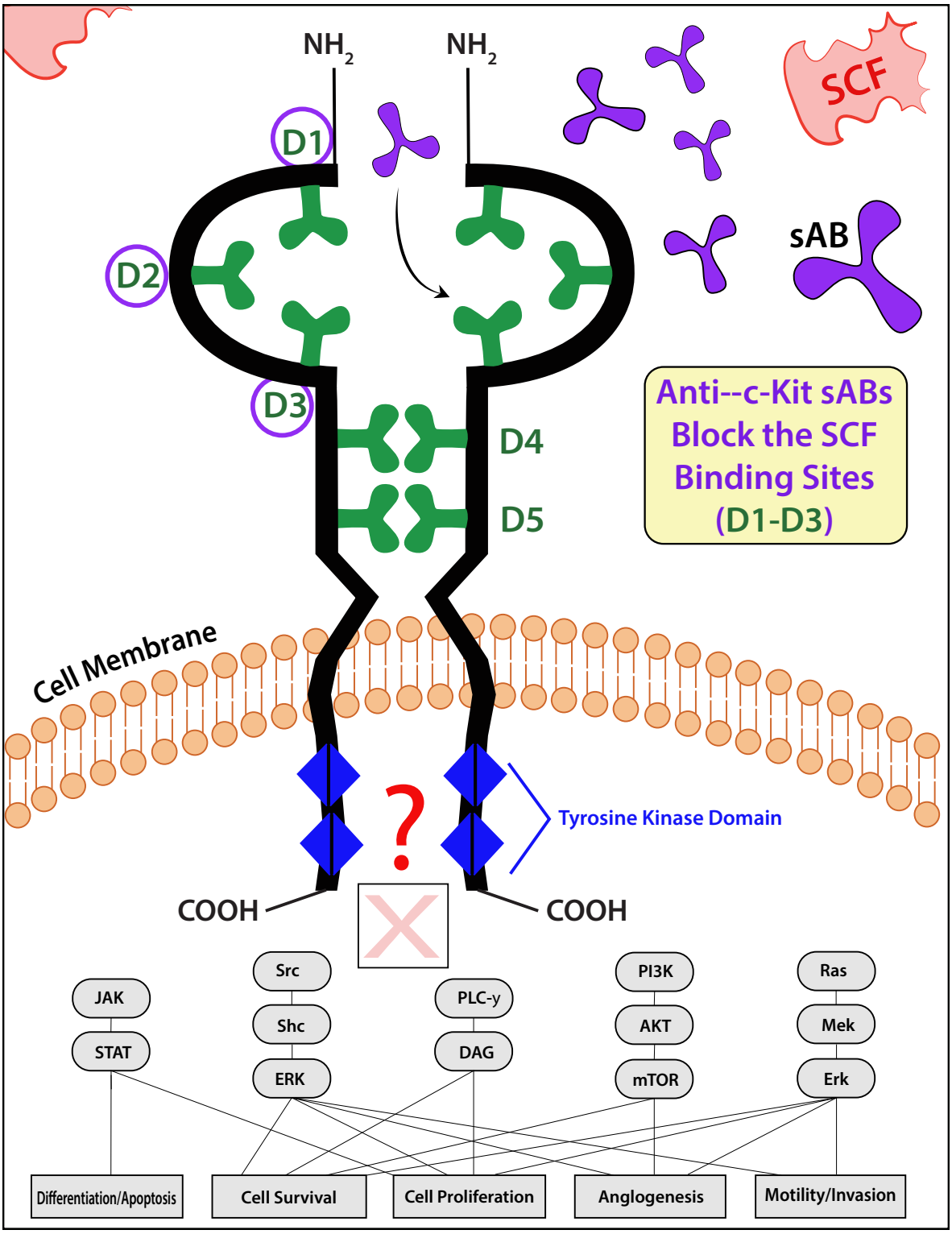

Figure 5.3: An Overview of How the SCF/c-Kit Pathway Should be Inhibited. Exploiting advances in the antibody phage display technology, sABs (purple) are generated with unique and specific characteristics (e.g., high affinity and high specificity) to target the essential binding sites of SCF on the receptor for pathway activation.

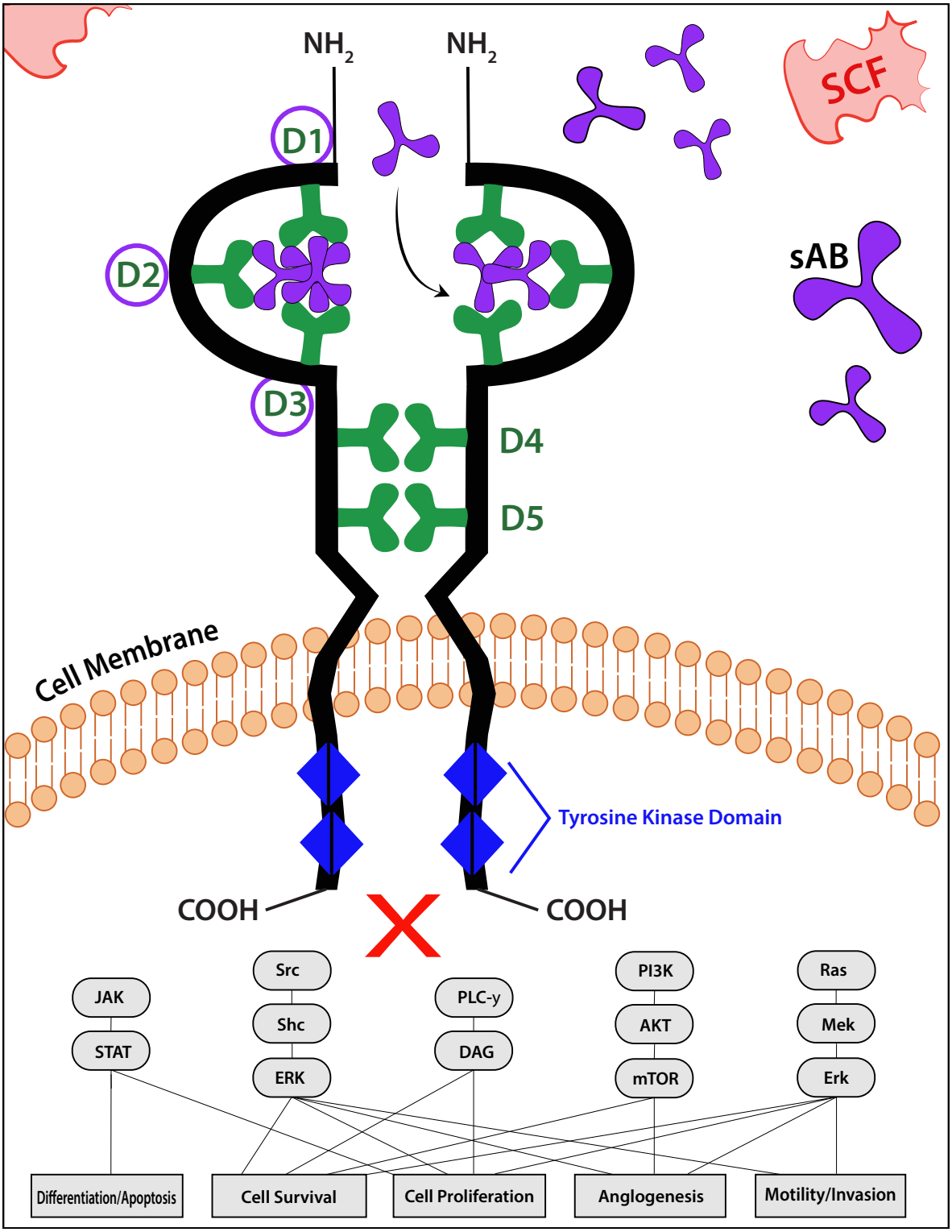

Figure 5.4: An Overview of Synthetic Antibodies Specifically Targeting D1–D2–D3 Domains on the Receptor c-Kit. To effectively inhibit the SCF/c-Kit pathway, sABs (purple) are utilized to specifically target D1–D2–D3 domains (SCF binding sites) on the receptor, thus causing a homodimerization of D4–D5 domains in order to deactivate downstream signal transduction pathways.

5.3 Overview of Anti–c-Kit sAB Generation

In the previous section, a combinatorial methodology involving two agents has been described. Clearly, to improve the likelihood of successfully deriving an effective combination, the starting points or input candidates need to possess promising properties. In this thesis, the drug agent is fixed to be nilotinib, while the promising sAB co-agent will be selected from a pool of c-Kit Fabs generated using the phage display technology. The goal is to produce sABs with the capacity to efficiently bind to specific domains on the c-Kit molecule, thus potentially inhibiting the SCF-mediated innate resistance pathway for a synergistic combinatorial treatment.

In Section 4.2, the protocols necessary to generate such sABs have been described in detail, and illustrated in Figures 4.1, 4.2, and 4.3. To summarize the generation process depicted in Figure 5.5, the three stages are pursued using the phage display technology [29, 30, 104–106]:

- **First stage** – generation of c-Kit Fabs specifically targeted to the c-Kit D1–D3 region from *in vitro* screening and selection strategies;
- **Second stage** – affinity maturation to produce alternative c-Kit Fabs with increased binding affinity for greater sensitivity in assays;
- **Third stage** – conversion of high affinity c-Kit Fabs into complete sABs, of the Immunoglobulin G (IgG) isotype, to perform subsequent tests on CML cells.

It should be noted that there are three other c-Kit Fabs generated: Apo B Fab, and two variants created from affinity maturation, i.e., Apo B1 Fab and Apo B2 Fab. However, the specific sequences with various substitutions in the CDR segments are not shown explicitly in this thesis, since these Fabs were found to fail the third stage, i.e., conversion of c-Kit Fabs into complete IgG antibodies.

In summary, of the six candidates anti–c-Kit sABs, only three were found to be the potential antibody co-agents. In other words, the subsequent assays will be pursued with Apo A, Apo A1 and Apo A2 sABs only, as described and conducted in Chapter 6.

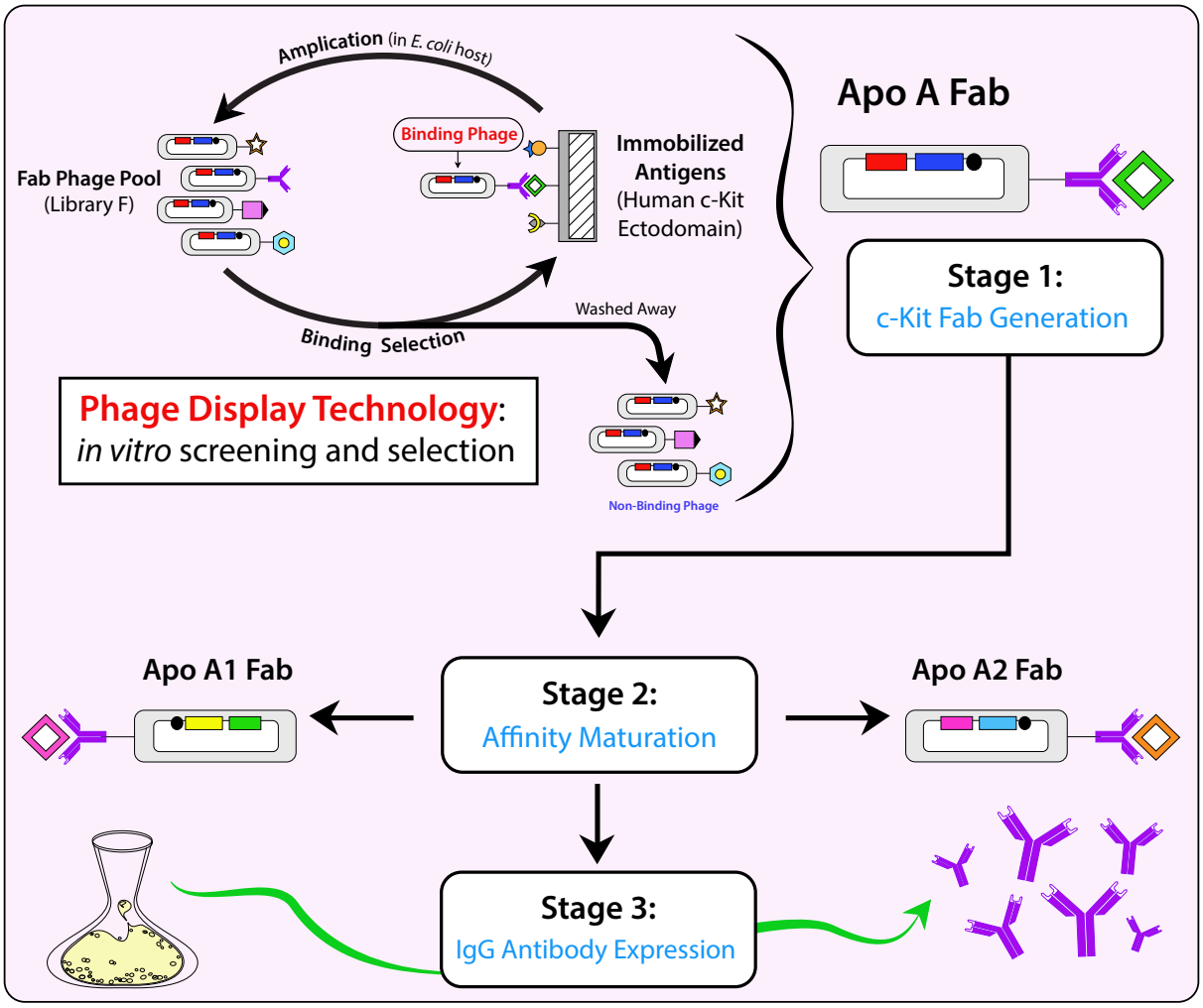

Figure 5.5: Three Stages Utilized to Generate and Express c-Kit Fabs into Human IgG sABs. 1) Using the phage display technology, Apo A Fab is generated to specifically target the c-Kit D1–D3 region; 2) With the goal of fine-tuning the binding affinity and specificity, alternative Fabs (i.e., Apo A1 Fab and Apo A2 Fab) are produced from an affinity maturation; and 3) c-Kit Fabs are expressed into human IgG sABs to perform tissue culture assays on CML cells.

6. Results and Data Analyses: Assessing the Ability of Anti–c-Kit sAB to Block SCF-Mediated Innate Resistance

In this chapter, the experimental results obtained from a strategically designed set of tests are first reported, followed by suitable data analysis in order to reveal the effectiveness of the proposed combinatorial approach. In particular, the ability of sABs to enhance combinatorial treatment with nilotinib for CML will be tested *in vitro* using kinetic, cell binding, viability, apoptosis, and colony forming cell assays. It will be seen that all tests support the promising potential of sABs to block the SCF pathway in order to mitigate LSCs, thus enhancing the effectiveness of nilotinib in addressing innate resistance.

Unless otherwise specified, all data analyses including statistical tests were performed in SPSS version 20 by IBM, with suitable graphs generated accordingly for subsequent interpretation.

6.1 Kinetic Test: Screening for Suitable Co-Agents Based on sAB Affinity

Since binding needs to at least occur before other types of interaction between sABs and cells can even be meaningfully considered, ensuring that binding tightness has in fact been achieved should be the first condition to be validated. Once this binding criterion has been successfully met, other follow-up tests will be investigated. Therefore, the first test applied was the kinetic test, with the objective of measuring the affinity of an antibody-protein interaction, which quantifies the binding tightness of an antibody to its target. This kinetic test was performed using the *forte*Bio Octet system, which includes an Octet $^{\text{Red}}$ 384 16-channel instrument, bio-layer interferometry (BLI) biosensors, reagents and assay kit to perform real-time quantification of IgG concentrations and high-sensitivity kinetic analysis of antibody-protein binding interactions in an accelerated and

efficient manner. The Octet system incorporates a Dip and Read BLI biosensor technology that emits incident white light down the biosensor and collects the reflected light from two surfaces: 1) a layer of immobilized protein on the biosensor tip, and 2) an internal reference layer. This system uses an optical technique to measure and analyze biomolecular interactions between immobilized antibodies (i.e., anti–c-Kit sABs) and protein molecules (i.e., c-Kit) in real-time. A layer of any molecules attached to the biosensor tip of an optical layer creates a wave interference pattern, which is captured by a spectrometer at the detector. Any change in the number of molecules bound to the tip triggers a spectral shift in the interference pattern and generates a response profile on the system, thus directly quantifying the change in optical thickness of the coating on the biological layer [107].

As illustrated in Figure 6.1, in the process of antibody loading, c-Kit sABs are first attached to the biosensor tip surface, which creates an interference pattern at the detector. Once the c-Kit molecules in solution bind or associate to immobilized sABs at the tip surface, this antibody-protein interaction causes a spectral shift in the interference pattern that directly quantifies an increase in optical thickness at the biosensor layer. In contrast, when the c-Kit molecules dissociate from immobilized sABs, this corresponding event causes another wavelength shift to quantify a decrease in optical thickness at the biosensor tip. Overall, the association and dissociation of interacting sABs bound to the c-Kit are assayed by the Octet system, thus quantifying the binding activity and producing the association and dissociation curves on the kinetic graph [107].

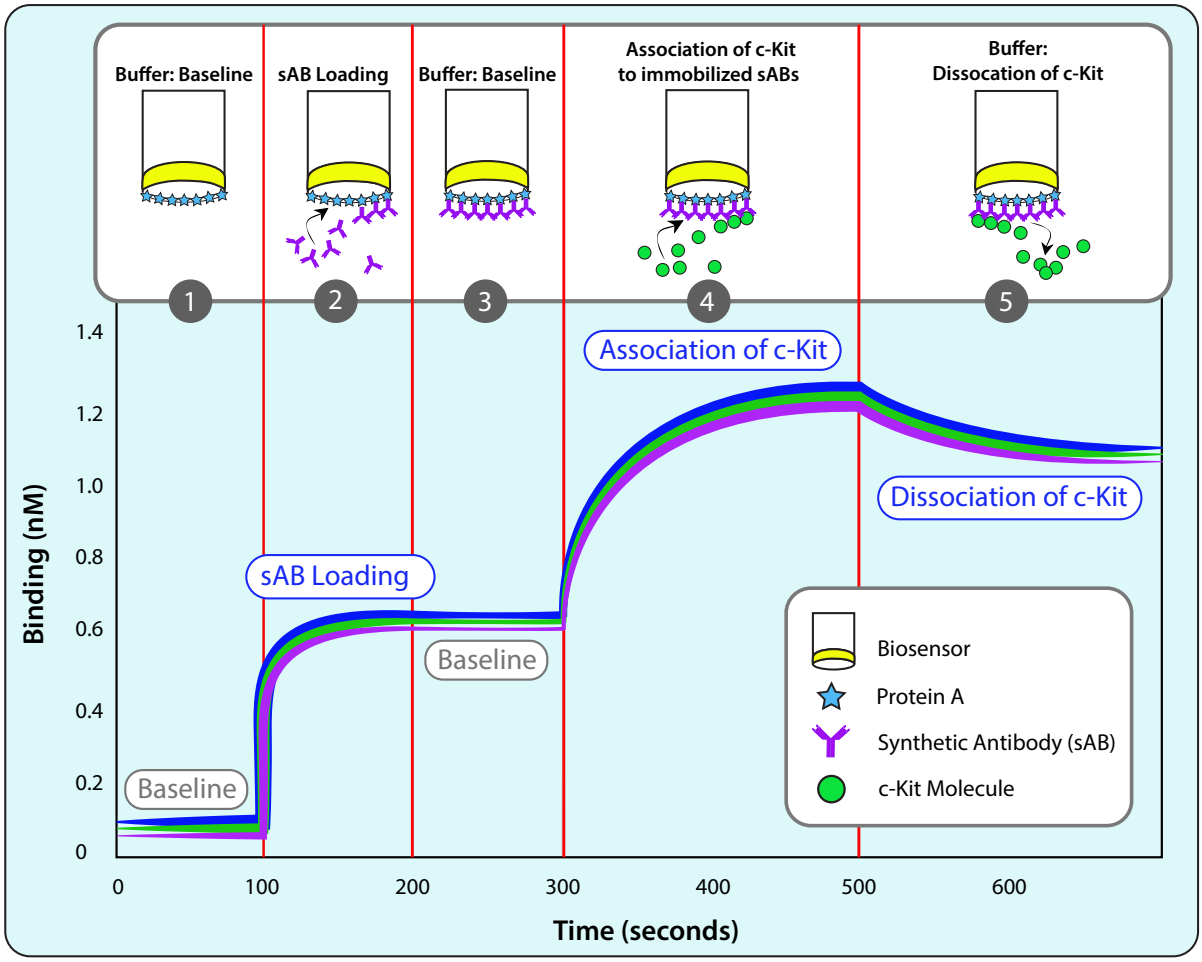

Figure 6.1: Schematic Diagram for Association and Dissociation of Anti–c-Kit sABs, as Delivered by the Octet System: 1) The Octet system uses buffer for the baseline step; 2) In the antibody loading step, sABs are first bound to the biosensor tip surface; 3) Next, the system uses buffer for another baseline step; 4) For association, the c-Kit molecules in solution bind to immobilized sABs at the tip surface to cause an antibody-protein interaction; and 5) For dissociation, the system uses buffer to separate the c-Kit molecules from immobilized sABs. The Octet system quantifies the association and dissociation of sABs bound to the c-Kit, in order to produce the association and dissociation curves on the kinetic graph.

For kinetic measurement, the *forte*Bio Octet $^{\text{Red}}$ 384 system — with protein A and amine reactive second-generation (AR2G) biosensors — was utilized to quantitatively determine the equilibrium dissociation constant (K_D). To enable useful visual characterization, the following kinetic parameters will be investigated: K_D and $K_{D,\text{error}}$, which respectively quantify: (i) the affinity of the antibody for its target; and (ii) accuracy and reliability of the K_D measurement.

$K_{D,\text{error}}$ is reported by the Octet instrumentation system, whereas K_D is calculated as follows [108, 109]:

$$K_D = \frac{k_d}{k_a}\ [M] \tag{6.1}$$

where

1. k_a, in units of 1 over molar over second $[1/(Ms)]$: an association constant characterizing how quickly an antibody binds to its specific target;
2. k_d, in units of 1 over second $[1/s]$: a dissociation constant characterizing how quickly an antibody separates off from its specific target.

6.1.1 Kinetic Data for the sABs

For this test, the kinetic experimental setup for each sAB was as follows:

- Apo A IgG with a titration series of 50, 100, 200 and 400 nM of c-Kit concentrations, using protein A biosensors;
- Apo A1 IgG with a titration series of 25, 50, 100, and 200 nM of c-Kit concentrations, using protein A biosensors;
- Apo A2 IgG with a titration series of 50, 100, 200, and 400 nM of c-Kit concentrations, using AR2G biosensors.

The corresponding protocol for this kinetic test is as described previously in Section 4.3.1. Then, the obtained kinetic plots for Apo A IgG, Apo A1 IgG, and Apo A2 IgG are respectively

shown in Figures 6.2, 6.3, and 6.4, and kinetic tables in Tables 6.1, 6.2, and 6.3. These data sets were analyzed with *forte*Bio Octet global curve fitting to produce the associated K_D and K_D error values, which are also reported in the respective tables.

The following general observations can be made (see also Figure 6.1 for guidelines on data interpretation):

- Figure 6.2 and Table 6.1 illustrate a full kinetic characterization of the interaction between Apo A IgG and each c-Kit concentration from a titration series, as described above in the experimental setup. Using this titration series, the average K_D calculated for **Apo A IgG** is 28.55 nM and the average K_D error is 0.82 nM.
- Similarly, from Figure 6.3 and Table 6.2, the average K_D for **Apo A1 IgG** is 2.90 nM and the average K_D error is 0.06 nM.
- And likewise, from Figure 6.4 and Table 6.3, the average K_D for **Apo A2 IgG** is 5.68 nM and the average K_D error is 0.32 nM.

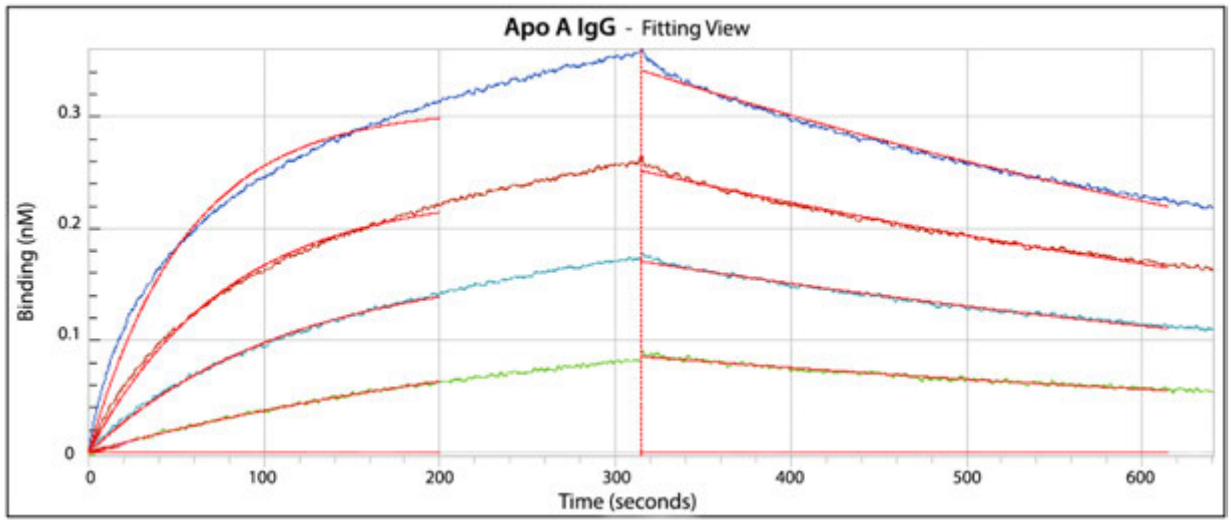

Figure 6.2: Kinetic Characterization of the Binding Interaction Between Apo A IgG and c-Kit: The kinetic graph illustrates association and dissociation curves for Apo A IgG and different c-Kit concentrations, using proteinA biosensors. The red curves represent the statistical fitting of curves; whereas the green, turquoise, brown, and blue curves represent experimental data of the binding interaction between Apo A IgG and a titration series of 50, 100, 200, and 400 nM of c-Kit concentrations, respectively.

Kinetic Characterization of the c-Kit:Apo A IgG Interaction (Using Protein A Biosensors)		
c-Kit Concentration (nM)	**K_D** (nM)	**K_D Error** (nM)
50	33.40	2.050
100	19.90	0.291
200	25.10	0.314
400	35.80	0.606
Mean K_D (nM)	**28.55**	
Mean K_D Error (nM)		**0.815**

Table 6.1: K_D and K_D error for Apo A IgG. The table lists K_D, K_D error, average K_D , and average K_D error, which are calculated based on four different c-Kit concentrations.

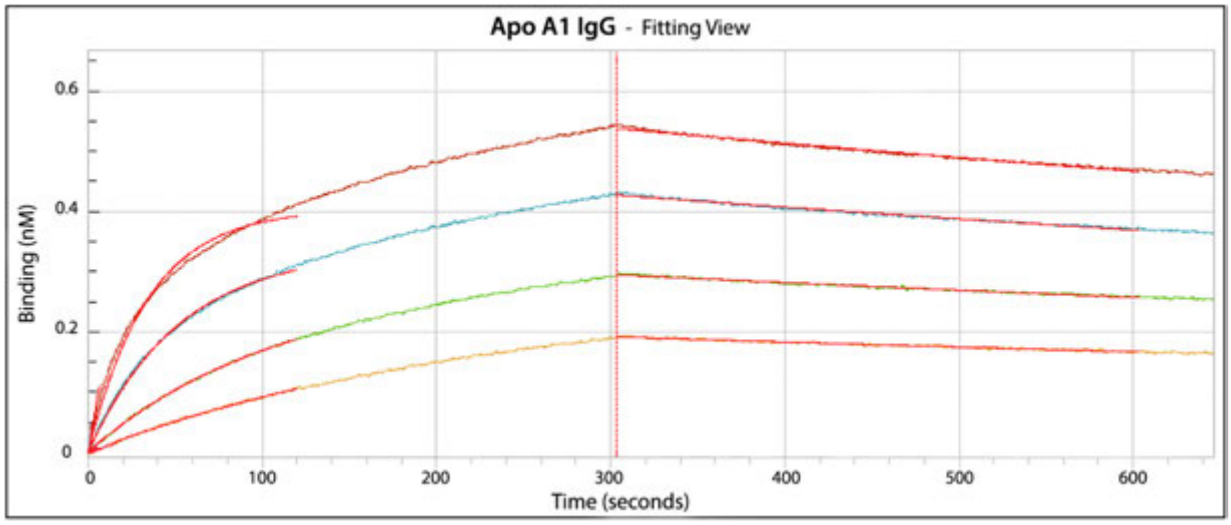

Figure 6.3: Kinetic Characterization of the Binding Interaction Between Apo A1 IgG and c-Kit: The kinetic graph illustrates association and dissociation curves for Apo A1 IgG and different c-Kit concentrations, using proteinA biosensors. The red curves represent the statistical fitting of curves; whereas the orange, green, turquoise, and brown curves represent experimental data of the binding interaction between Apo A1 IgG and a titration series of 25, 50, 100, and 200 nM of c-Kit concentrations, respectively.

Kinetic Characterization of the c-Kit:Apo A1 IgG Interaction (Using Protein A Biosensors)		
c-Kit Concentration (nM)	**K_D** (nM)	**K_D Error** (nM)
25	2.93	0.1200
50	2.66	0.0355
100	2.64	0.0298
200	3.35	0.0657
Mean K_D (nM)	**2.90**	
Mean K_D Error (nM)		**0.0628**

Table 6.2: K_D and K_D error for Apo A1 IgG. The table lists K_D, K_D error, average K_D , and average K_D error, which are calculated based on four different c-Kit concentrations.

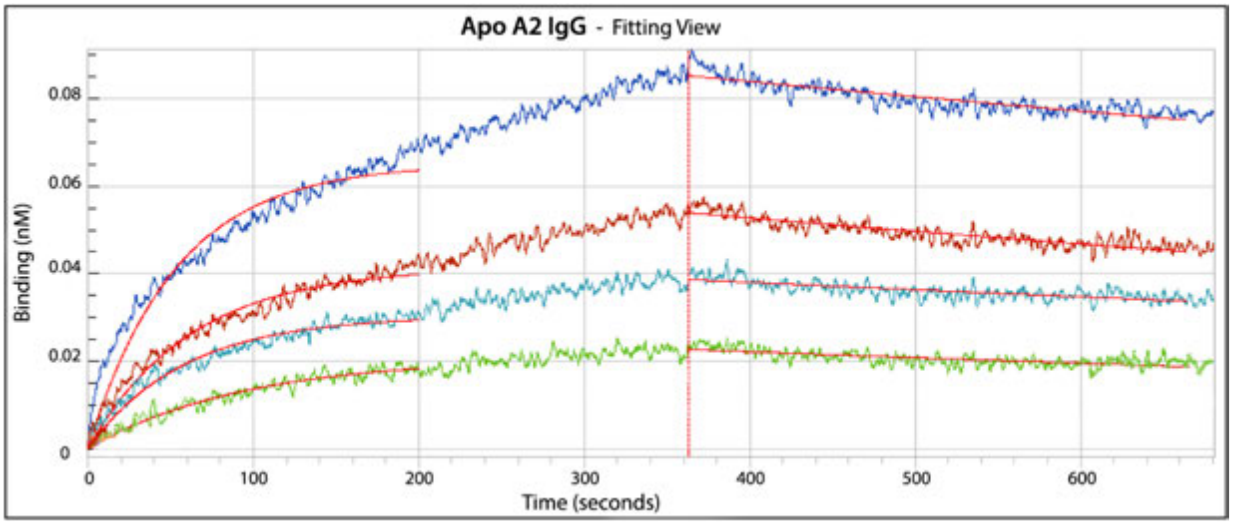

Figure 6.4: Kinetic Characterization of the Binding Interaction Between Apo A2 IgG and c-Kit: The kinetic graph illustrates association and dissociation curves for Apo A2 IgG and different c-Kit concentrations, using AR2G biosensors. The red curves represent the statistical fitting of curves; whereas the green, turquoise, brown, and blue curves represent experimental data of the binding interaction between Apo A2 IgG and a titration series of 50, 100, 200, and 400 nM of c-Kit concentrations, respectively.

Kinetic Characterization of the c-Kit:Apo A2 IgG Interaction (Using Amine Reactive 2nd Generation Biosensors)		
c-Kit Concentration (nM)	**K_D** (nM)	**K_D Error** (nM)
50	3.10	0.251
100	2.71	0.170
200	7.75	0.340
400	9.14	0.522
Mean K_D (nM)	**5.68**	
Mean K_D Error (nM)		**0.321**

Table 6.3: K_D and K_D error for Apo A2 IgG. The table lists K_D, K_D error, average K_D , and average K_D error, which are calculated based on four different c-Kit concentrations.

6.1.2 Data Analysis and Discussion: All Candidate Co-Agents Are Feasible After Screening

The K_D values generated from the obtained graphs and tables quantify the binding affinity due to each sAB with a titration series of c-Kit target measured against an immobilized antibody. In other words, high affinity antibodies (i.e., with low K_D values) have strong binding to their specific targets and low affinity antibodies (i.e., with high K_D values) have weak binding. Clearly, for therapeutic cancer applications, we seek to develop high affinity sABs for effective treatment.

According to known literature, most antibodies have K_D values in the low micromolar (10^{-6}) to nanomolar (10^{-9}) range. In particular, high affinity antibodies are usually considered to be in the low nanomolar range (10^{-9}) [108–112]. With this reference threshold, in the context of the binding affinity data obtained from the *forte*Bio Octet System, the following corresponding observations can be made:

- Apo A IgG has a high affinity for its target on the receptor c-Kit, since the obtained K_D is in the low nanomolar range.
- Apo A1 IgG exhibits an even higher affinity for its specific antigen compared to Apo A IgG.
- Apo A2 IgG shows the highest affinity for its target.

Overall, the kinetic test reveals that all three sABs have small K_D in the low nanomolar range with the Apo A2 IgG being the preferred candidate according to this test.

With significantly low K_D data, all three sABs exhibit high affinity and sensitivity. These results indicate that all candidates are feasible and further tests should be pursued for each antibody, in order to develop the suitable CML treatment solution from multiple test perspectives.

6.2 Cell Binding Test: Assessing the Quantity of sABs Binding to the Cell Surface of CML Cells

After kinetic test has confirmed tight binding, the next procedure to be performed should be cell binding test for the sABs. This test measures the number of sABs binding to the cell surface

on various CML cell lines, in order to assess how many sABs actually achieve tight binding. This is a significant quantity, to complement the tight binding confirmation provided by the kinetic test, since it indicates the effectiveness of cell and sAB interactions.

The cell binding test involves immunofluorescence staining and flow cytometry to optically estimate the level of cell binding. This is achieved by probing with a receptor-specific antibody indirectly tagged with a fluorophore and measuring the level of c-Kit fluorescence, in order to investigate the binding events of sABs to c-Kit molecules on various CML cell lines. In this test, as illustrated in Figure 6.5, CML cells are stained and incubated with: 1) primary antibody (i.e., anti–c-Kit sAB); and 2) secondary antibody, which is conjugated with a fluorochrome. This labeled secondary antibody binds to the primary antibody's fragment crystallizable region (Fc region) to indirectly detect target antigens. Specifically, a gating procedure is applied for this test, in which unstained cells represent a *negative* cell population, stained cells with a fluorochrome-labeled secondary antibody correspond to a *reference* cell population of the gating system, and stained cells with both primary and secondary antibodies represent a *positive* cell population. In other words, flow cytometry histograms measure c-Kit antibody fluorescence by assessing a percentage of CML cells exhibiting binding events between sABs and c-Kit. A histogram of the *negative* cell population shows the background fluorescence in the absence of both primary and secondary antibodies; whereas a histogram of a *reference* cell population exhibits the conjugated antibody fluorescence in the presence of secondary antibody, but devoid of the primary antibody; and a histogram of the *positive* cell population measures the c-Kit fluorescence in the presence of primary antibody. Therefore, given such a gating system, a significant increase or right shift in immunofluorescence intensity passing the gating system on a *reference* cell population is a desirable outcome, since a positive result implies that there are significant binding activities between sAB and receptor surface proteins on various CML cell lines.

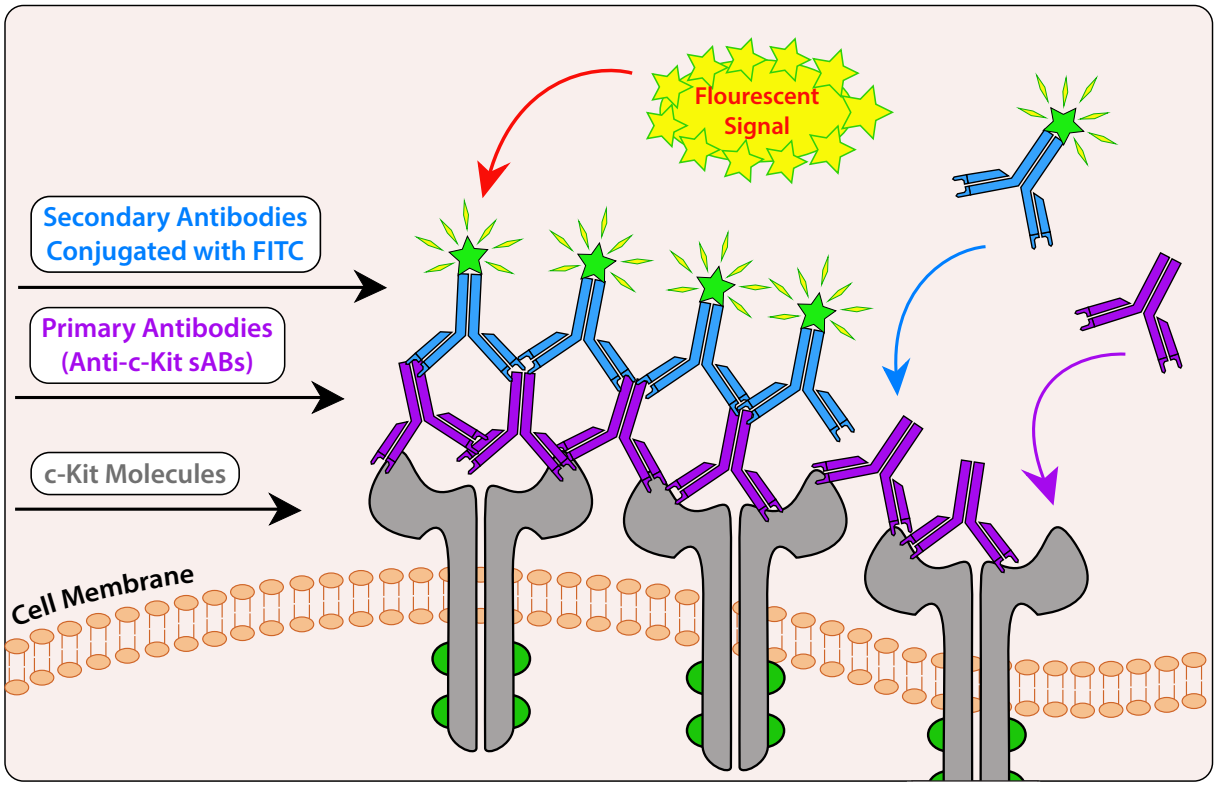

Figure 6.5: Schematic Diagram for Cell Binding of sABs to c-Kit Molecules on Cell Membrane: Cell binding test involves immunofluorescence staining and flow cytometry to optically measure the level of c-Kit fluorescence, by probing with primary antibodies (i.e., anti–c-Kit sABs in purple) indirectly tagged with a fluorophore (green star). This fluorescence measurement allows estimation of the number of binding events of sABs to c-Kit molecules (gray).

6.2.1 Data for Cell Binding Test with CML Cell Lines

As described in the procedure in Section 4.3.2, the immunofluorescence staining involves the following cells:

- unstained cells;
- stained cells, comprising of:
  - unconjugated primary antibody (i.e., anti–c-Kit sAB);
  - labeled secondary antibody conjugated to a fluorochrome, e.g., fluorescein isothiocyanate (FITC) with operational wavelength range of 494–520 nm, or phycoerythrin (PE), an accessory photosynthetic pigment found in red algae, with operational wavelength of 496–578 nm.

It should be noted that, in this case, the antibody staining procedure facilitates the estimation of the cell population of interest using a conjugated fluorochrome-labeled secondary antibody (as such, the unconjugated primary antibody is not fluorochrome labeled).

For this cell binding test, the experimental setup was as follows:

- murine CML cell line (CJ cells) was stained with primary antibody (i.e., anti–c-Kit sAB) and secondary antibody (conjugated to PE);
- human CML cell lines (KU-812 cells and JURL-MK1 cells) were stained with primary antibody and secondary antibody (conjugated to FITC).

In the following graphs showing the intensity output, as delivered by the analytical software FlowJo Version 8.8.7, a right shift in immunofluorescence intensity passing a *reference* cell population corresponds to a desirable result. Figures 6.6, 6.7, 6.8 show the binding test results respectively for CJ, KU-812, and JURL-MK1 cell lines.

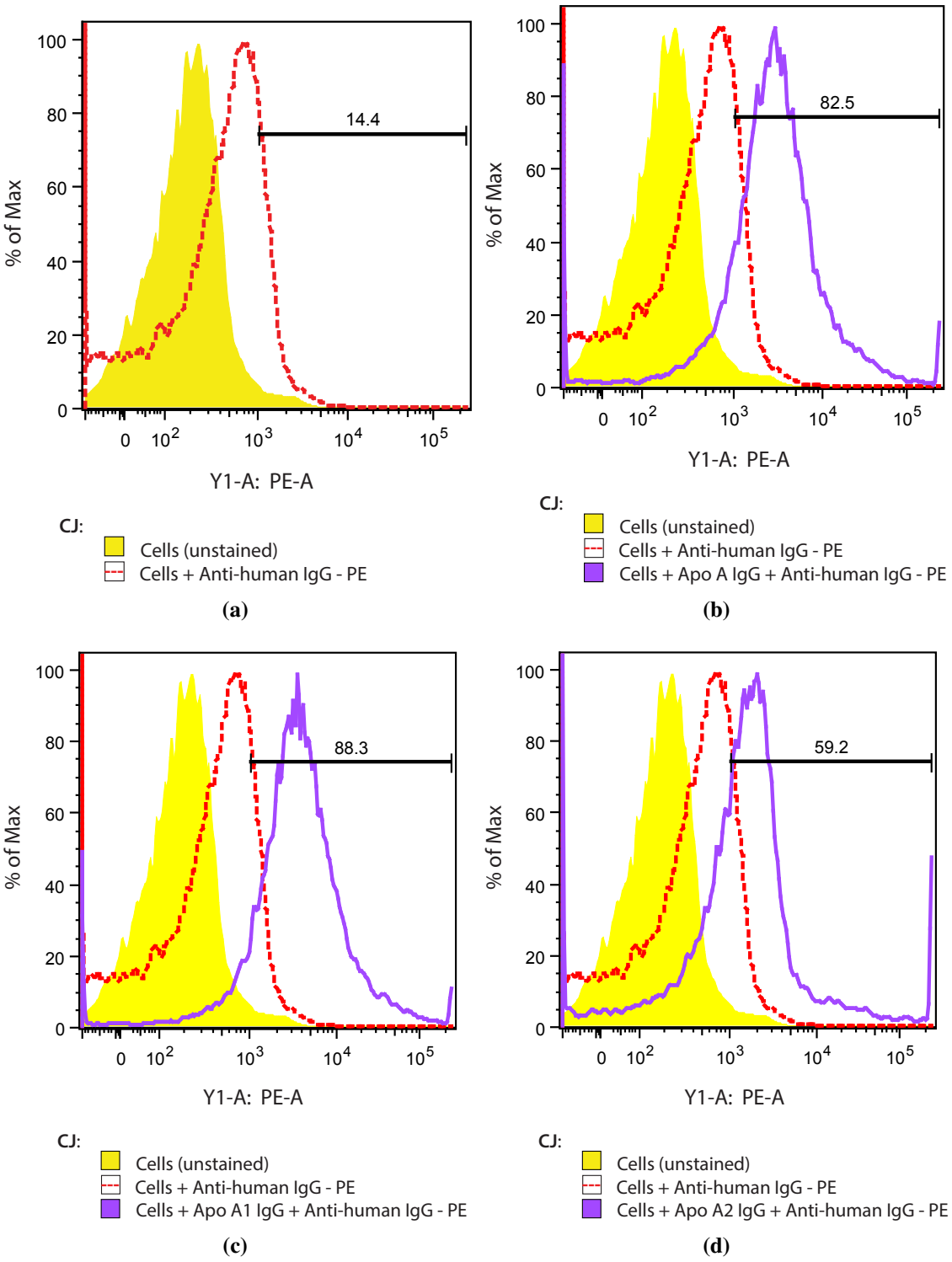

Figure 6.6: Cell Binding Test on CJ Cells for: (a) Anti-human IgG - PE (secondary antibody); (b) Apo A IgG; (c) Apo A1 IgG; and (d) Apo A2 IgG. A yellow shaded histogram represents a *negative* cell population; whereas a red dashed histogram corresponds to a *reference* cell population in the presence of conjugated antibody; and a purple solid histogram represents a *positive* cell population in the presence of primary antibody.

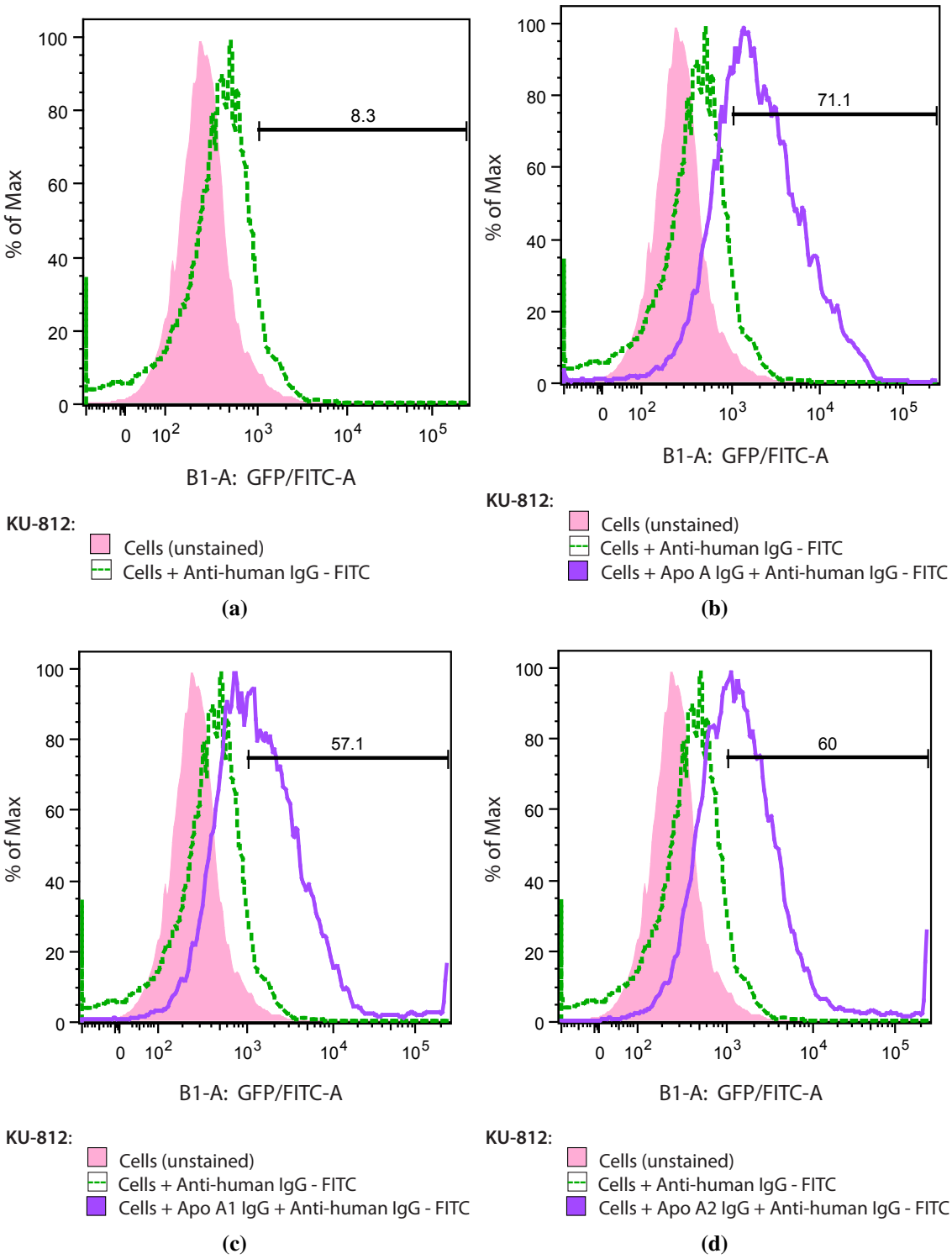

Figure 6.7: Cell Binding Test on KU-812 Cells for: (a) Anti-human IgG - FITC (secondary antibody); (b) Apo A IgG; (c) Apo A1 IgG; and (d) Apo A2 IgG. A pink shaded histogram represents a *negative* cell population; whereas a green dashed histogram corresponds to a *reference* cell population in the presence of conjugated antibody; and a purple solid histogram represents a *positive* cell population in the presence of primary antibody.

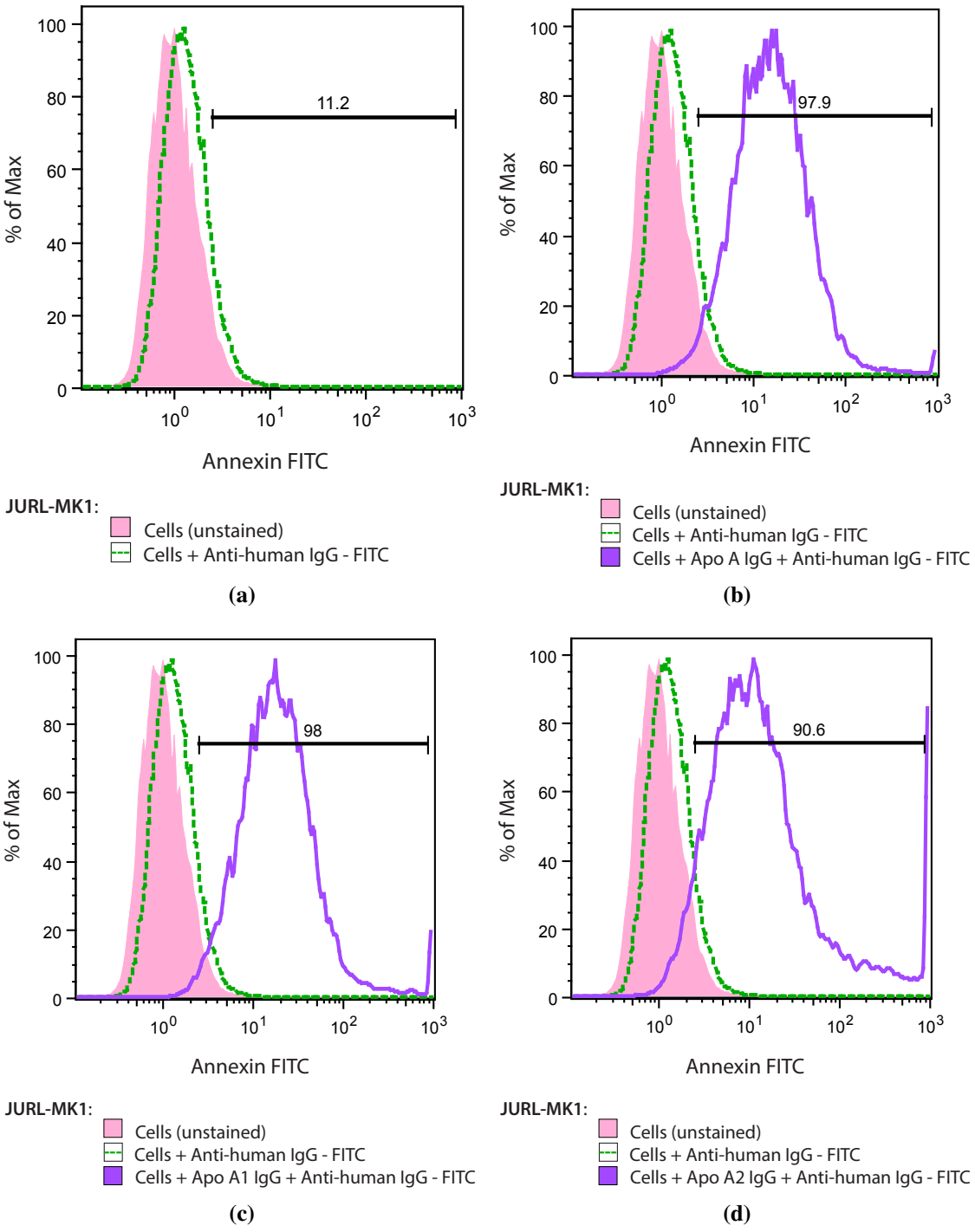

Figure 6.8: Cell Binding Test on JURL-MK1 Cells for: (a) Anti-human IgG - FITC (secondary antibody); (b) Apo A IgG; (c) Apo A1 IgG; and (d) Apo A2 IgG. A pink shaded histogram represents a *negative* cell population; whereas a green dashed histogram corresponds to a *reference* cell population in the presence of conjugated antibody; and a purple solid histogram represents a *positive* cell population in the presence of primary antibody.

6.2.2 Data Analysis and Discussion: A Majority of Anti–c-Kit sABs for Each Candidate Achieves Tight Binding to the Cell Surface

In all cases, the developed sABs successfully induced a right shift in immunofluorescence intensity. This implies that the majority of the c-Kit antibodies achieved tight binding for various CML cell lines, and as such should be good candidates for CML treatment from a cell binding perspective. Notably, the JURL-MK1 cell line exhibits the best cell binding data, with the highest shift values, compared to other CML cell lines tested. This means that the developed sABs bound well to receptor proteins (i.e., c-Kit molecules) on the cell surface of this particular cell line, thus achieving a strong binding interaction.

6.3 Specific Binding (SB) and Non-Specific Binding (NSB) Tests: Assessing the sAB Binding Activity, with Respect to the Target c-Kit Domains

While the previous cell binding test reveals insights about the quantity of sABs binding to the cell surface of various CML cell lines, it is unable to differentiate the different binding activities occurring on different cell surface types: surface with c-Kit molecules (i.e., specific case of interest) versus surface without c-Kit, but with other molecule types (i.e., non-specific cases not of interest, including other receptors, transporters, or proteins). This differentiation is important to assess the effectiveness of the sABs in specifically targeting cKit molecules. Therefore, the next procedure to be performed is a pair of tests: the non-specific binding (NSB) test, and specific binding (SB) test. Designed to quantify the binding activities of interest, the SB test involves measuring the number of binding events for sABs to cells with specific receptors of interest (i.e., c-Kit molecules) on their surface. By contrast, the NSB test involves measuring the number of binding events for sABs to cells without specific receptors of interest (i.e., no c-Kit molecules).

It should be noted that, since the underlying flow cytometry technique is not inherently suitable for distinguishing different binding types, the two tests are conducted separately, while keeping the same experimental parameters, except for the c-Kit presence in the former SB test, and absence in the latter NSB test. In other words, the goal of this procedure is to quantify binding events between sABs and different surface molecular targets presented in two different cell populations, which are configured with the same measurement settings (e.g., volume, cell concentration, and primary and

secondary antibody staining, etc.). For a successful treatment, it is clear that more binding activities should be observed for the sABs in the cell population with c-Kit molecules (i.e., SB case). This would mean that the specifically designed sABs are in fact behaving as expected: targeting specific c-Kit domains, resulting in higher binding events when c-Kit molecules are actually present on the cell surface.

Procedurally, to prepare two different cell populations, the pre-step uses a specific cell line originally derived from human embryonic kidney (HEK) cells, to facilitate controlling the presence or absence of c-Kit on the cell surface. In particular, the HEK 293F is a specific cell line amenable to the use of polyethylenimine (PEI) transfection with c-Kit plasmid DNA for SB test. This experiment is based on similar cell preparation and immunofluorescence staining as in the cell binding test, which means that a right shift in immunofluorescence intensity is also a desirable outcome.

6.3.1 Data for SB and NSB Tests with the HEK 293F Cell Line

As procedurally described in Section 4.3.3, the experimental setup was as follows:

- For SB, the HEK 293F cell line (transfected with c-Kit plasmid DNA) was stained with primary antibody (i.e., anti–c-Kit sAB) and secondary antibody (conjugated to FITC);
- For NSB, the HEK 293F cell line was also stained both primary and secondary antibodies.

First, for the gating system, Figure 6.9 shows unstained cells and stained cells with secondary antibodies conjugated to FITC. Then, Figures 6.10, 6.11, and 6.12 show the SB and NSB test results for the HEK 293F cell line with respectively Apo A, Apo A1, and Apo A2 IgG's. For NSB on the HEK 293F cells, the data show no significant right shift in immunofluorescence intensity. By contrast, for the SB on the HEK 293F cells with c-Kit molecules, the results indicate a significant right shift as expected. For this test, data were also processed using FlowJo Version 8.8.7 to generate suitable graphs for subsequent data analysis.

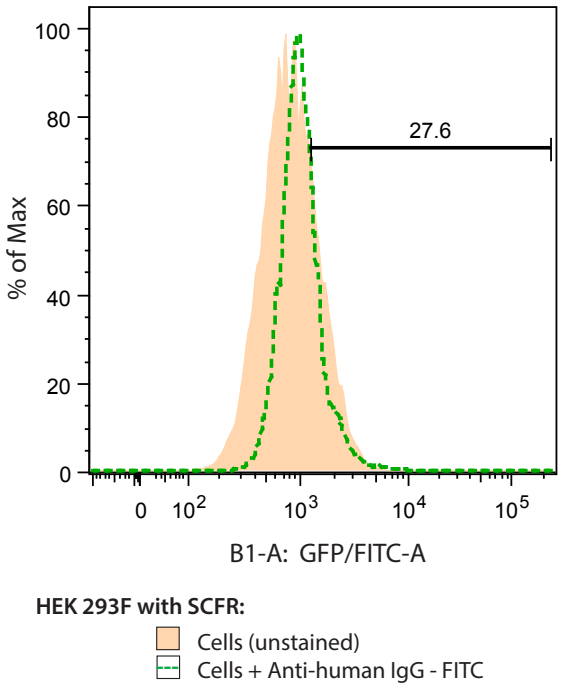

(a) SB – Cell Surface with c-Kit Molecules

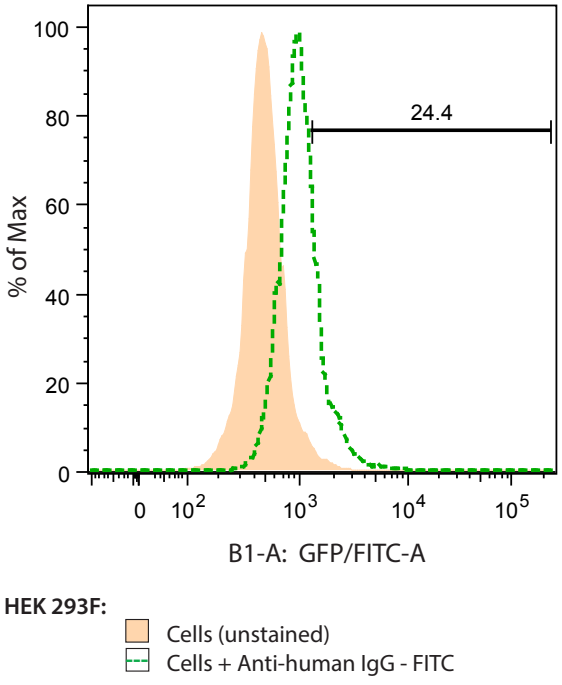

(b) NSB – Cell Surface without c-Kit Molecules

Figure 6.9: Cell Binding Tests for Secondary Antibody on the HEK 293F cells: (a) Specific Binding (SB) Case – binding activities on cells with the presence of c-Kit molecules; (b) Non-Specific binding (NSB) Case – binding activities on cells with the absence of c-Kit molecules. A peach shaded histogram represents a *negative* cell population; whereas a green dashed histogram corresponds to a *reference* cell population in the presence of conjugated antibody.

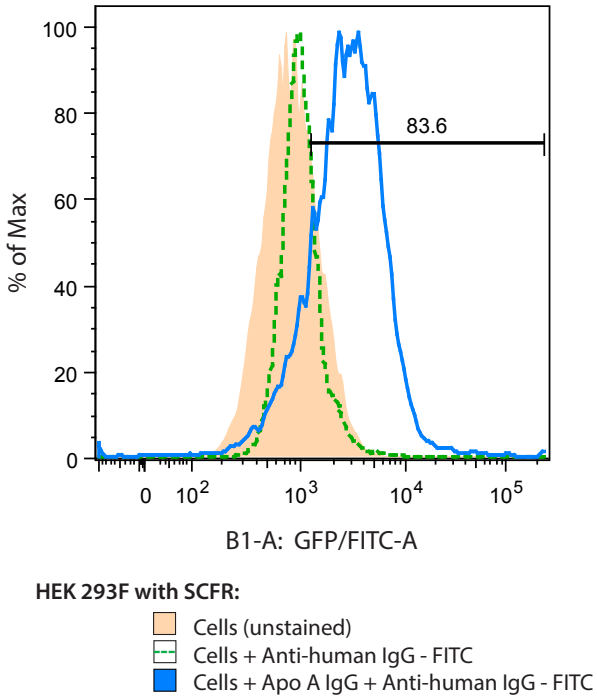

(a) SB – Cell Surface with c-Kit Molecules

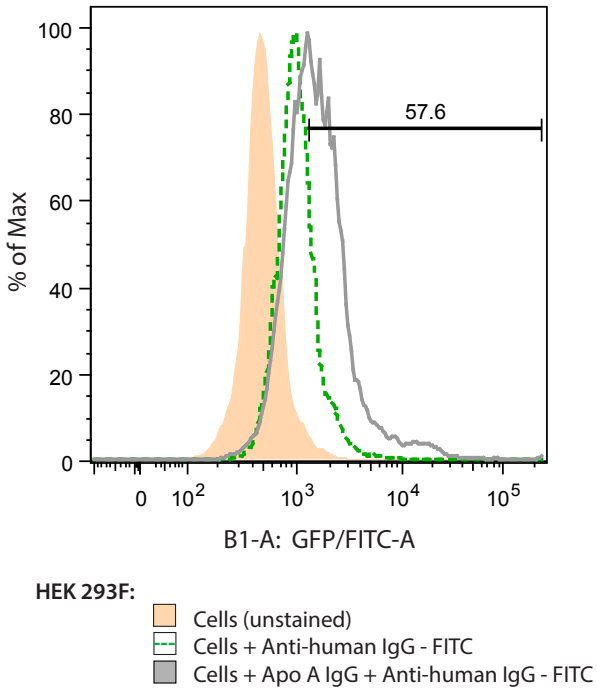

(b) NSB – Cell Surface without c-Kit Molecules

Figure 6.10: Cell Binding Tests for Apo A IgG on the HEK 293F Cells: (a) Specific Binding (SB) Case – binding activities on cells with the presence of c-Kit molecules; (b) Non-Specific binding (NSB) Case – binding activities on cells with the absence of c-Kit molecules. A peach shaded histogram represents a *negative* cell population; whereas a green dashed histogram corresponds to a *reference* cell population in the presence of conjugated antibody; and a blue or gray solid histogram represents a *positive* cell population in the presence of Apo A IgG.

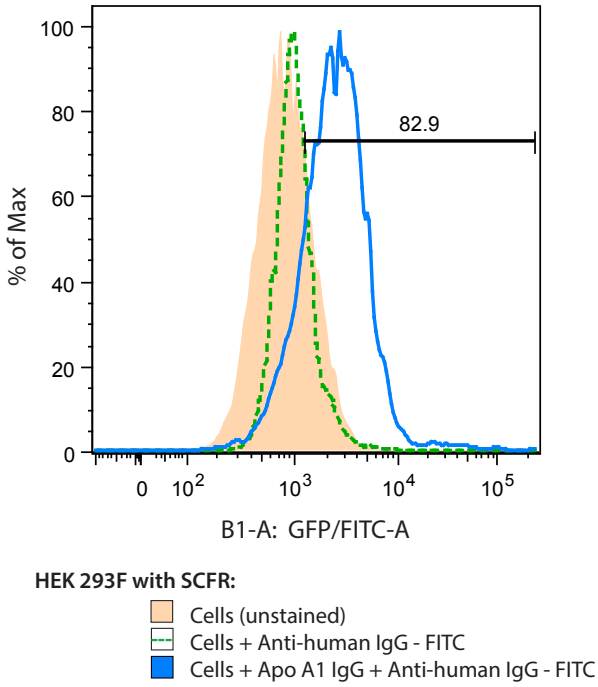

(a) SB – Cell Surface with c-Kit Molecules

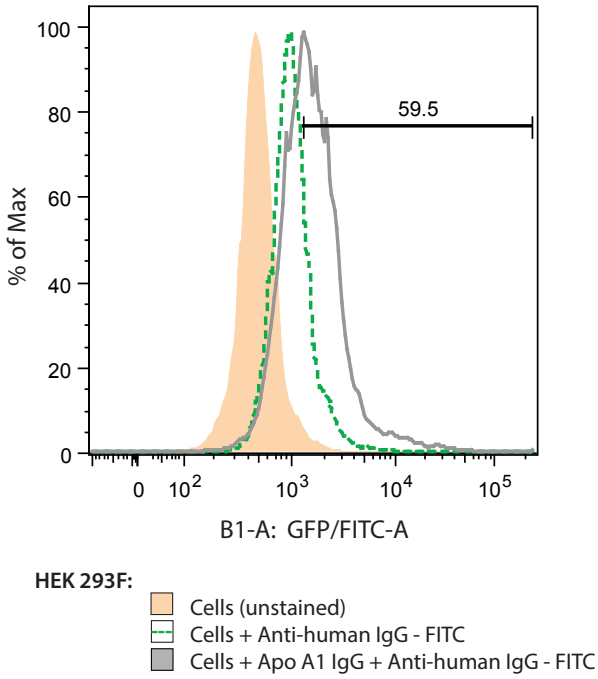

(b) NSB – Cell Surface without c-Kit Molecules

Figure 6.11: Cell Binding Tests for Apo A1 IgG on the HEK 293F Cells: (a) Specific Binding (SB) Case – binding activities on cells with the presence of c-Kit molecules; (b) Non-Specific binding (NSB) Case – binding activities on cells with the absence of c-Kit molecules. A peach shaded histogram represents a *negative* cell population; whereas a green dashed histogram corresponds to a *reference* cell population in the presence of conjugated antibody; and a blue or gray solid histogram represents a *positive* cell population in the presence of Apo A1 IgG.

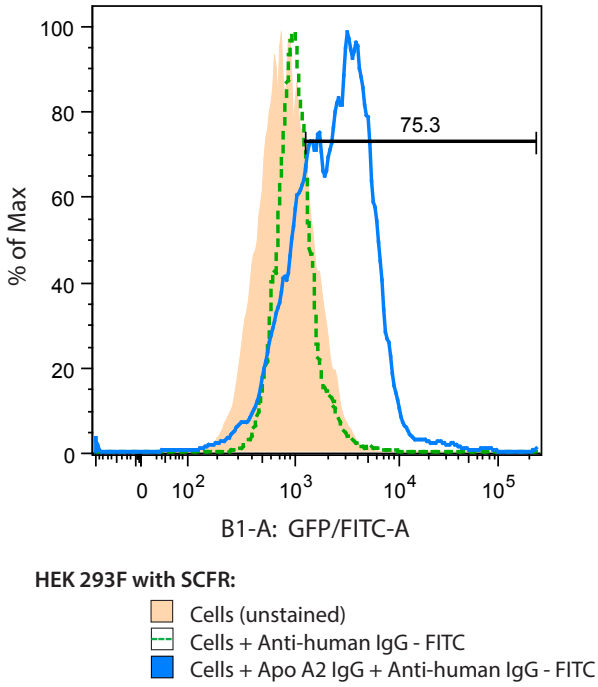

(a) SB – Cell Surface with c-Kit Molecules

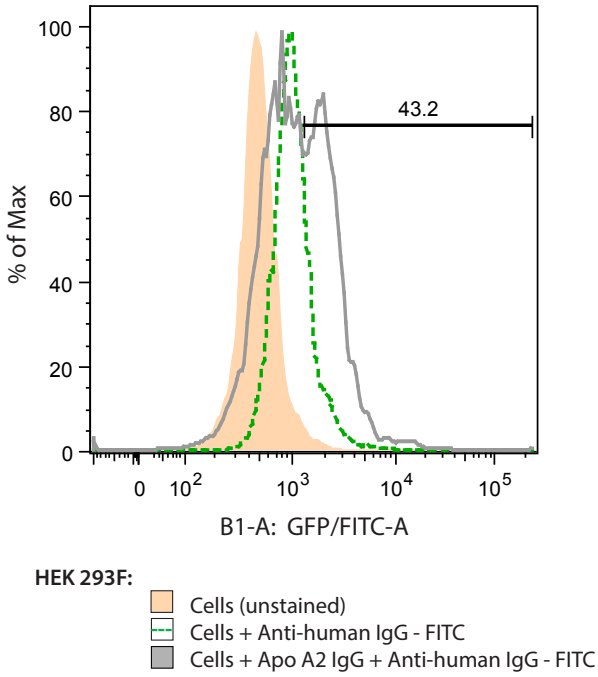

(b) NSB – Cell Surface without c-Kit Molecules

Figure 6.12: Cell Binding Tests for Apo A2 IgG on the HEK 293F Cells: (a) Specific Binding (SB) Case – binding activities on cells with the presence of c-Kit molecules; (b) Non-Specific binding (NSB) Case – binding activities on cells with the absence of c-Kit molecules. A peach shaded histogram represents a *negative* cell population; whereas a green dashed histogram corresponds to a *reference* cell population in the presence of conjugated antibody; and a blue or gray solid histogram represents a *positive* cell population in the presence of Apo A2 IgG.

6.3.2 Data Analysis and Discussion: The sABs Are Indeed Specifically Bound to c-Kit Domains

Given the obtained immunofluorescence data, it can be seen that:

- In the SB case, more significant binding activities of sABs and receptor proteins of interest were measured on the HEK 293F cells in the presence of c-Kit domains;
- In the NSB case, weak binding interactions of sABs and other cell surface proteins were observed on the HEK 293F cells in the absence of c-Kit domains.

With these NSB and SB tests, the flow system quantifies binding events of sABs to their targets in two separate cell populations. The key of this procedure is to confirm more significant binding activities for sABs to their specific targets in the SB case (with c-Kit molecules on cell surface), compared with those in the NSB case (without c-Kit molecules). As expected, the immunofluorescence histograms from the obtained data confirmed that more significant binding of sABs to cells with c-Kit molecules. And the higher SB activities consistently occurred with all three candidates of anti–c-Kit sABs. In other words, this result is indeed compatible with the desired requirements on binding specificity: the presence of c-Kit molecules on the HEK 293F cells should determine, or be correlated with, the binding activities of the candidate sABs. As such, the NSB test exhibits fewer binding activities compared to SB test, since by design the former scenario corresponds to cells devoid of c-Kit molecules. By contrast, in the latter SB test, with HEK 293F cells transfected with c-Kit plasmid DNA, there are more significant binding activities on the cell surface due to c-Kit presence. This finding quantitatively demonstrates that the specifically developed sABs were indeed able to bind c-Kit molecules on cell surface, thus conducive to high affinity and specificity, which are certainly crucial characteristics of effective and efficient cancer treatment. To this end, the next set of tests will focus on the treatment effects of the proposed combinations of drug and sABs.

6.4 Cell Viability Assay: Investigation of Growth Inhibition Using a Combinatorial Treatment

The tests conducted hitherto focus only on the binding criteria of the candidate sABs. Therefore, an investigation of cell behaviors in response to a combinatorial effect is assessed on various CML cell lines after the kinetic and cell binding tests. To this end, the next test to be performed is the cell viability assay, to confirm that a combination of sABs and drug treatments promotes more significant cell death compared to a single drug treatment alone. This test utilizes microscopic cell counting technique with trypan blue stain to investigate cell death and cell density. In this case, the test is applied on various combinations of sABs and drug treatments, for several CML cell lines. In other words, cell viability is statistically estimated as the number of viable cells divided by the total number of cells within selected grids of the hemacytometer, under a microscope. Trypan blue staining facilitates the visualization of cell morphology, thus enhancing the discrimination between viable and non-viable cells. Specifically, non-viable cells take up the trypan blue dye, whereas viable cells remain unstained due to intact cell membranes. Under a microscope, the staining process can thus visually separate non-viable cells (blue color) from viable cells (clear).

6.4.1 Data for Cell Viability Assay with CML Cell Lines

For this viability assay, the following scenarios were considered:

- [1] - Cells (untreated)
- [2] - Cells + stem cell factor (SCF)
- [3] - Cells + nilotinib (Nil)
- [4] - Cells + SCF + Nil
- [5] - Cells + antibody (Ab)
- [6] - Cells + Ab + SCF
- [7] - Cells + Ab + Nil
- [8] - Cells + Ab + SCF + Nil

Each of the above test scenarios was performed in triplicate, with all CML cell lines. The corresponding experimental setup is summarized in Table 4.5 (Section 4.3.4) for nilotinib, sAB (including Apo A, Apo A1, and Apo A2 IgG's), and SCF concentrations. Furthermore, cell counting was determined after 40–48 hours of incubation, in a humidified atmosphere containing 5% CO_2 at 37º C.

To facilitate subsequent interpretation and comparison, the graphs were grouped according to cell line as follows:

- CJ: results shown in Figures 6.13–6.15;
- KU-812: results shown in Figures 6.16–6.18;
- JURL-MK1: results shown in Figures 6.19–6.21.

In each group, the combination consists of nilotinib and one of the sABs (Apo A, Apo A1, or Apo A2 IgG's). The effect of SCF is also investigated, i.e., measurements were made both in the absence and in the presence of SCF conditions. Using one-tailed Student's t-test, p-values for cell viability were also evaluated to enable statistical significance assessment, specifically for comparative pairs of a single drug application versus a combination of treatments, with and without SCF conditions.

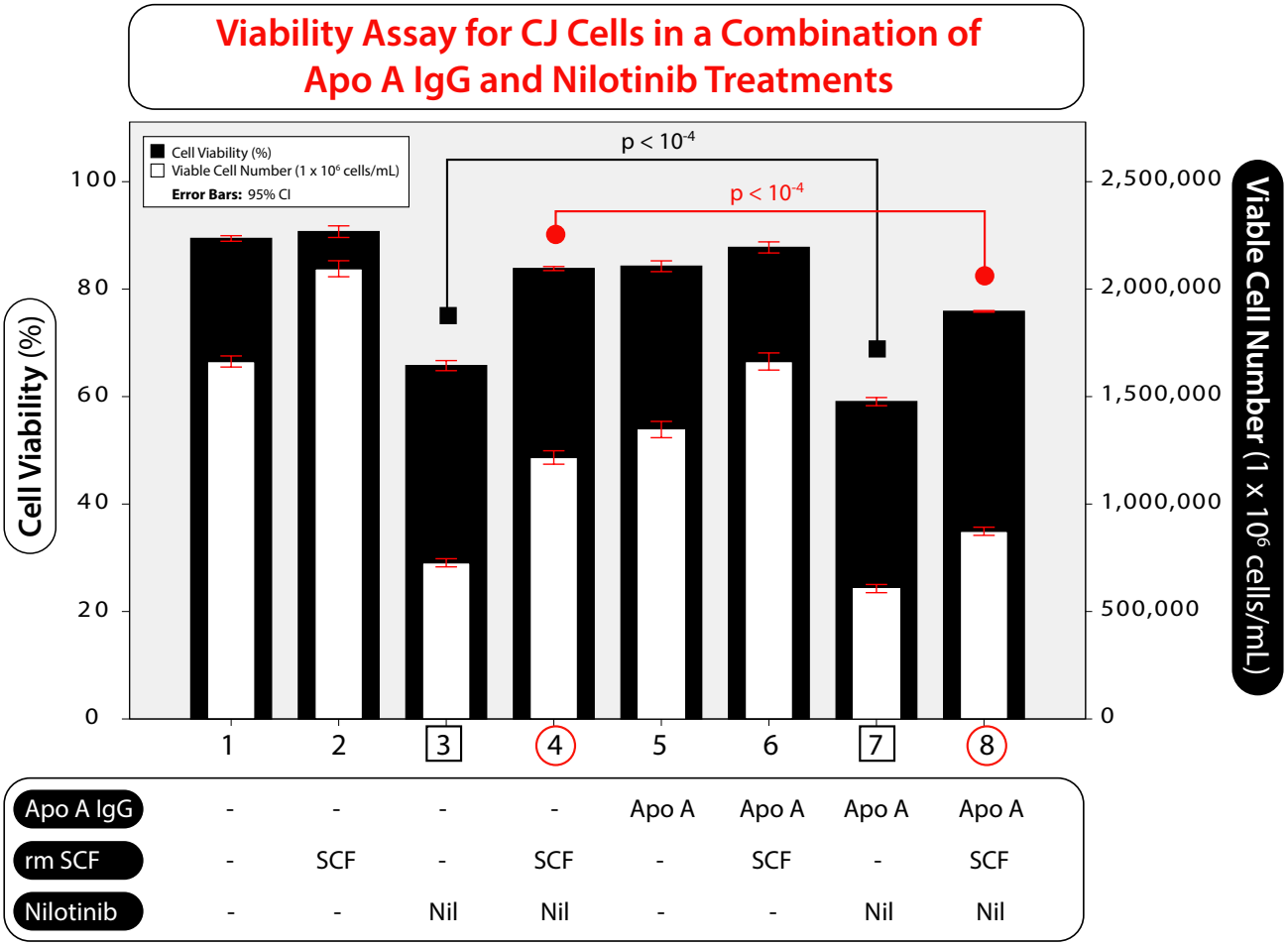

Figure 6.13: Viability Assay for CJ Cells in a Combination of Apo A IgG and Nilotinib Treatments. The combinatorial treatment consists of 3 μg/mL Apo A IgG and 50 nM nilotinib (Nil), applied with 200 ng/mL recombinant mouse stem cell factor (rm SCF). Cells were cultured in RPMI 1640 medium supplemented with 20% v/v FBS, and maintained in a humidified incubator containing 5% CO_2 at 37° C for 40 hours before the assay. In the graph, black shaded bars represent the cell viability (%), whereas white shaded bars denote the viable cell number (1 x 10^6 cells/mL). P-values for cell viability were calculated in the test pair labeled 3 and 7, and pair 4 and 8 to compare a combinatorial treatment versus one drug solution. In the treatment annotation table below the graph, a dash (-) stands for the absence of the corresponding treatment factor. For example, the first column with 3 dashes corresponds to a null condition, i.e., without an antibody, SCF, or drug.

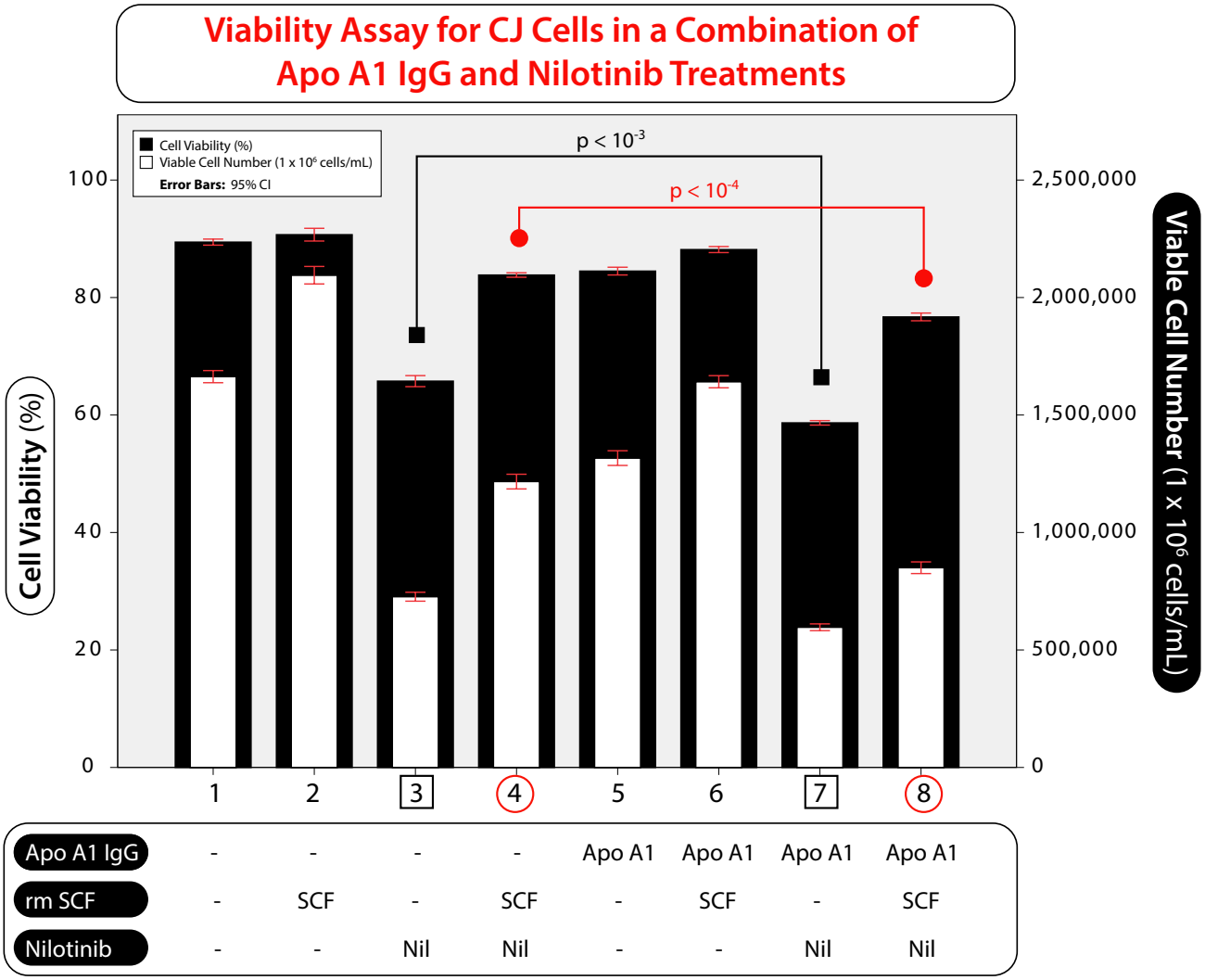

Figure 6.14: Viability Assay for CJ Cells in a Combination of Apo A1 IgG and Nilotinib Treatments. The combinatorial treatment consists of 3 μg/mL Apo A1 IgG and 50 nM nilotinib (Nil), applied with 200 ng/mL recombinant mouse stem cell factor (rm SCF). Cells were cultured in RPMI 1640 medium supplemented with 20% v/v FBS, and maintained in a humidified incubator containing 5% CO_2 at 37° C for 40 hours before the assay. In the graph, black shaded bars represent the cell viability (%), whereas white shaded bars denote the viable cell number (1 x 10^6 cells/mL). P-values for cell viability were calculated in the test pair labeled 3 and 7, and pair 4 and 8 to compare a combinatorial treatment versus one drug solution. In the treatment annotation table below the graph, a dash (-) stands for the absence of the corresponding treatment factor.

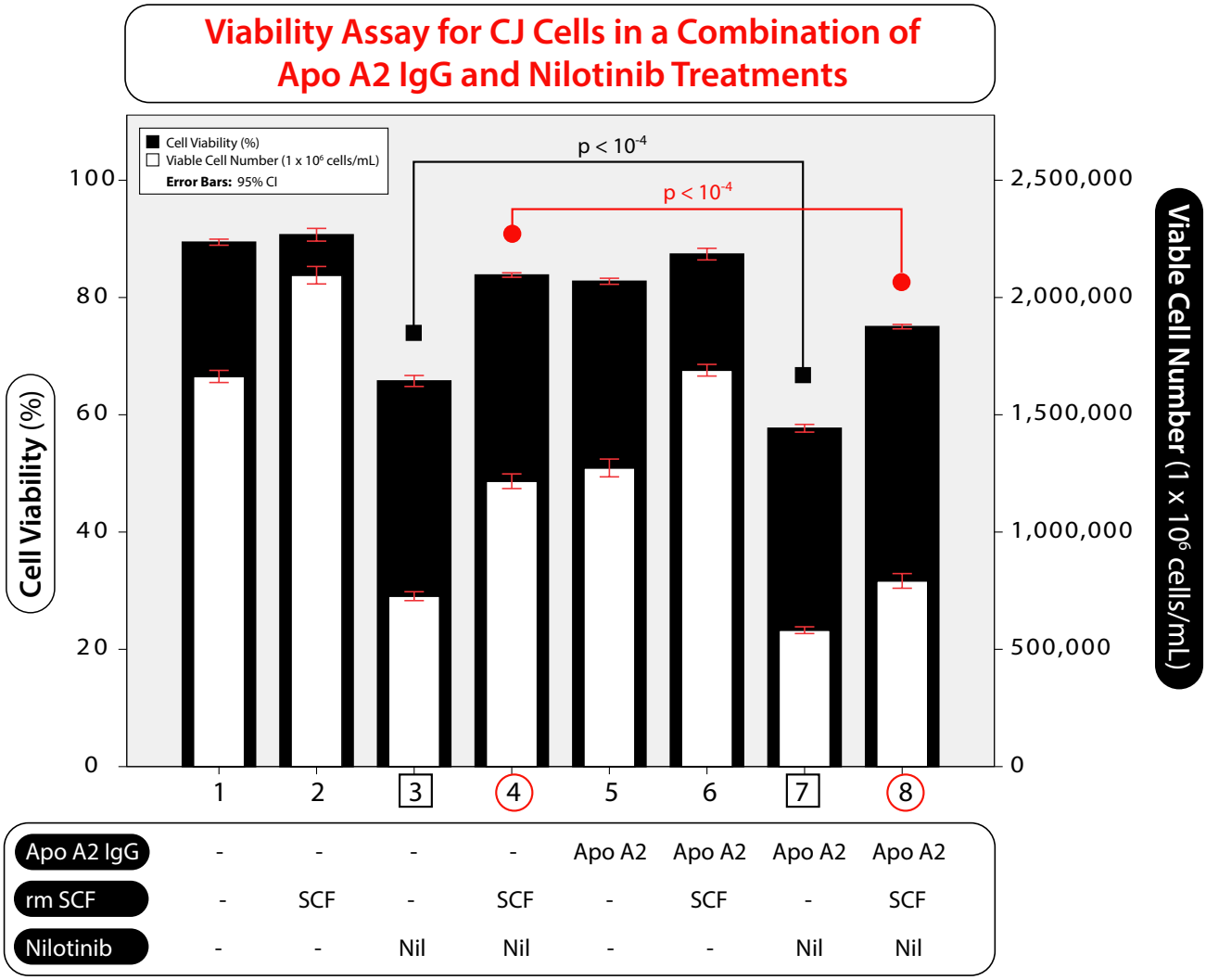

Figure 6.15: Viability Assay for CJ Cells in a Combination of Apo A2 IgG and Nilotinib Treatments. The combinatorial treatment consists of 3 μg/mL Apo A2 IgG and 50 nM nilotinib (Nil), applied with 200 ng/mL recombinant mouse stem cell factor (rm SCF). Cells were cultured in RPMI 1640 medium supplemented with 20% v/v FBS, and maintained in a humidified incubator containing 5% CO_2 at 37° C for 40 hours before the assay. In the graph, black shaded bars represent the cell viability (%), whereas white shaded bars denote the viable cell number (1 x 10^6 cells/mL). P-values for cell viability were calculated in the test pair labeled 3 and 7, and pair 4 and 8 to compare a combinatorial treatment versus one drug solution. In the treatment annotation table below the graph, a dash (-) stands for the absence of the corresponding treatment factor.

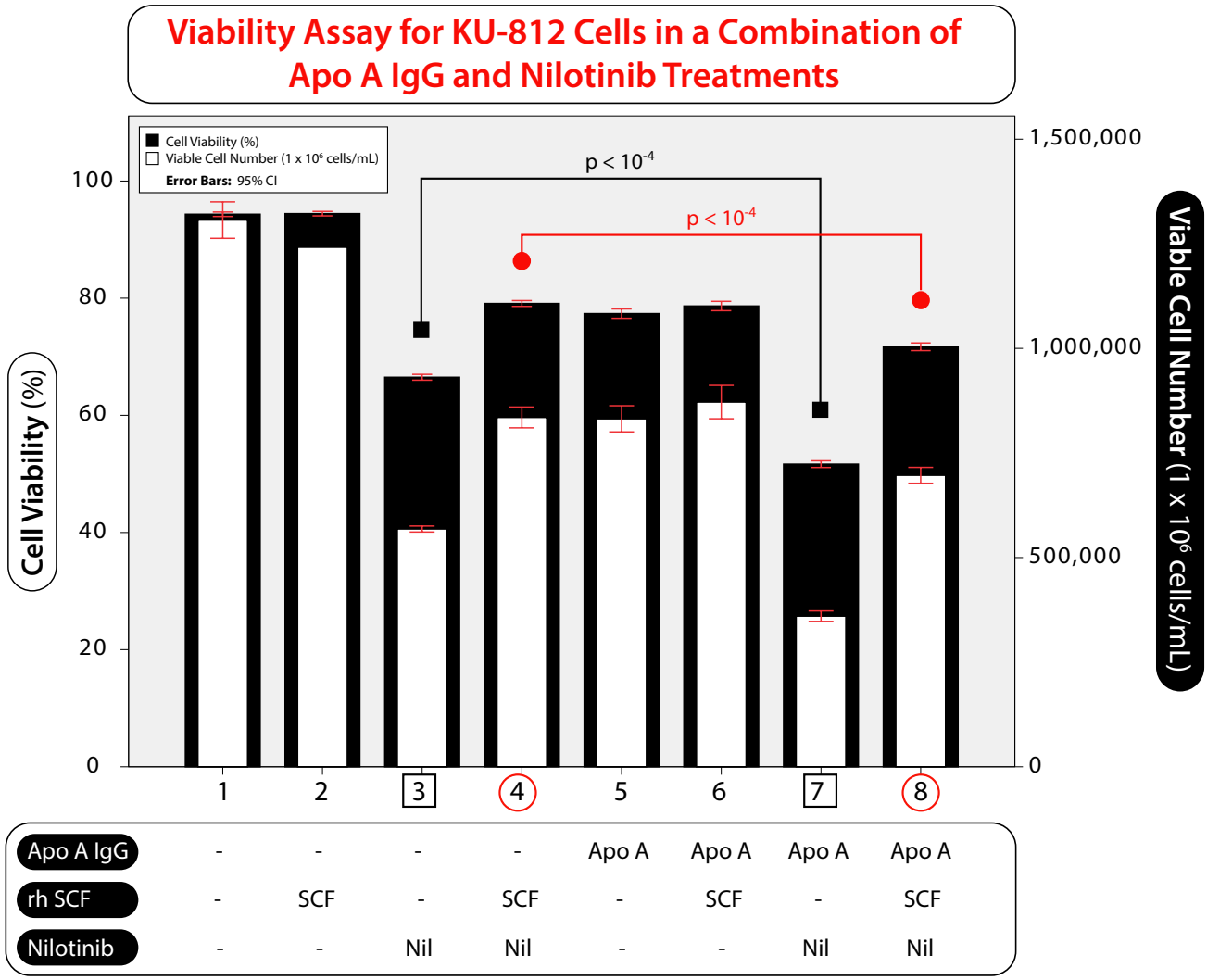

Figure 6.16: Viability Assay for KU-812 Cells in a Combination of Apo A IgG and Nilotinib Treatments. The combinatorial treatment consists of 3 μg/mL Apo A IgG and 10 nM nilotinib (Nil), applied with 200 ng/mL recombinant human stem cell factor (rh SCF). Cells were cultured in RPMI 1640 medium supplemented with 10% v/v FBS and 1% v/v penicillin-streptomycin solution, and maintained in a humidified incubator containing 5% CO_2 at 37° C for 48 hours before the assay. In the graph, black shaded bars represent the cell viability (%), whereas white shaded bars denote the viable cell number (1 x 10^6 cells/mL). P-values for cell viability were calculated in the test pair labeled 3 and 7, and pair 4 and 8 to compare a combinatorial treatment versus one drug solution. In the treatment annotation table below the graph, a dash (-) stands for the absence of the corresponding treatment factor. For example, the first column with 3 dashes corresponds to a null condition, i.e., without an antibody, SCF, or drug.

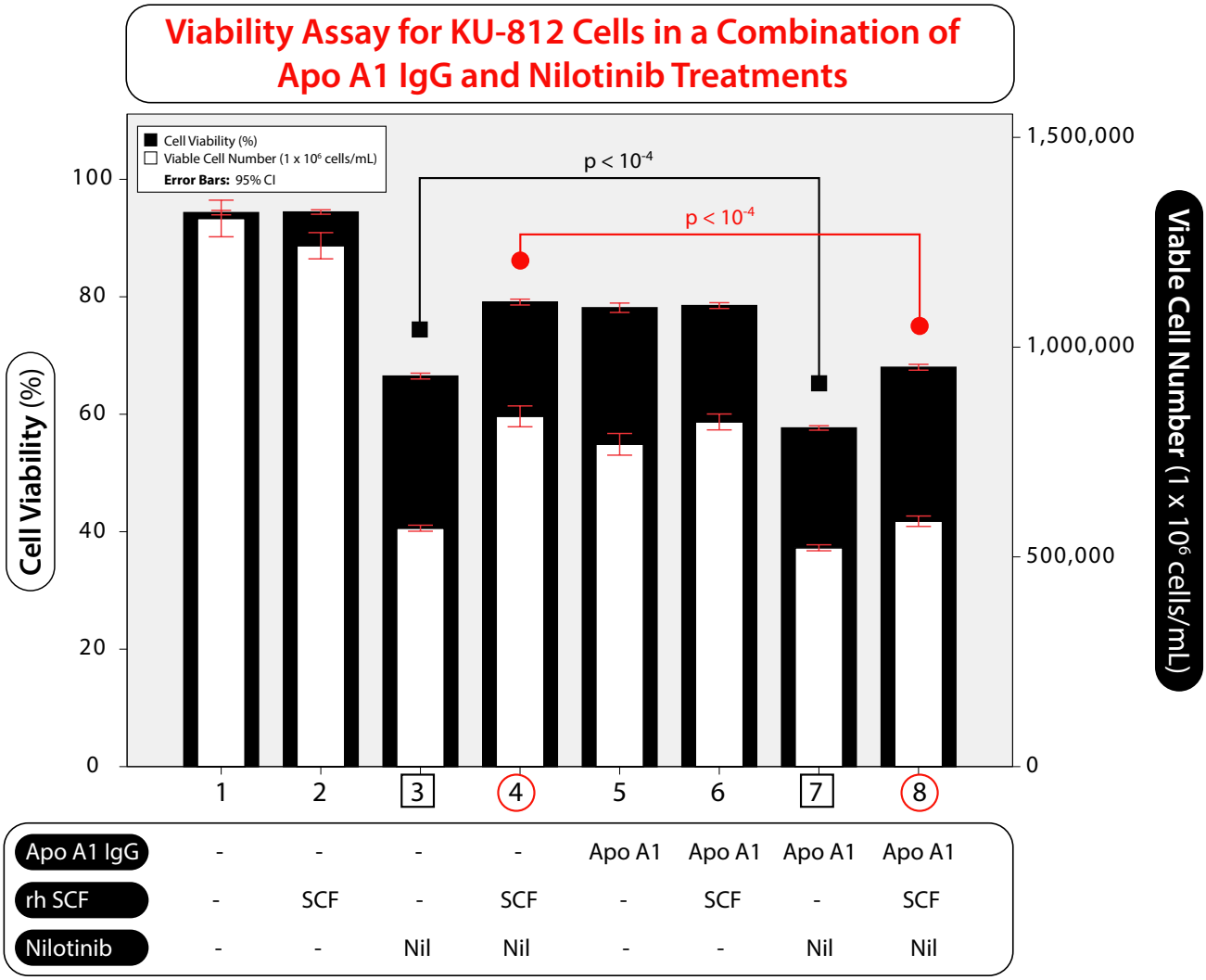

Figure 6.17: Viability Assay for KU-812 Cells in a Combination of Apo A1 IgG and Nilotinib Treatments. The combinatorial treatment consists of 3 μg/mL Apo A1 IgG and 10 nM nilotinib (Nil), applied with 200 ng/mL recombinant human stem cell factor (rh SCF). Cells were cultured in RPMI 1640 medium supplemented with 10% v/v FBS and 1% v/v penicillin-streptomycin solution, and maintained in a humidified incubator containing 5% CO_2 at 37° C for 48 hours before the assay. In the graph, black shaded bars represent the cell viability (%), whereas white shaded bars denote the viable cell number (1 x 10^6 cells/mL). P-values for cell viability were calculated in the test pair labeled 3 and 7, and pair 4 and 8 to compare a combinatorial treatment versus one drug solution. In the treatment annotation table below the graph, a dash (-) stands for the absence of the corresponding treatment factor.

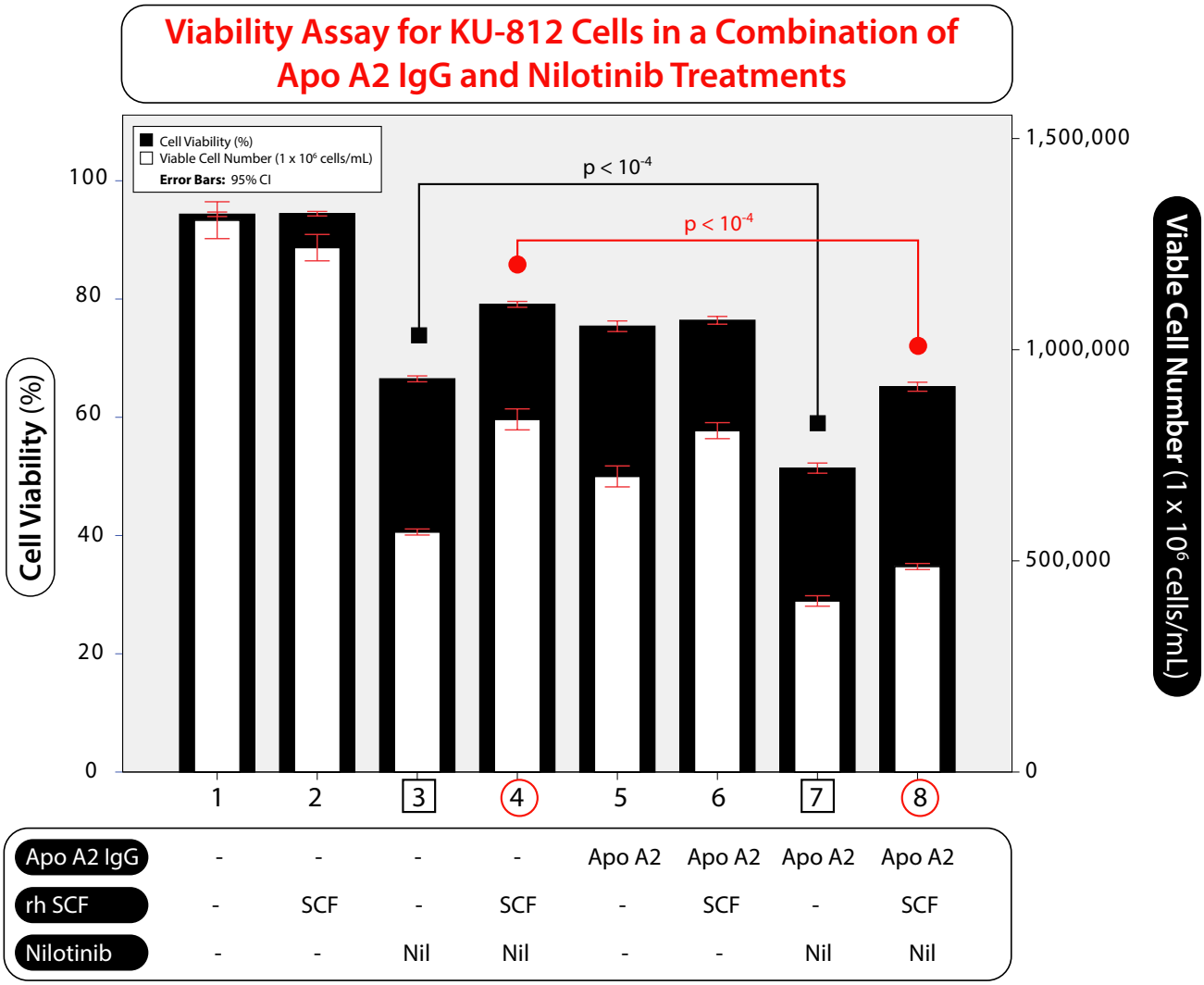

Figure 6.18: Viability Assay for KU-812 Cells in a Combination of Apo A2 IgG and Nilotinib Treatments. The combinatorial treatment consists of 3 μg/mL Apo A2 IgG and 10 nM nilotinib (Nil), applied with 200 ng/mL recombinant human stem cell factor (rh SCF). Cells were cultured in RPMI 1640 medium supplemented with 10% v/v FBS and 1% v/v penicillin-streptomycin solution, and maintained in a humidified incubator containing 5% CO_2 at 37° C for 48 hours before the assay. In the graph, black shaded bars represent the cell viability (%), whereas white shaded bars denote the viable cell number (1 x 10^6 cells/mL). P-values for cell viability were calculated in the test pair labeled 3 and 7, and pair 4 and 8 to compare a combinatorial treatment versus one drug solution. In the treatment annotation table below the graph, a dash (-) stands for the absence of the corresponding treatment factor.

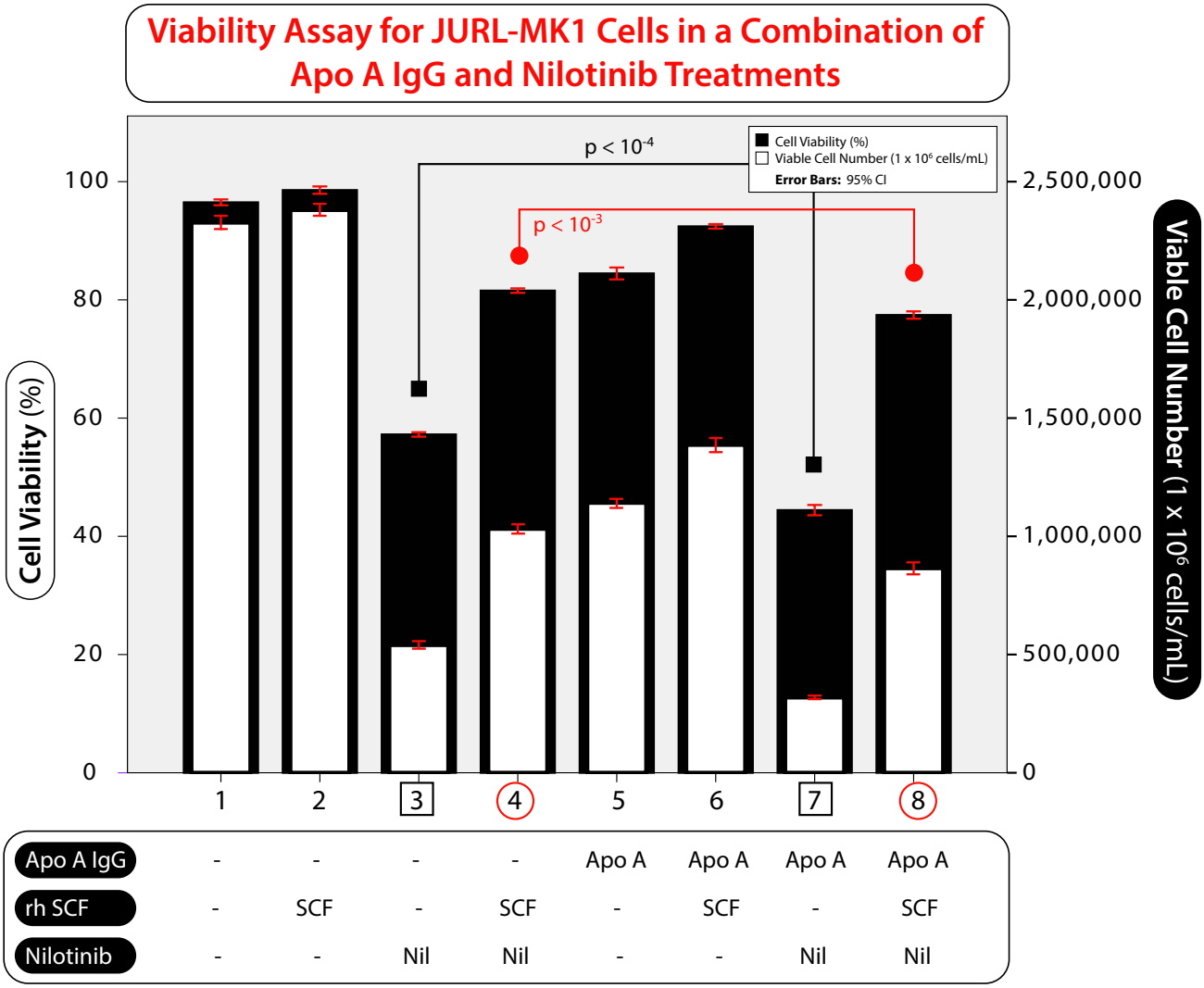

Figure 6.19: Viability Assay for JURL-MK1 Cells in a Combination of Apo A IgG and Nilotinib Treatments. The combinatorial treatment consists of 3 μg/mL Apo A IgG and 30 nM nilotinib (Nil), applied with 200 ng/mL recombinant human stem cell factor (rh SCF). Cells were cultured in RPMI 1640 medium supplemented with 10% v/v FBS and 1% v/v penicillin-streptomycin solution, and maintained in a humidified incubator containing 5% CO_2 at 37° C for 48 hours before the assay. In the graph, black shaded bars represent the cell viability (%), whereas white shaded bars denote the viable cell number (1 x 10^6 cells/mL). P-values for cell viability were calculated in the test pair labeled 3 and 7, and pair 4 and 8 to compare a combinatorial treatment versus one drug solution. In the treatment annotation table below the graph, a dash (-) stands for the absence of the corresponding treatment factor. For example, the first column with 3 dashes corresponds to a null condition, i.e., without an antibody, SCF, or drug.

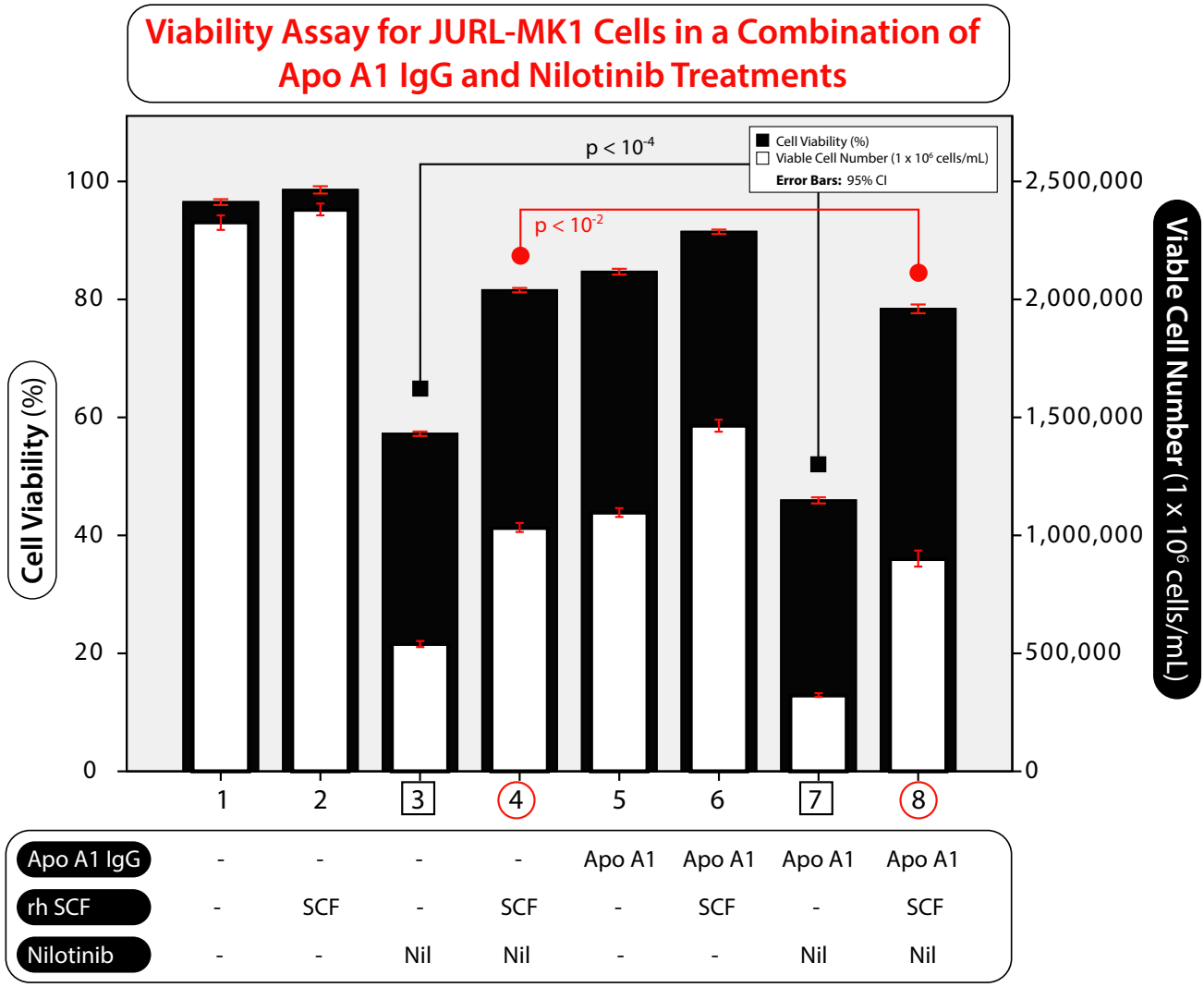

Figure 6.20: Viability Assay for JURL-MK1 Cells in a Combination of Apo A1 IgG and Nilotinib Treatments. The combinatorial treatment consists of 3 μg/mL Apo A1 IgG and 30 nM nilotinib (Nil), applied with 200 ng/mL recombinant human stem cell factor (rh SCF). Cells were cultured in RPMI 1640 medium supplemented with 10% v/v FBS and 1% v/v penicillin-streptomycin solution, and maintained in a humidified incubator containing 5% CO_2 at 37° C for 48 hours before the assay. In the graph, black shaded bars represent the cell viability (%), whereas white shaded bars denote the viable cell number (1 x 10^6 cells/mL). P-values for cell viability were calculated in the test pair labeled 3 and 7, and pair 4 and 8 to compare a combinatorial treatment versus one drug solution. In the treatment annotation table below the graph, a dash (-) stands for the absence of the corresponding treatment factor.

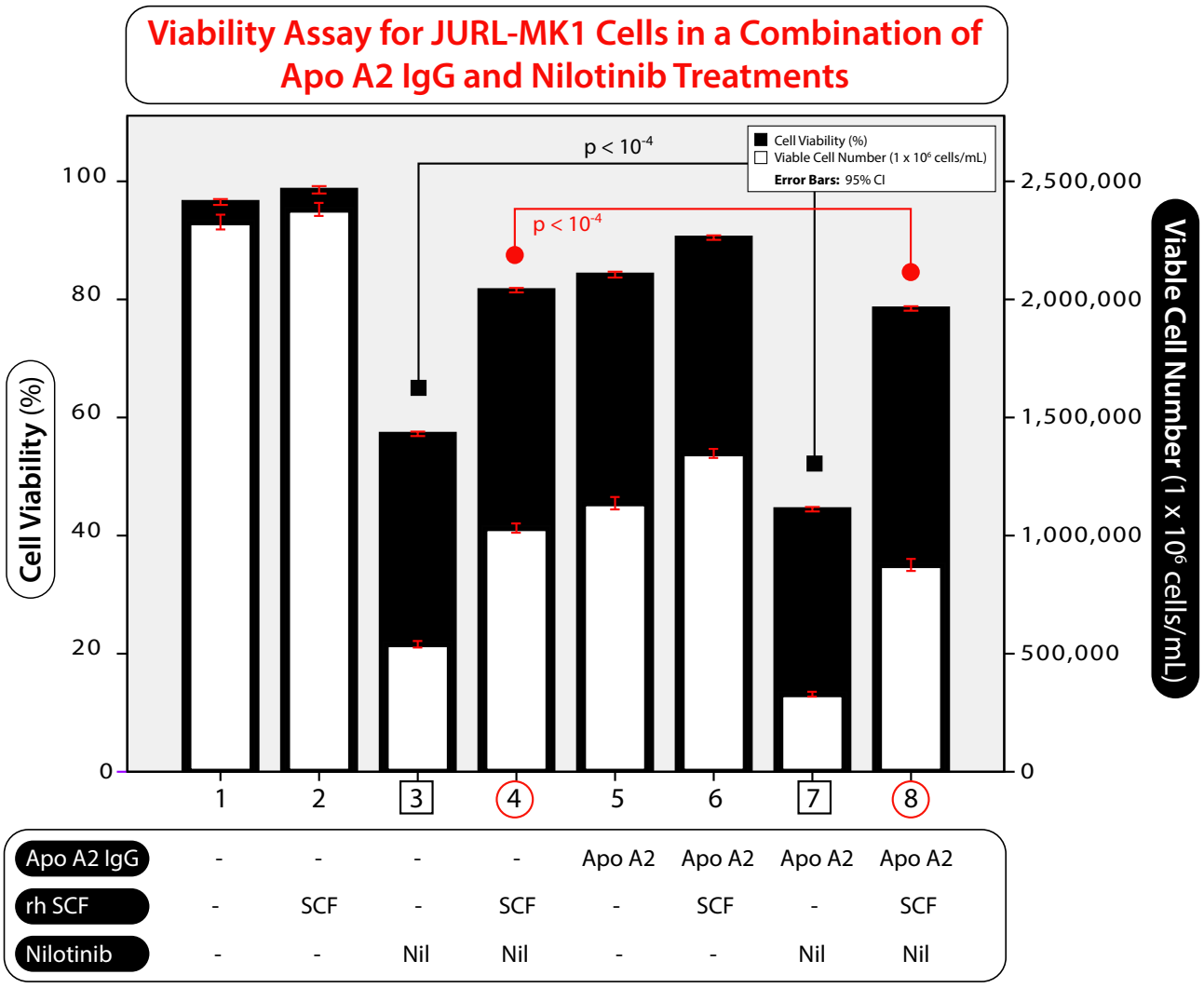

Figure 6.21: Viability Assay for JURL-MK1 Cells in a Combination of Apo A2 IgG and Nilotinib Treatments. The combinatorial treatment consists of 3 μg/mL Apo A2 IgG and 30 nM nilotinib (Nil), applied with 200 ng/mL recombinant human stem cell factor (rh SCF). Cells were cultured in RPMI 1640 medium supplemented with 10% v/v FBS and 1% v/v penicillin-streptomycin solution, and maintained in a humidified incubator containing 5% CO_2 at 37° C for 48 hours before the assay. In the graph, black shaded bars represent the cell viability (%), whereas white shaded bars denote the viable cell number (1 x 10^6 cells/mL). P-values for cell viability were calculated in the test pair labeled 3 and 7, and pair 4 and 8 to compare a combinatorial treatment versus one drug solution. In the treatment annotation table below the graph, a dash (-) stands for the absence of the corresponding treatment factor.

6.4.2 Data Analysis and Discussion: By Successfully Inhibiting the c-Kit Pathway, the sABs Induced Increased Cell Deaths

In all cases with the presence of SCF, both cell viability and cell number increased compared to those respective values in the absence of SCF condition. SCF is a cytokine that provides a protective effect occurred through the SCF signaling on the BCR-ABL and c-Kit expressing cells. This means the presence of SCF condition is able to compensate for the BCR-ABL inhibition in CML cells. In other words, the environmental presentation of SCF supports the survival of CML cells by partially rescuing them from the nilotinib activity. Hence, by reversing a protective effect from the SCF condition, a combination of sABs and nilotinib promotes more cell death by simultaneously targeting both c-Kit and BCR-ABL pathways. As such, it is vital to block the SCF-mediated innate resistance, in order to develop an effective strategy for improved CML treatment, which is one of the proposed signal-pathway approaches in this thesis.

Indeed, for cases with SCF condition, it is still possible to induce cell death with an appropriately designed combination of drug and sABs, which specifically target the c-Kit pathway. In fact, Figure 6.18 demonstrates this phenomenon, where even with an addition of SCF, a suitable combination of sABs and nilotinib treatments significantly reduced cell viability and cell number. In other words, the obtained data suggest that a specifically designed combination of sABs and nilotinib treatments may act in synergy to promote more significant cell death compared to a single drug application alone.

It should be noted that, to ensure repeatability and consistency of data, a triplicate setup was performed. The corresponding error bars are statistically small in size, and do not overlap between associated pairs of test scenarios. In addition, for cell viability assay with the developed sABs, the data indicate that KU-812 was the most compatible cell line, with the lowest cell viability and cell number values, consistently across all c-Kit antibodies.

In brief, cell viability assay on various CML cell lines showed that SCF treatment reduced the activity of nilotinib drug, but this drug activity could be restored by co-treating cells with c-Kit antibodies.

6.5 Apoptosis Assay: Examination of Nilotinib Apoptotic Effect Using a Combinatorial Treatment

The cell viability assay performed in the previous section substantiates that the proposed combinatorial approach promotes cell death more significantly compared to a single drug application alone, but it is unable to specifically identify the effects of apoptosis, which is a biochemical process causing programmed cell death that is particularly relevant for this research. From a therapeutic perspective, the combinatorial treatment should be designed to induce apoptosis, in order to eliminate the cancer cells of interest. Therefore, to investigate the treatment effectiveness, an apoptosis assay should be performed. This assay measures the apoptotic effect of CML cells in response to a combinatorial treatment in two different cases, i.e., in the presence and absence of SCF. Then, by comparing the results from these two cases, it can be determined whether a majority of the cell deaths can indeed be ascribed to the applied combinatorial treatment.

In particular, since apoptosis causes death by inducing characteristic cellular changes, an appropriate assay may be designed to detect these effects. Such effects include: a) loss of plasma membrane asymmetry and attachment; b) cytoplasmic and nuclear condensation; and c) chromatin degradation. Importantly, the loss of membrane integrity occurs in the early stage of apoptosis. Therefore, the assay in this section is designed to target this loss of membrane in order to quantify the apoptotic effect [113, 114].

The apoptosis assay involves Annexin V staining and flow cytometric analysis of cells in order to detect this morphological change. Specifically, the phospholipid phosphatidylserine (PS), normally hidden in the inner layer of the plasma membrane, is translocated to the outer leaflet of the membrane, thereby exposing PS on the cellular surface. As such, Annexin V is used to bind to apoptotic cells with this exposed PS on the external cellular environment. This is feasible because this Annexin V is a 35-36 kDa Ca^{2+} dependent phospholipid-binding protein that has a high affinity for PS, which in turn makes it a sensitive probe to perform flow cytometric analysis.

In addition, it should be noted that Annexin V is conjugated to a fluorochrome such as FITC, PE, and allophycocyanin conjugate (APC) to distinguish cells in the early stage of apoptosis, and the stain is typically used in conjunction with a vital dye (e.g., sytox blue or propidium iodide (PI))

to identify dead and damaged cells in the late stage of apoptosis. As will be reported in the subsequent results, the relevant fluorochromes for this research are FITC and APC, for distinguishing cells in the early stage of apoptosis, used in conjunction with either sytox blue or PI as necessary, for identifying dead and damaged cells in the late stage of apoptosis.

6.5.1 Data for Apoptosis Assay with CML Cell Lines

The initial steps of this experiment are similar to those in the cell viability assay, consisting of appropriate preparation and incubation criteria as described in Section 4.3.5. Then, Annexin V staining was performed in accordance with the manufacturer's instructions to enable apoptosis analysis using flow cytometry, with each test scenario in triplicate for all CML cell lines. Once the flow cytometric results were obtained, FlowJo Version 8.8.7 was utilized to generate analytical data for the following graphs, presented according to cell line:

- CJ: results shown in Figures 6.22–6.24;
- KU-812: results shown in Figures 6.25–6.27;
- JURL-MK1: results shown in Figures 6.28–6.30.

As in the cell viability test in Section 6.4, each combination consists of a drug and an sAB co-agent, along with the presence or absence of SCF investigated. However, instead of the number of general cell deaths due to various causes, the flow cytometric measurements assess this death quantity specifically due to apoptosis in this case. For statistical validation, the one-tailed Student's t-test was used to specifically compare pairs of test scenarios consisting of a drug application alone versus a combinatorial therapy, with and without SCF conditions, thus generating corresponding p-values for statistical significance testing.

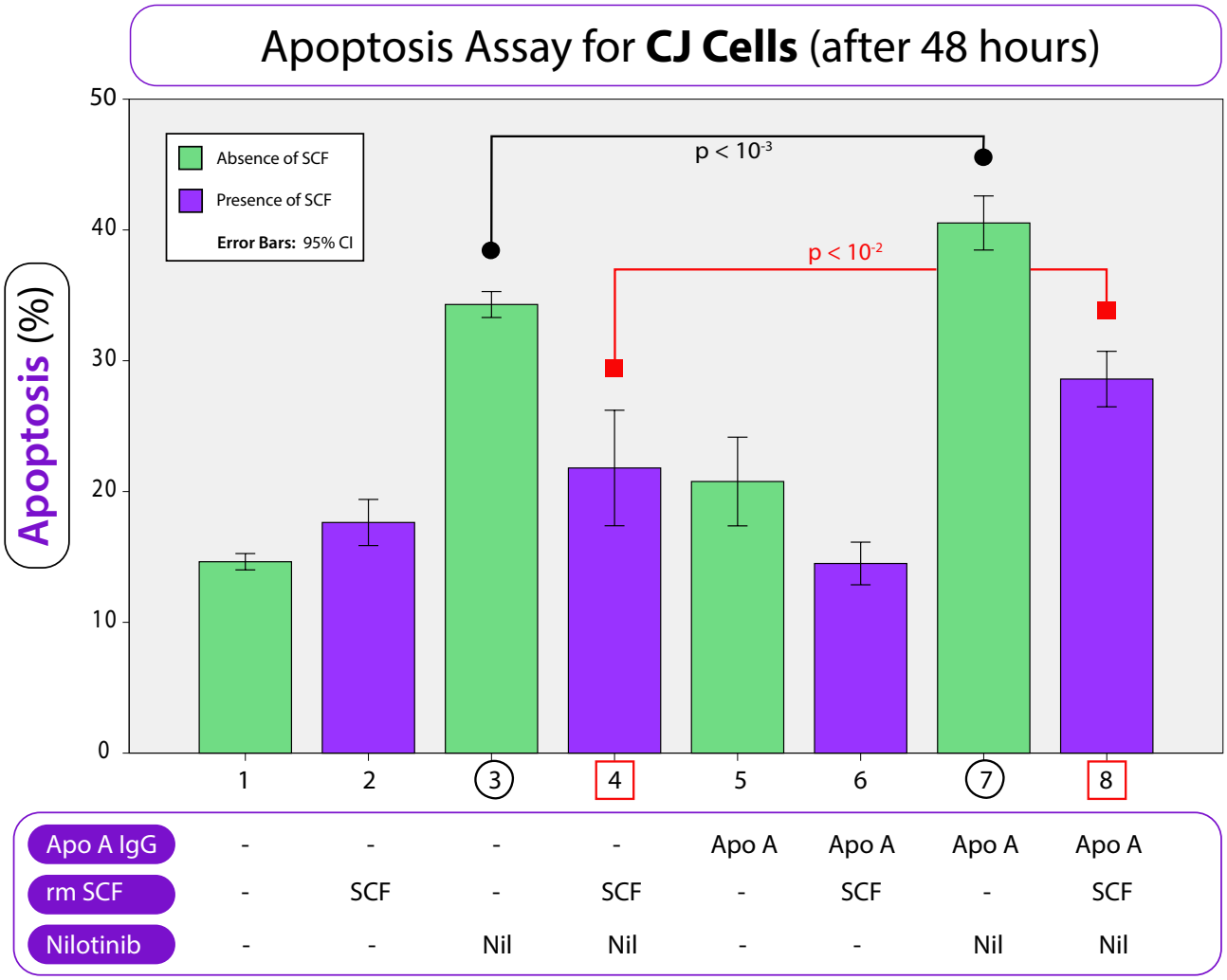

Figure 6.22: Apoptosis Assay for CJ Cells in a Combination of Apo A IgG and Nilotinib Treatments. The combinatorial treatment consists of 3 μg/mL Apo A IgG and 50 nM nilotinib (Nil), applied with 200 ng/mL recombinant mouse stem cell factor (rm SCF). Cells were cultured in RPMI 1640 medium supplemented with 20% v/v FBS, and maintained in a humidified incubator containing 5% CO_2 at 37° C for 40 hours before the assay. In the graph, green shaded bars are used to specify an absence of SCF, whereas purple shaded bars indicate a presence of SCF. P-values for apoptosis (%) were calculated in the test pair labeled 3 and 7, and pair 4 and 8 to compare a combinatorial treatment versus one drug solution. In the treatment annotation table below the graph, a dash (-) stands for the absence of the corresponding treatment factor. For example, the first column with 3 dashes corresponds to a null condition, i.e., without an antibody, SCF, or drug.

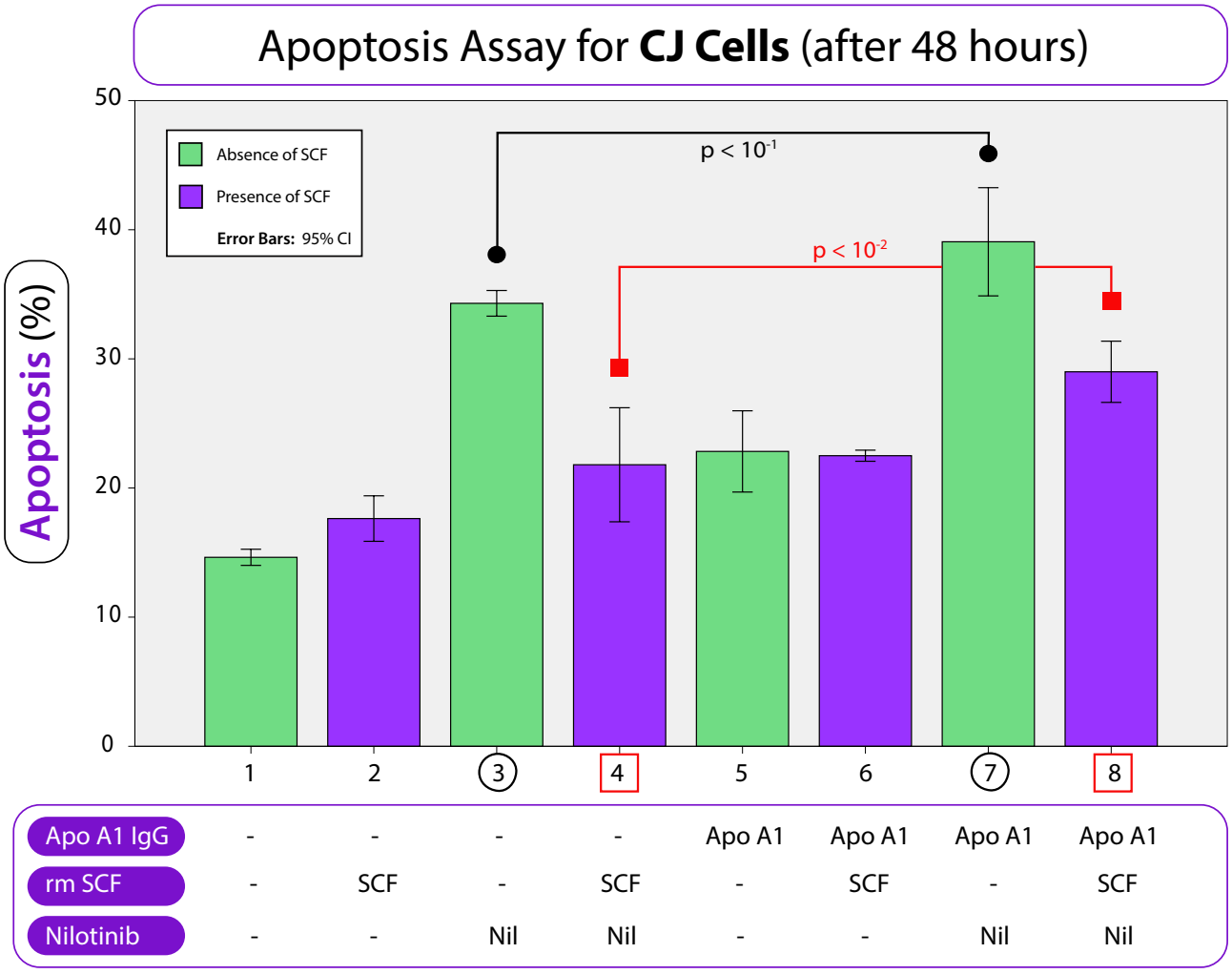

Figure 6.23: Apoptosis Assay for CJ Cells in a Combination of Apo A1 IgG and Nilotinib Treatments. The combinatorial treatment consists of 3 μg/mL Apo A1 IgG and 50 nM nilotinib (Nil), applied with 200 ng/mL recombinant mouse stem cell factor (rm SCF). Cells were cultured in RPMI 1640 medium supplemented with 20% v/v FBS, and maintained in a humidified incubator containing 5% CO_2 at 37° C for 40 hours before the assay. In the graph, green shaded bars are used to specify an absence of SCF, whereas purple shaded bars indicate a presence of SCF. P-values for apoptosis (%) were calculated in the test pair labeled 3 and 7, and pair 4 and 8 to compare a combinatorial treatment versus one drug solution. In the treatment annotation table below the graph, a dash (-) stands for the absence of the corresponding treatment factor.

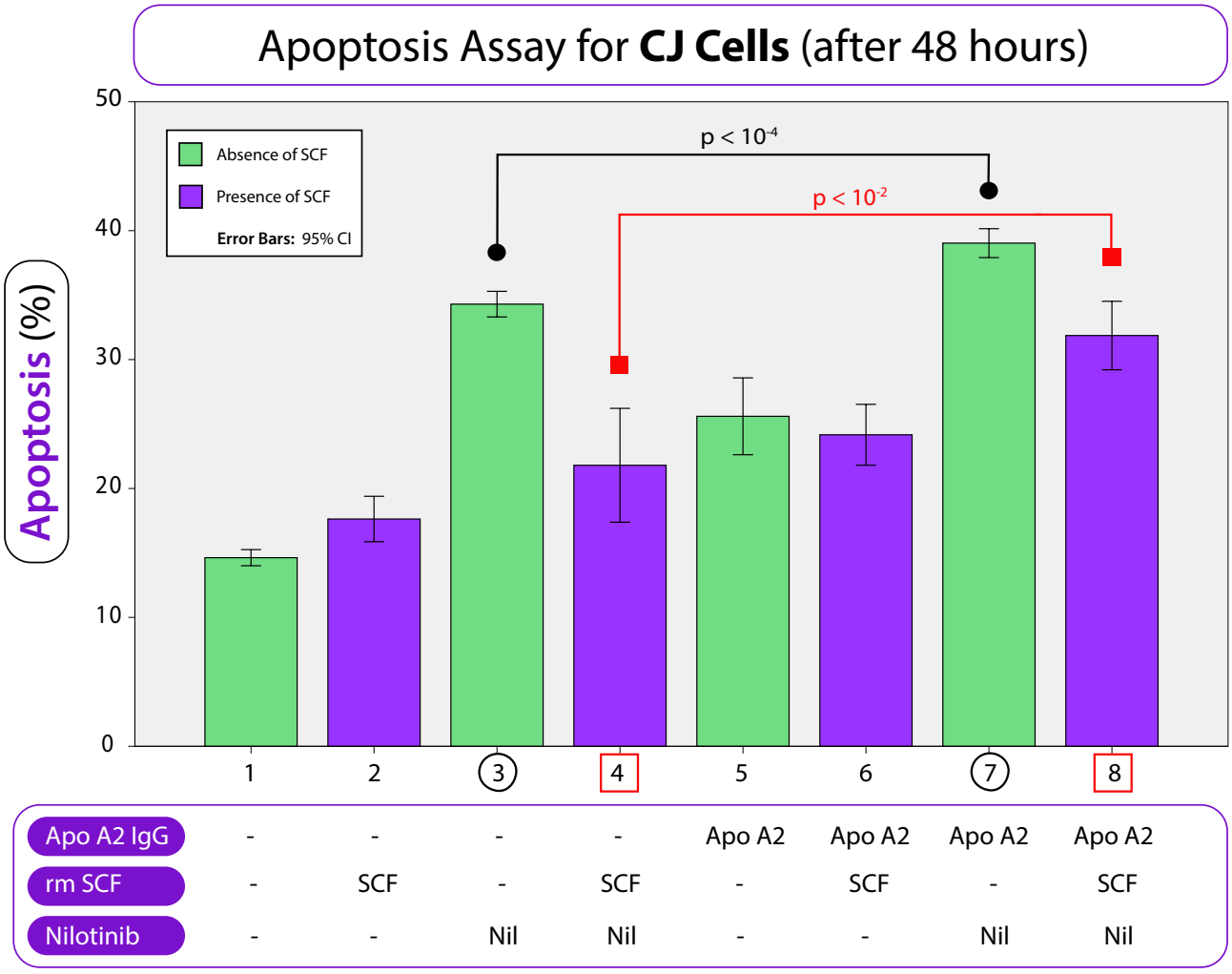

Figure 6.24: Apoptosis Assay for CJ Cells in a Combination of Apo A2 IgG and Nilotinib Treatments. The combinatorial treatment consists of 3 μg/mL Apo A2 IgG and 50 nM nilotinib (Nil), applied with 200 ng/mL recombinant mouse stem cell factor (rm SCF). Cells were cultured in RPMI 1640 medium supplemented with 20% v/v FBS, and maintained in a humidified incubator containing 5% CO_2 at 37° C for 40 hours before the assay. In the graph, green shaded bars are used to specify an absence of SCF, whereas purple shaded bars indicate a presence of SCF. P-values for apoptosis (%) were calculated in the test pair labeled 3 and 7, and pair 4 and 8 to compare a combinatorial treatment versus one drug solution. In the treatment annotation table below the graph, a dash (-) stands for the absence of the corresponding treatment factor.

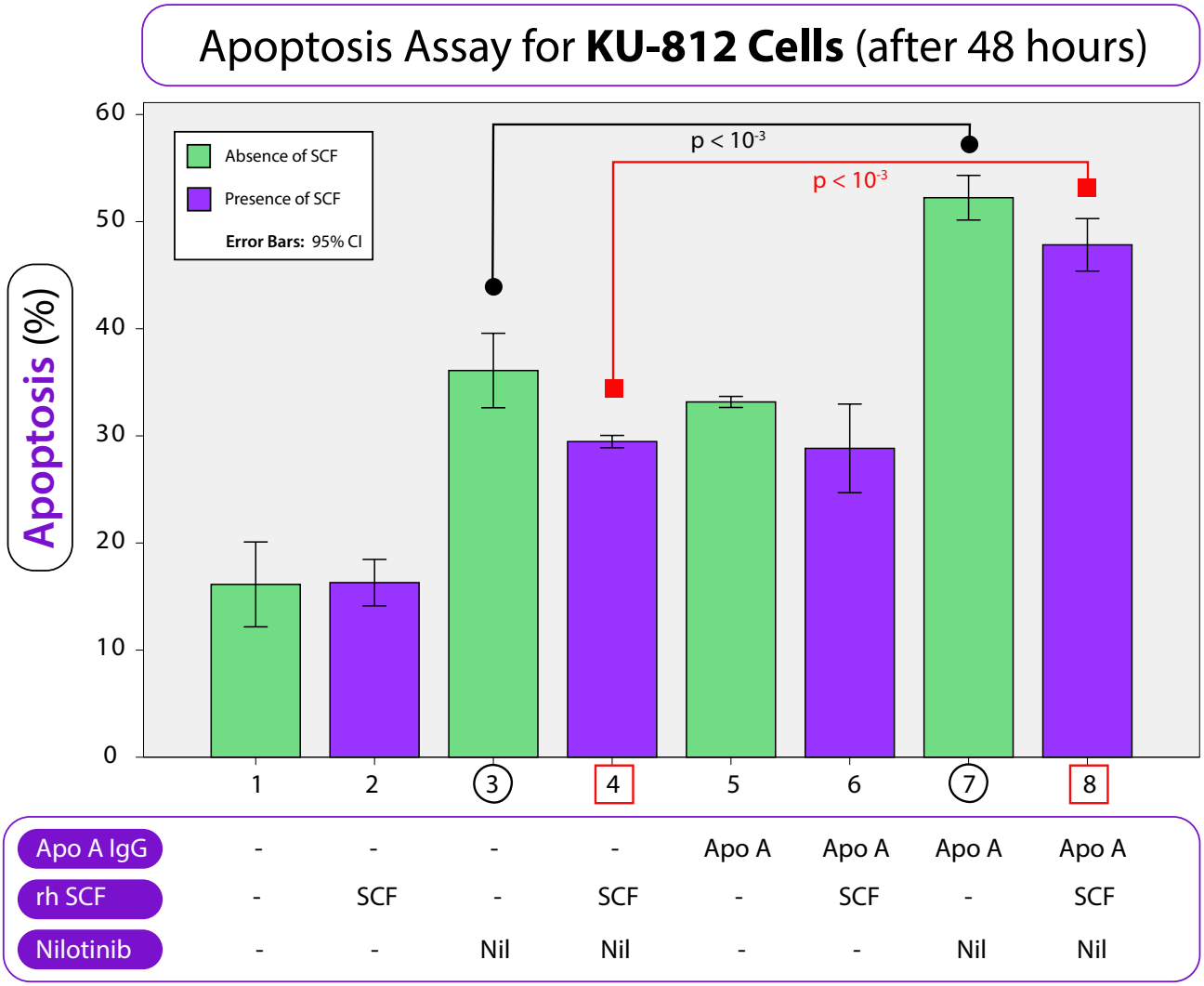

Figure 6.25: Apoptosis Assay for KU-812 Cells in a Combination of Apo A IgG and Nilotinib Treatments. The combinatorial treatment consists of 3 μg/mL Apo A IgG and 10 nM nilotinib (Nil), applied with 200 ng/mL recombinant human stem cell factor (rh SCF). Cells were cultured in RPMI 1640 medium supplemented with 10% v/v FBS and 1% v/v penicillin-streptomycin solution, and maintained in a humidified incubator containing 5% CO_2 at 37° C for 48 hours before the assay. In the graph, green shaded bars are used to specify an absence of SCF, whereas purple shaded bars indicate a presence of SCF. P-values for apoptosis (%) were calculated in the test pair labeled 3 and 7, and pair 4 and 8 to compare a combinatorial treatment versus one drug solution. In the treatment annotation table below the graph, a dash (-) stands for the absence of the corresponding treatment factor. For example, the first column with 3 dashes corresponds to a null condition, i.e., without an antibody, SCF, or drug.

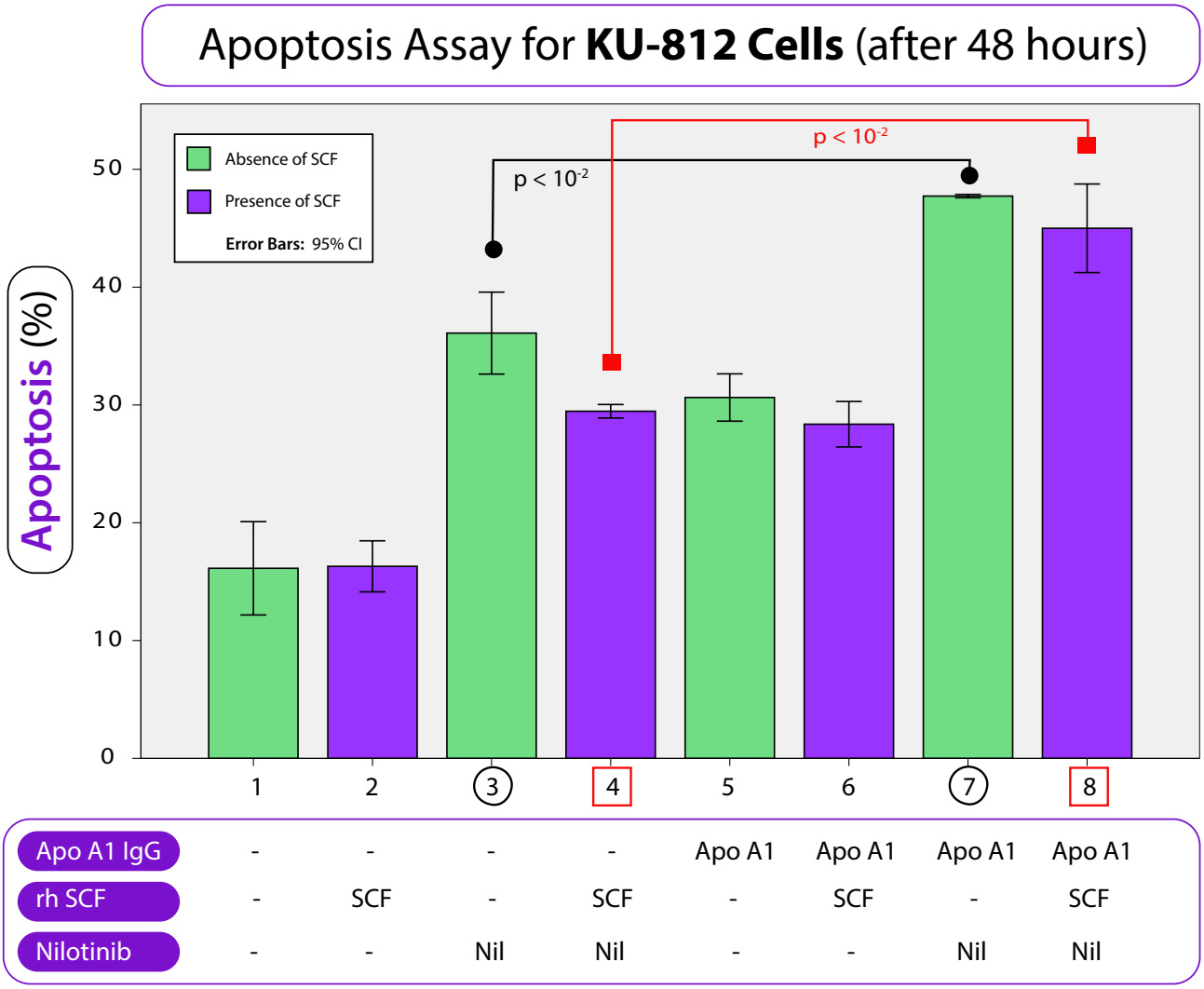

Figure 6.26: Apoptosis Assay for KU-812 Cells in a Combination of Apo A1 IgG and Nilotinib Treatments. The combinatorial treatment consists of 3 μg/mL Apo A1 IgG and 10 nM nilotinib (Nil), applied with 200 ng/mL recombinant human stem cell factor (rh SCF). Cells were cultured in RPMI 1640 medium supplemented with 10% v/v FBS and 1% v/v penicillin-streptomycin solution, and maintained in a humidified incubator containing 5% CO_2 at 37° C for 48 hours before the assay. In the graph, green shaded bars are used to specify an absence of SCF, whereas purple shaded bars indicate a presence of SCF. P-values for apoptosis (%) were calculated in the test pair labeled 3 and 7, and pair 4 and 8 to compare a combinatorial treatment versus one drug solution. In the treatment annotation table below the graph, a dash (-) stands for the absence of the corresponding treatment factor.

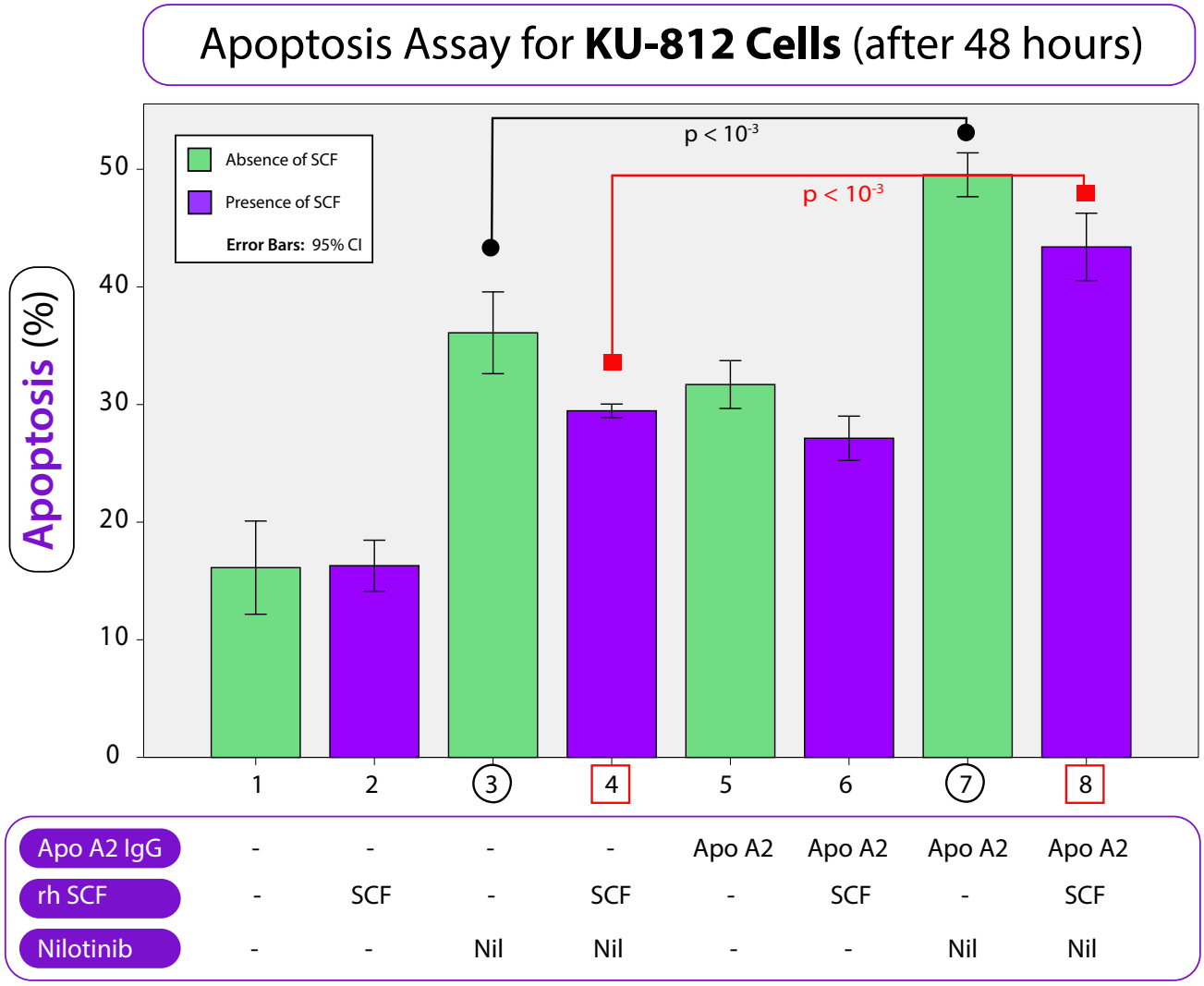

Figure 6.27: Apoptosis Assay for KU-812 Cells in a Combination of Apo A2 IgG and Nilotinib Treatments. The combinatorial treatment consists of 3 μg/mL Apo A2 IgG and 10 nM nilotinib (Nil), applied with 200 ng/mL recombinant human stem cell factor (rh SCF). Cells were cultured in RPMI 1640 medium supplemented with 10% v/v FBS and 1% v/v penicillin-streptomycin solution, and maintained in a humidified incubator containing 5% CO_2 at 37° C for 48 hours before the assay. In the graph, green shaded bars are used to specify an absence of SCF, whereas purple shaded bars indicate a presence of SCF. P-values for apoptosis (%) were calculated in the test pair labeled 3 and 7, and pair 4 and 8 to compare a combinatorial treatment versus one drug solution. In the treatment annotation table below the graph, a dash (-) stands for the absence of the corresponding treatment factor.

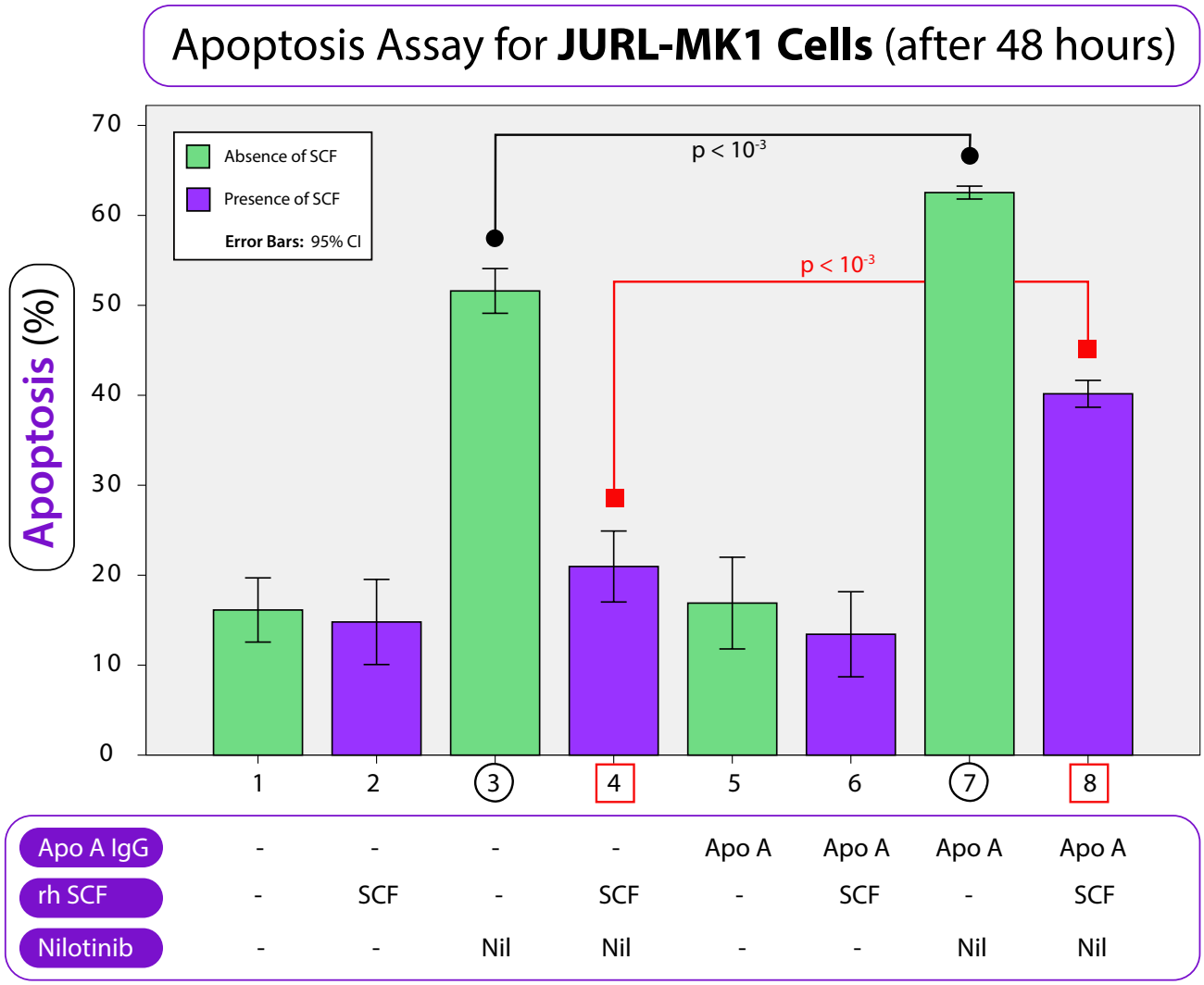

Figure 6.28: Apoptosis Assay for JURL-MK1 Cells in a Combination of Apo A IgG and Nilotinib Treatments. The combinatorial treatment consists of 3 μg/mL Apo A IgG and 30 nM nilotinib (Nil), applied with 200 ng/mL recombinant human stem cell factor (rh SCF). Cells were cultured in RPMI 1640 medium supplemented with 10% v/v FBS and 1% v/v penicillin-streptomycin solution, and maintained in a humidified incubator containing 5% CO_2 at 37° C for 48 hours before the assay. In the graph, green shaded bars are used to specify an absence of SCF, whereas purple shaded bars indicate a presence of SCF. P-values for apoptosis (%) were calculated in the test pair labeled 3 and 7, and pair 4 and 8 to compare a combinatorial treatment versus one drug solution. In the treatment annotation table below the graph, a dash (-) stands for the absence of the corresponding treatment factor. For example, the first column with 3 dashes corresponds to a null condition, i.e., without an antibody, SCF, or drug.

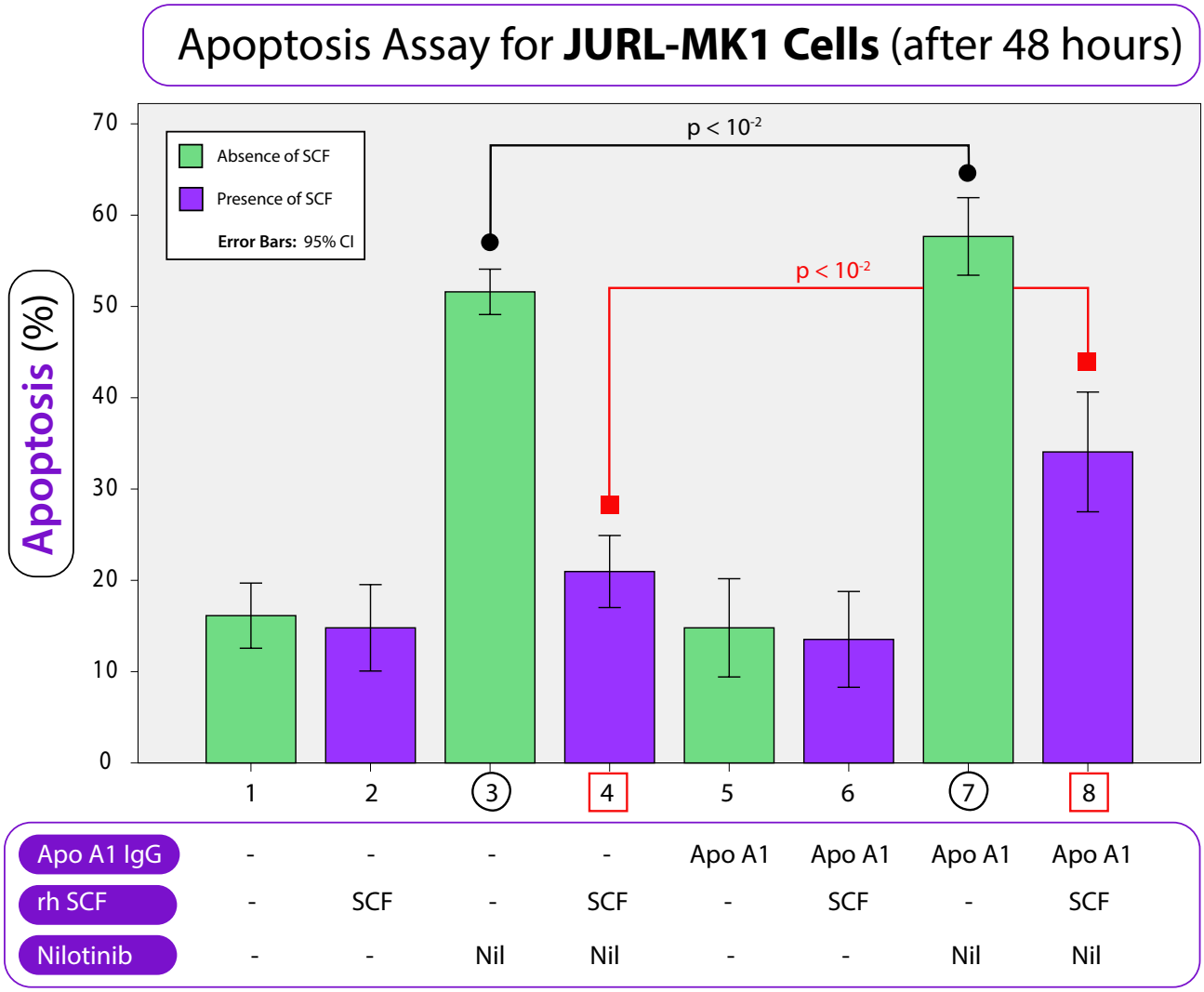

Figure 6.29: Apoptosis Assay for JURL-MK1 Cells in a Combination of Apo A1 IgG and Nilotinib Treatments. The combinatorial treatment consists of 3 μg/mL Apo A1 IgG and 30 nM nilotinib (Nil), applied with 200 ng/mL recombinant human stem cell factor (rh SCF). Cells were cultured in RPMI 1640 medium supplemented with 10% v/v FBS and 1% v/v penicillin-streptomycin solution, and maintained in a humidified incubator containing 5% CO_2 at 37° C for 48 hours before the assay. In the graph, green shaded bars are used to specify an absence of SCF, whereas purple shaded bars indicate a presence of SCF. P-values for apoptosis (%) were calculated in the test pair labeled 3 and 7, and pair 4 and 8 to compare a combinatorial treatment versus one drug solution. In the treatment annotation table below the graph, a dash (-) stands for the absence of the corresponding treatment factor.

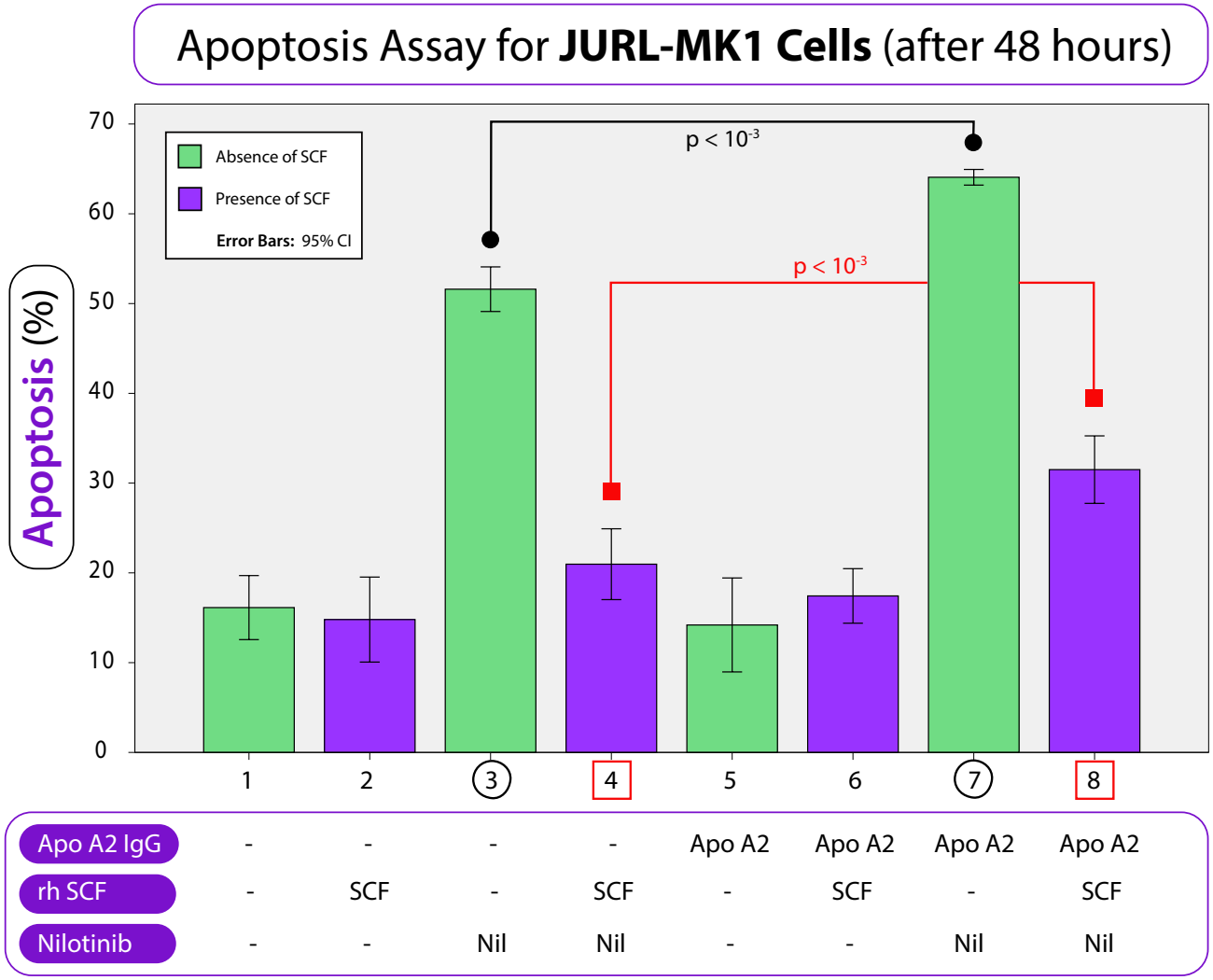

Figure 6.30: Apoptosis Assay for JURL-MK1 Cells in a Combination of Apo A2 IgG and Nilotinib Treatments. The combinatorial treatment consists of 3 μg/mL Apo A2 IgG and 30 nM nilotinib (Nil), applied with 200 ng/mL recombinant human stem cell factor (rh SCF). Cells were cultured in RPMI 1640 medium supplemented with 10% v/v FBS and 1% v/v penicillin-streptomycin solution, and maintained in a humidified incubator containing 5% CO_2 at 37° C for 48 hours before the assay. In the graph, green shaded bars are used to specify an absence of SCF, whereas purple shaded bars indicate a presence of SCF. P-values for apoptosis (%) were calculated in the test pair labeled 3 and 7, and pair 4 and 8 to compare a combinatorial treatment versus one drug solution. In the treatment annotation table below the graph, a dash (-) stands for the absence of the corresponding treatment factor.

6.5.2 Data Analysis and Discussion: By Blocking the Innate Resistance, the sABs Promoted Nilotinib Apoptotic Activity

In all cases with the presence of SCF, apoptotic activity quantified by percentage values decreased compared to those respective values in the absence of SCF condition (e.g., see Figure 6.25). This means that the addition of SCF reduces drug effect, in partially rescuing the cells from the nilotinib treatment, but this effect can be counteracted with an appropriate sAB co-agent. Therefore, from an apoptotic perspective, the rationale for blocking the SCF-mediated innate resistance is reaffirmed for CML treatment. This can be achieved by inhibiting the corresponding receptor c-Kit in order to suppress the pathway responsible for this innate resistance.

As in the cell viability assay, a triplicate setup was performed to enable data consistency. Also, the obtained error bars do not overlap between associated pairs of test scenarios. In addition, according to the apoptosis assay with the developed sABs, the data suggest that Apo A IgG and Apo A2 IgG should be the preferred candidates, since they induced the highest apoptotic activity with all CML cell lines investigated.

All in all, compatible with all the tests conducted so far, apoptosis assay also demonstrated that, even though SCF stimulation hindered nilotinib in treating CML, this challenge may be overcome by recruiting a suitable ally in the form of c-Kit antibody co-agents.

6.6 Colony Forming Cell (CFC) Assay: Investigation of the Progenitor Ability of CML Cells Using a Combinatorial Approach

The tests conducted thus far focused on various aspects of the cells within their individual life cycle, e.g., cell death and apoptosis. However, cancer development involves more than just independent behavior of the cells in isolation. For instance, among some well known hallmarks, cancer cells exhibit the ability to affect other cells or to reproduce progenies with anomalous characteristics, as well as resistance to drug treatment and relapse occurrence [115, 116]. In fact, it is now known that many cancers are able to sustain these characteristics via specialized entities known as the progenitor cells [13, 117]. Clearly, in developing suitable cancer therapy, it is important to understand the effects of the treatment on these progenitor cells to completely suppress the disease. Therefore, last but not least, a test that is able to assess the status of these progenitor cells is immensely relevant here. To this end, since a characteristic behavior of the progenitor cells is that they proliferate and differentiate into colonies, a corresponding colony forming cell (CFC) assay can be applied to measure this phenomenon in order to quantify the progenitor ability.

Procedurally, the CFC assay involves using various cytokines to stimulate growth in a methylcellulose-based medium to form colonies. This means that the number of progenitor cells can be enumerated by counting the number of colonies under an inverted microscope. Then, this assay allows for investigating how a combinatorial drug treatment affects progenitor cells. In particular, for a successful drug combination, it is expected that the number of colonies should be significantly decreased when the treatment is applied.

6.6.1 Data for CFC Assay with CML Cell Lines

Fundamentally, CFC assay is a cell counting technique without staining, which means that it is most similar to cell viability assay in Section 6.4, and as such, also necessitates similar initial preparation steps as described in Section 4.3.6. Colony formation was quantitated using MethoCult™ methylcellulose-based medium in accordance with the manufacturer's instructions. However, within methylcellulose-based medium, the progenitor cells require sufficient time to differentiate into visually distinguishable clusters. In particular, the incubation time is significantly longer compared to other tests, ranging from 7–14 days in a humidified incubator containing 5%

CO_2 at 37º C before quantifying the resulting colonies under an inverted microscope. This test is therefore highly time-consuming, resource demanding (i.e., costly) and attention-intensive.

The obtained CFC assay data are grouped according to cell line in the following graphs:

- CJ: results shown in Figures 6.31–6.33;
- KU-812: results shown in Figures 6.34–6.36;
- JURL-MK1: results shown in Figures 6.37–6.39.

As already noted, this technique is related to cell viability assay and it also has similar output format, with one crucial difference, i.e., the histograms depicting the number of colonies instead of the number of cells.

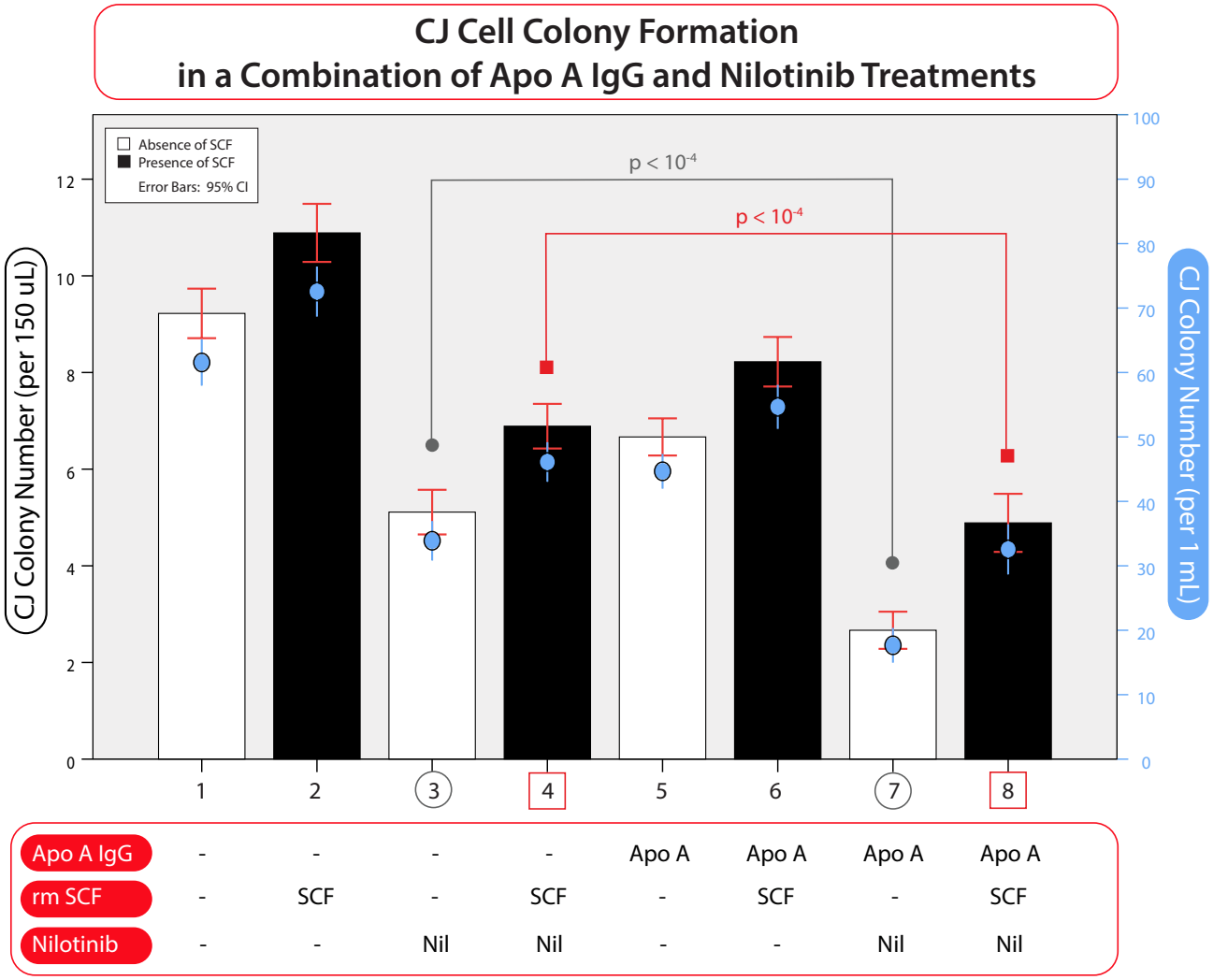

Figure 6.31: Colony Forming Cell Assay for CJ Cells in a Combination of Apo A IgG and Nilotinib Treatments. The combinatorial treatment consists of 3 μg/mL Apo A IgG and 50 nM nilotinib (Nil), applied with 200 ng/mL recombinant mouse stem cell factor (rm SCF). Cells were first prepared in RPMI 1640 medium supplemented with 20% v/v FBS, and maintained in a humidified incubator containing 5% CO_2 at 37° C for 40 hours before the CFC assay setup. Next, cells were then cultured in MethoCult™ GF M3434 methylcellulose medium, and maintained in a humidified incubator for 7-14 days. In the graph, white bars are used to specify an absence of SCF, whereas black shaded bars indicate a presence of SCF. P-values for colony number were calculated in the test pair labeled 3 and 7, and pair 4 and 8 to compare a combinatorial treatment versus one drug solution. In the treatment annotation table below the graph, a dash (-) stands for the absence of the corresponding treatment factor. For example, the first column with 3 dashes corresponds to a null condition, i.e., without an antibody, SCF, or drug.

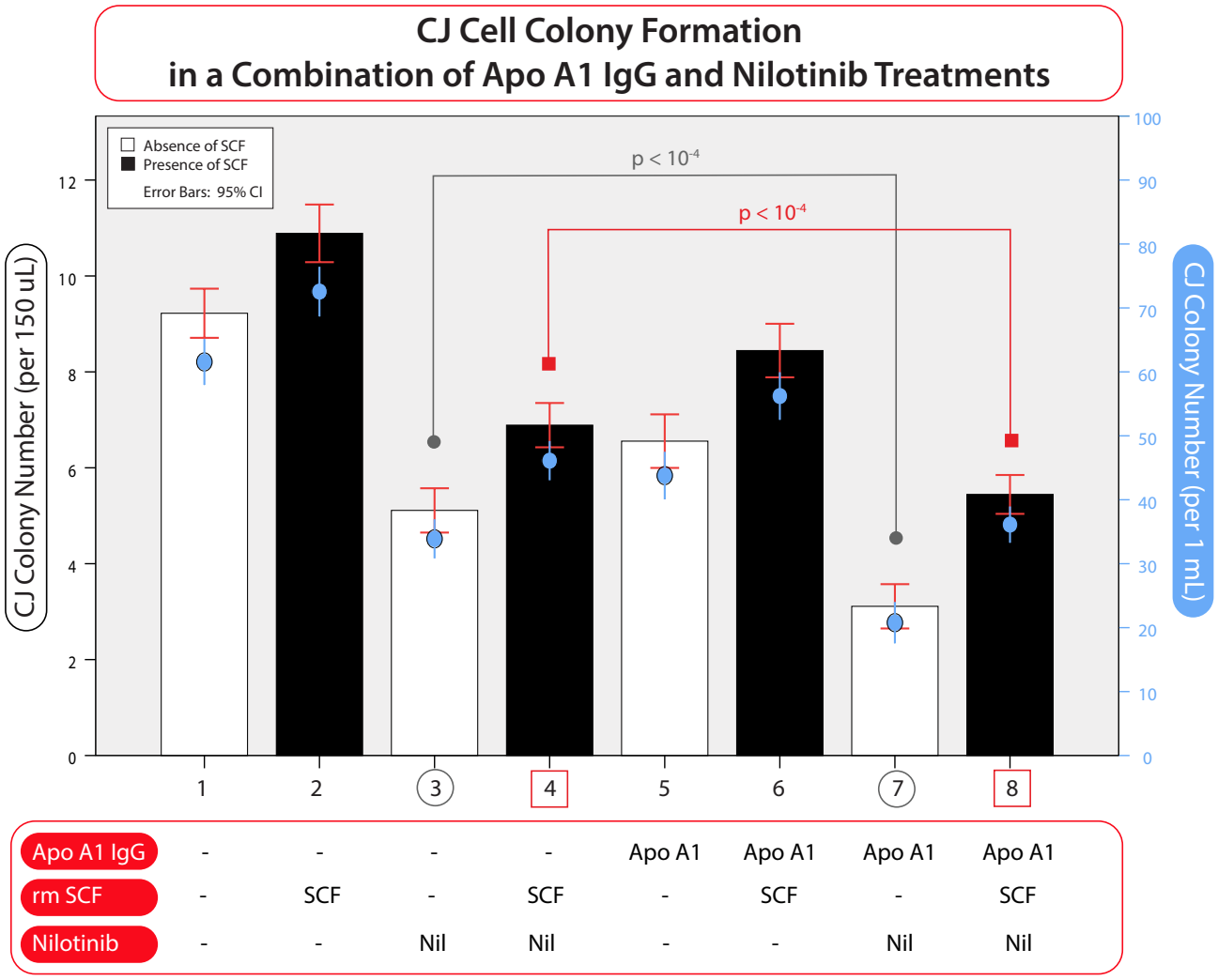

Figure 6.32: Colony Forming Cell Assay for CJ Cells in a Combination of Apo A1 IgG and Nilotinib Treatments. The combinatorial treatment consists of 3 μg/mL Apo A1 IgG and 50 nM nilotinib (Nil), applied with 200 ng/mL recombinant mouse stem cell factor (rm SCF). Cells were first prepared in RPMI 1640 medium supplemented with 20% v/v FBS, and maintained in a humidified incubator containing 5% CO_2 at 37° C for 40 hours before the CFC assay setup. Next, cells were then cultured in MethoCult™ GF M3434 methylcellulose medium, and maintained in a humidified incubator for 7-14 days. In the graph, white bars are used to specify an absence of SCF, whereas black shaded bars indicate a presence of SCF. P-values for colony number were calculated in the test pair labeled 3 and 7, and pair 4 and 8 to compare a combinatorial treatment versus one drug solution. In the treatment annotation table below the graph, a dash (-) stands for the absence of the corresponding treatment factor.

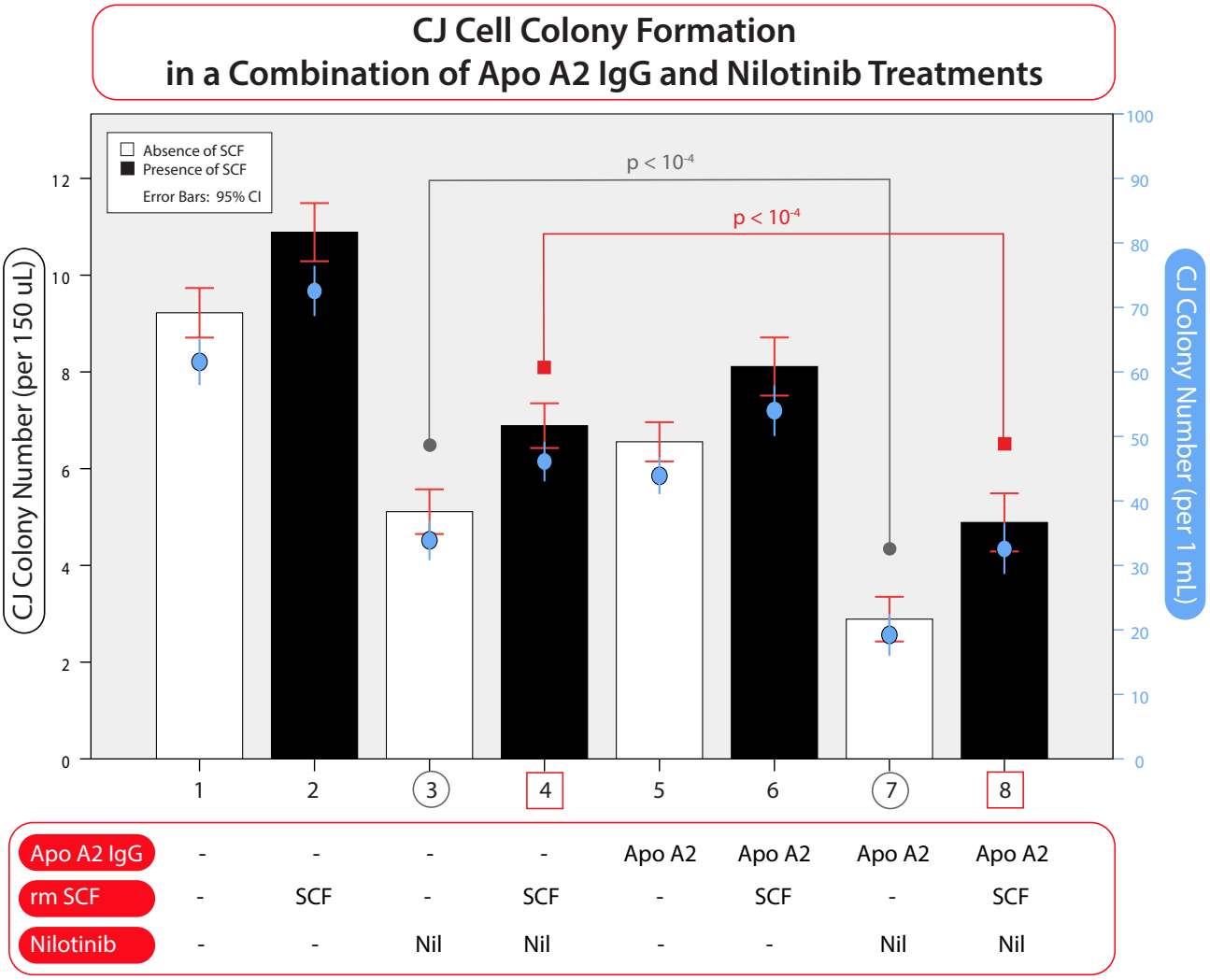

Figure 6.33: Colony Forming Cell Assay for CJ Cells in a Combination of Apo A2 IgG and Nilotinib Treatments. The combinatorial treatment consists of 3 μg/mL Apo A2 IgG and 50 nM nilotinib (Nil), applied with 200 ng/mL recombinant mouse stem cell factor (rm SCF). Cells were first prepared in RPMI 1640 medium supplemented with 20% v/v FBS, and maintained in a humidified incubator containing 5% CO_2 at 37° C for 40 hours before the CFC assay setup. Next, cells were then cultured in MethoCult™ GF M3434 methylcellulose medium, and maintained in a humidified incubator for 7-14 days. In the graph, white bars are used to specify an absence of SCF, whereas black shaded bars indicate a presence of SCF. P-values for colony number were calculated in the test pair labeled 3 and 7, and pair 4 and 8 to compare a combinatorial treatment versus one drug solution. In the treatment annotation table below the graph, a dash (-) stands for the absence of the corresponding treatment factor.

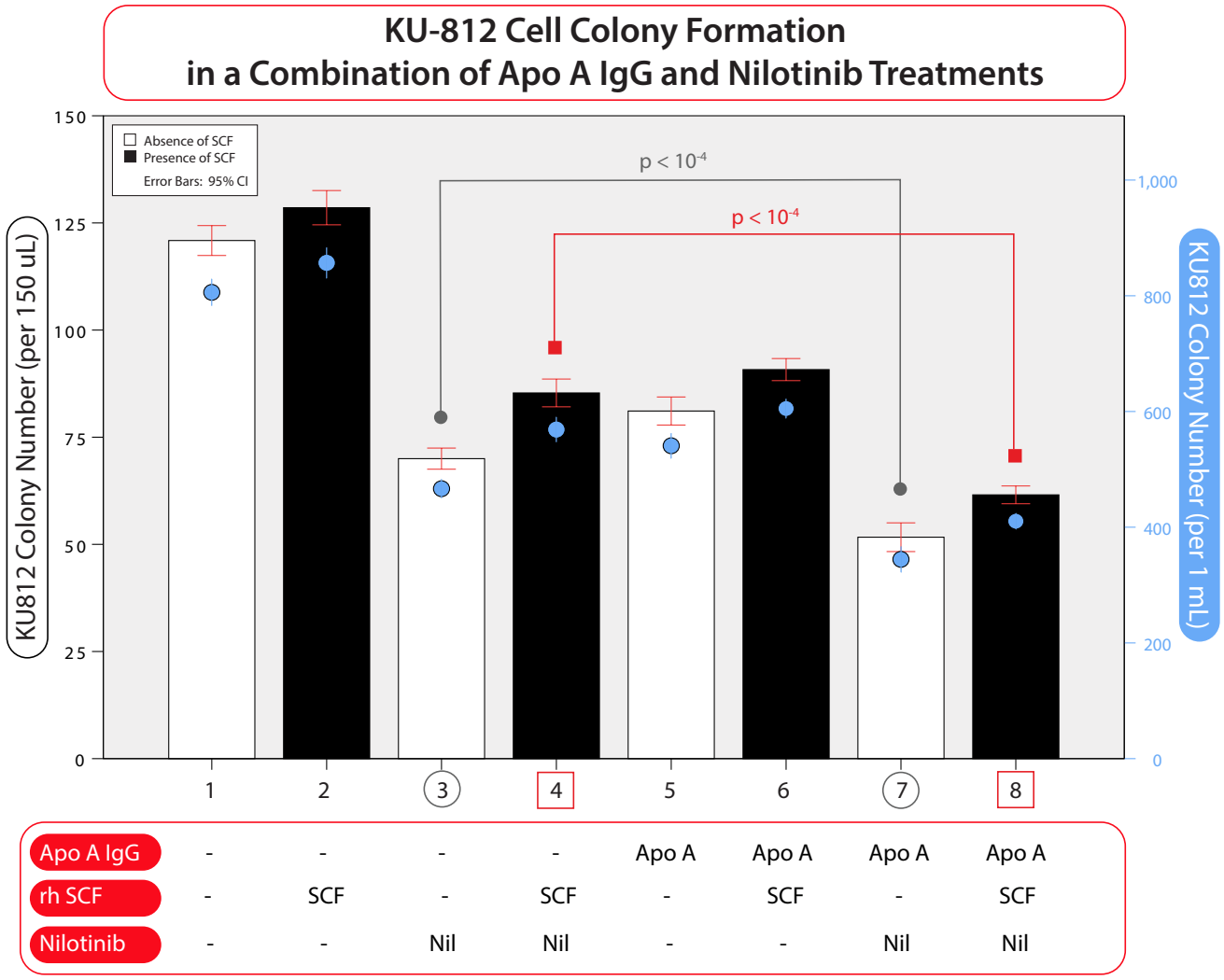

Figure 6.34: Colony Forming Cell Assay for KU-812 Cells in a Combination of Apo A IgG and Nilotinib Treatments. The combinatorial treatment consists of 3 μg/mL Apo A IgG and 10 nM nilotinib (Nil), applied with 200 ng/mL recombinant human stem cell factor (rh SCF). Cells were first prepared in RPMI 1640 medium supplemented with 10% v/v FBS and 1% v/v penicillin-streptomycin solution, and maintained in a humidified incubator containing 5% CO_2 at 37° C C for 48 hours before the CFC assay setup. Next, cells were then cultured in MethoCult™ H4434 methylcellulose medium, and maintained in a humidified incubator for 7-14 days. In the graph, white bars are used to specify an absence of SCF, whereas black shaded bars indicate a presence of SCF. P-values for colony number were calculated in the test pair labeled 3 and 7, and pair 4 and 8 to compare a combinatorial treatment versus one drug solution. In the treatment annotation table below the graph, a dash (-) stands for the absence of the corresponding treatment factor. For example, the first column with 3 dashes corresponds to a null condition, i.e., without an antibody, SCF, or drug.

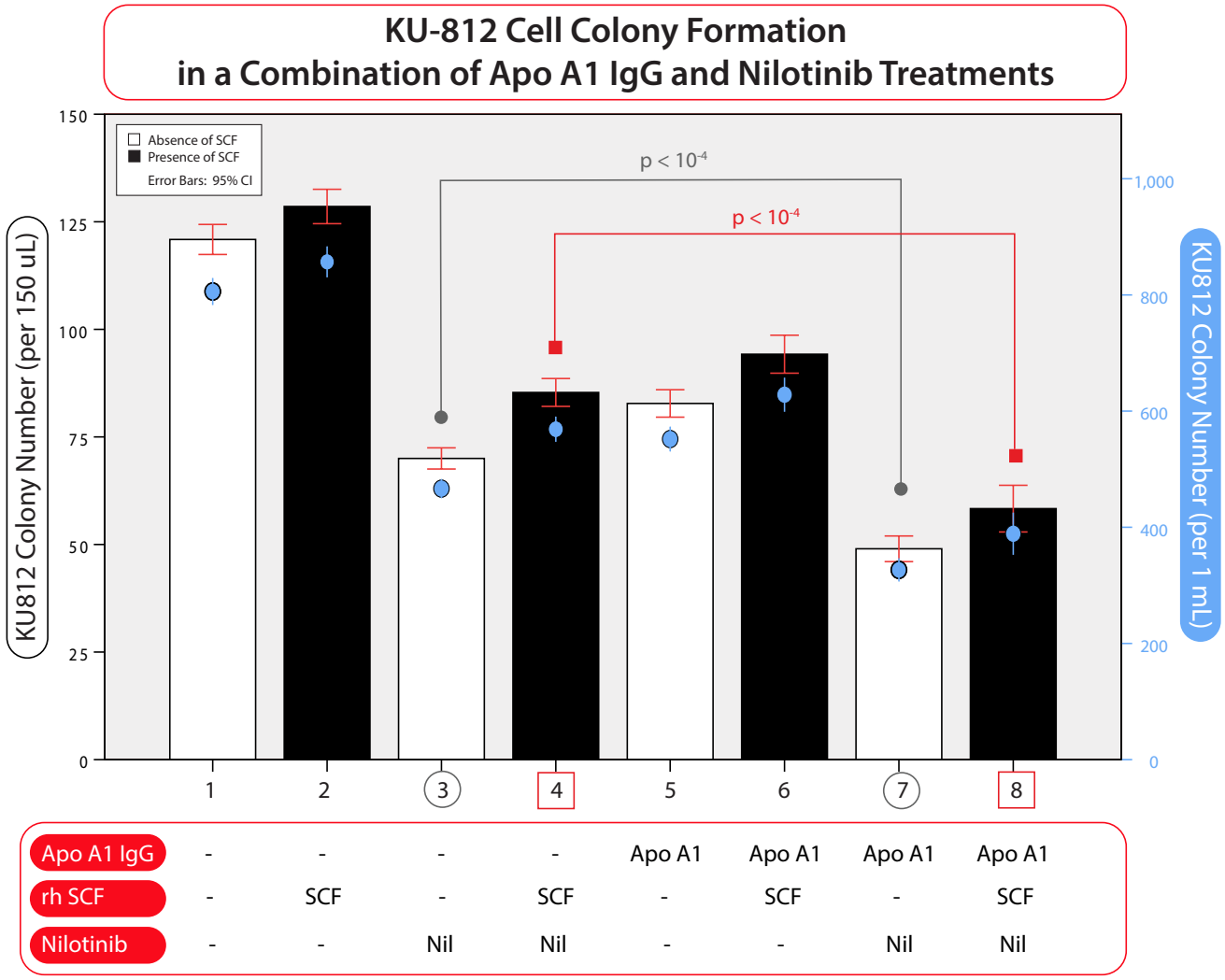

Figure 6.35: Colony Forming Cell Assay for KU-812 Cells in a Combination of Apo A1 IgG and Nilotinib Treatments. The combinatorial treatment consists of 3 μg/mL Apo A1 IgG and 10 nM nilotinib (Nil), applied with 200 ng/mL recombinant human stem cell factor (rh SCF). Cells were first prepared in RPMI 1640 medium supplemented with 10% v/v FBS and 1% v/v penicillin-streptomycin solution, and maintained in a humidified incubator containing 5% CO_2 at 37° C for 48 hours before the CFC assay setup. Next, cells were then cultured in MethoCult™ H4434 methylcellulose medium, and maintained in a humidified incubator for 7-14 days. In the graph, white bars are used to specify an absence of SCF, whereas black shaded bars indicate a presence of SCF. P-values for colony number were calculated in the test pair labeled 3 and 7, and pair 4 and 8 to compare a combinatorial treatment versus one drug solution. In the treatment annotation table below the graph, a dash (-) stands for the absence of the corresponding treatment factor.

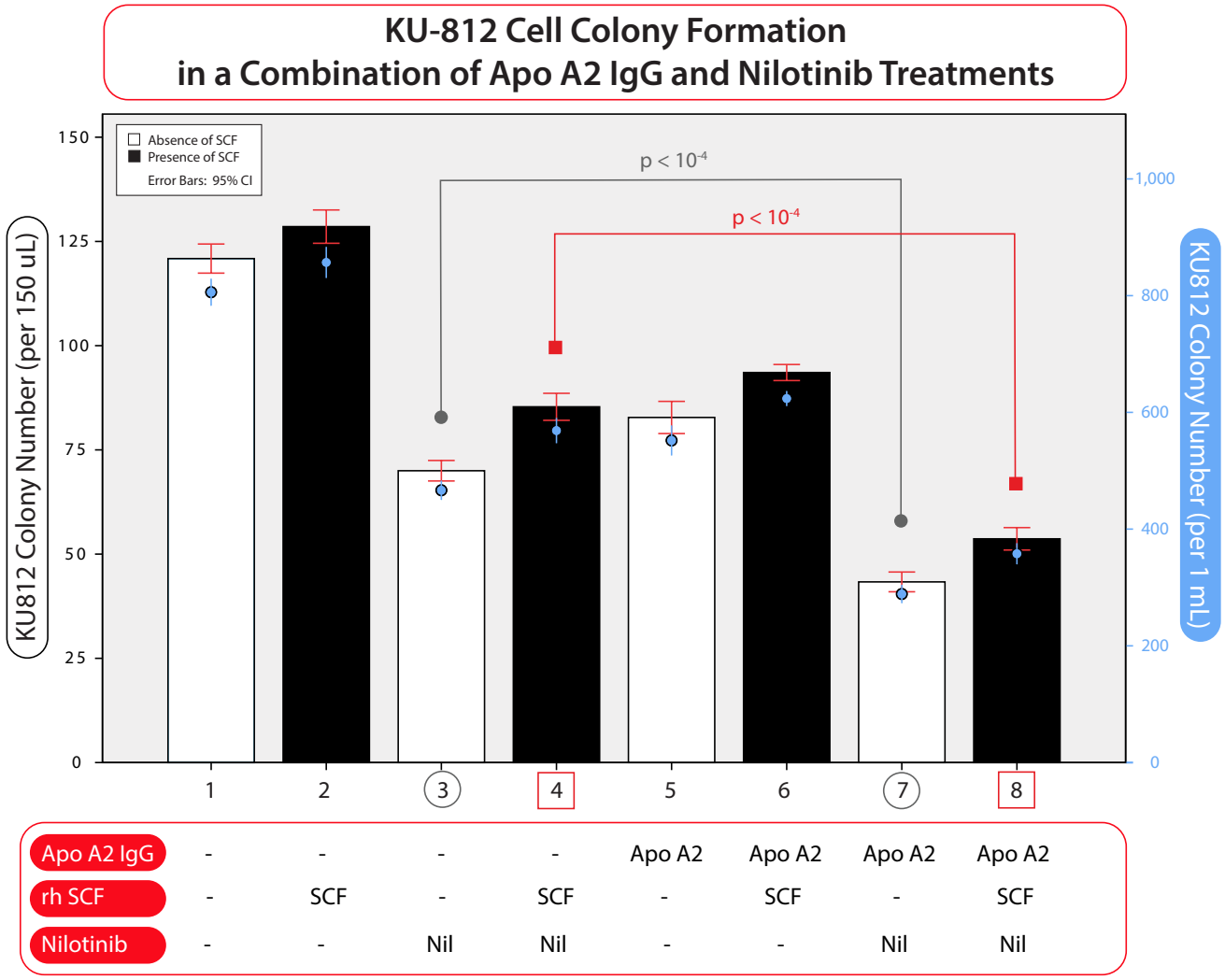

Figure 6.36: Colony Forming Cell Assay for KU-812 Cells in a Combination of Apo A2 IgG and Nilotinib Treatments. The combinatorial treatment consists of 3 μg/mL Apo A2 IgG and 10 nM nilotinib (Nil), applied with 200 ng/mL recombinant human stem cell factor (rh SCF). Cells were first prepared in RPMI 1640 medium supplemented with 10% v/v FBS and 1% v/v penicillin-streptomycin solution, and maintained in a humidified incubator containing 5% CO_2 at 37° C for 48 hours before the CFC assay setup. Next, cells were then cultured in MethoCult™ H4434 methylcellulose medium, and maintained in a humidified incubator for 7-14 days. In the graph, white bars are used to specify an absence of SCF, whereas black shaded bars indicate a presence of SCF. P-values for colony number were calculated in the test pair labeled 3 and 7, and pair 4 and 8 to compare a combinatorial treatment versus one drug solution. In the treatment annotation table below the graph, a dash (-) stands for the absence of the corresponding treatment factor.

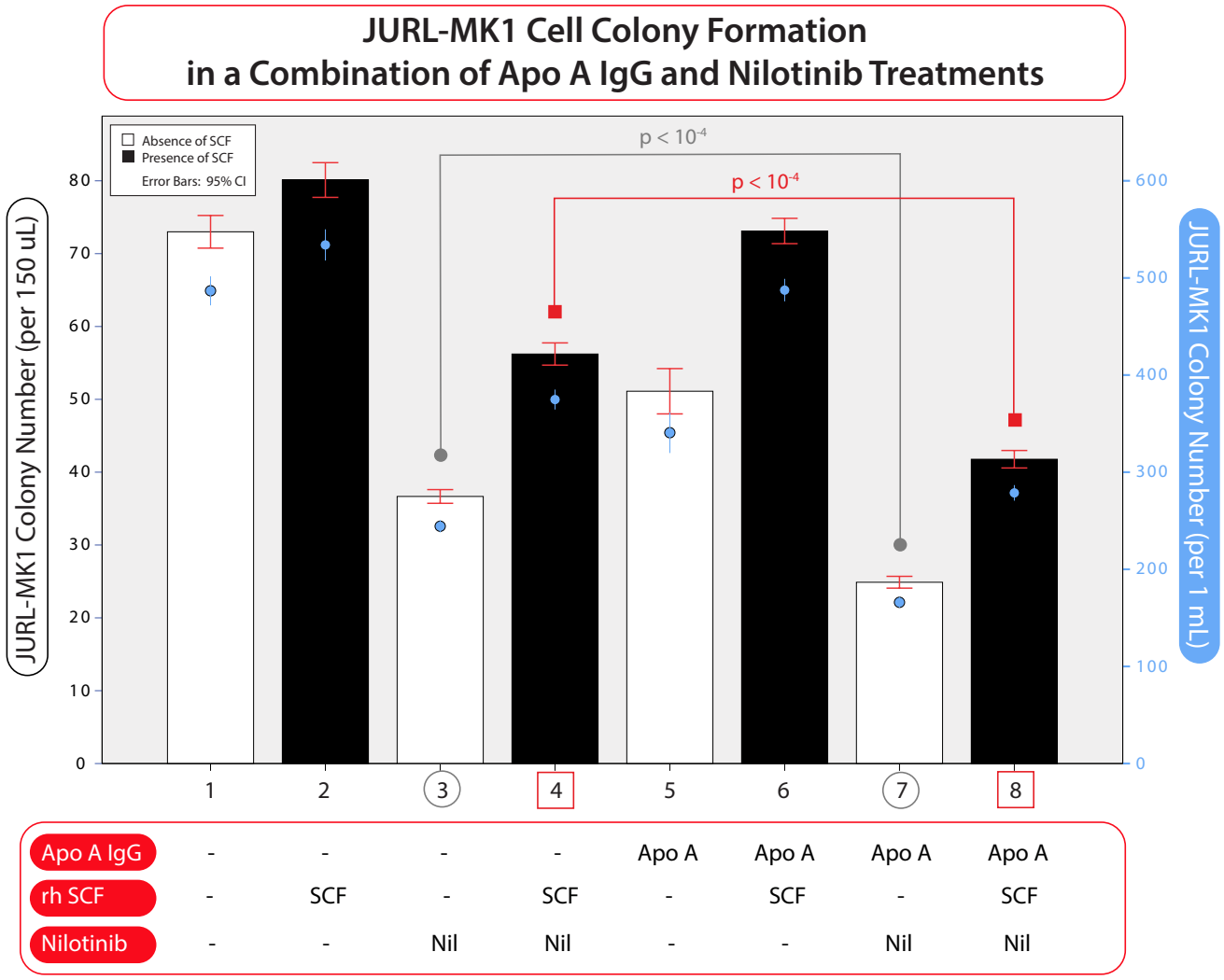

Figure 6.37: Colony Forming Cell Assay for JURL-MK1 Cells in a Combination of Apo A IgG and Nilotinib Treatments. The combinatorial treatment consists of 3 μg/mL Apo A IgG and 30 nM nilotinib (Nil), applied with 200 ng/mL recombinant human stem cell factor (rh SCF). Cells were first prepared in RPMI 1640 medium supplemented with 10% v/v FBS and 1% v/v penicillin-streptomycin solution, and maintained in a humidified incubator containing 5% CO_2 at 37° C for 48 hours before the CFC assay setup. Next, cells were then cultured in MethoCult™ H4434 methylcellulose medium, and maintained in a humidified incubator for 7-14 days. In the graph, white bars are used to specify an absence of SCF, whereas black shaded bars indicate a presence of SCF. P-values for colony number were calculated in the test pair labeled 3 and 7, and pair 4 and 8 to compare a combinatorial treatment versus one drug solution. In the treatment annotation table below the graph, a dash (-) stands for the absence of the corresponding treatment factor. For example, the first column with 3 dashes corresponds to a null condition, i.e., without an antibody, SCF, or drug.

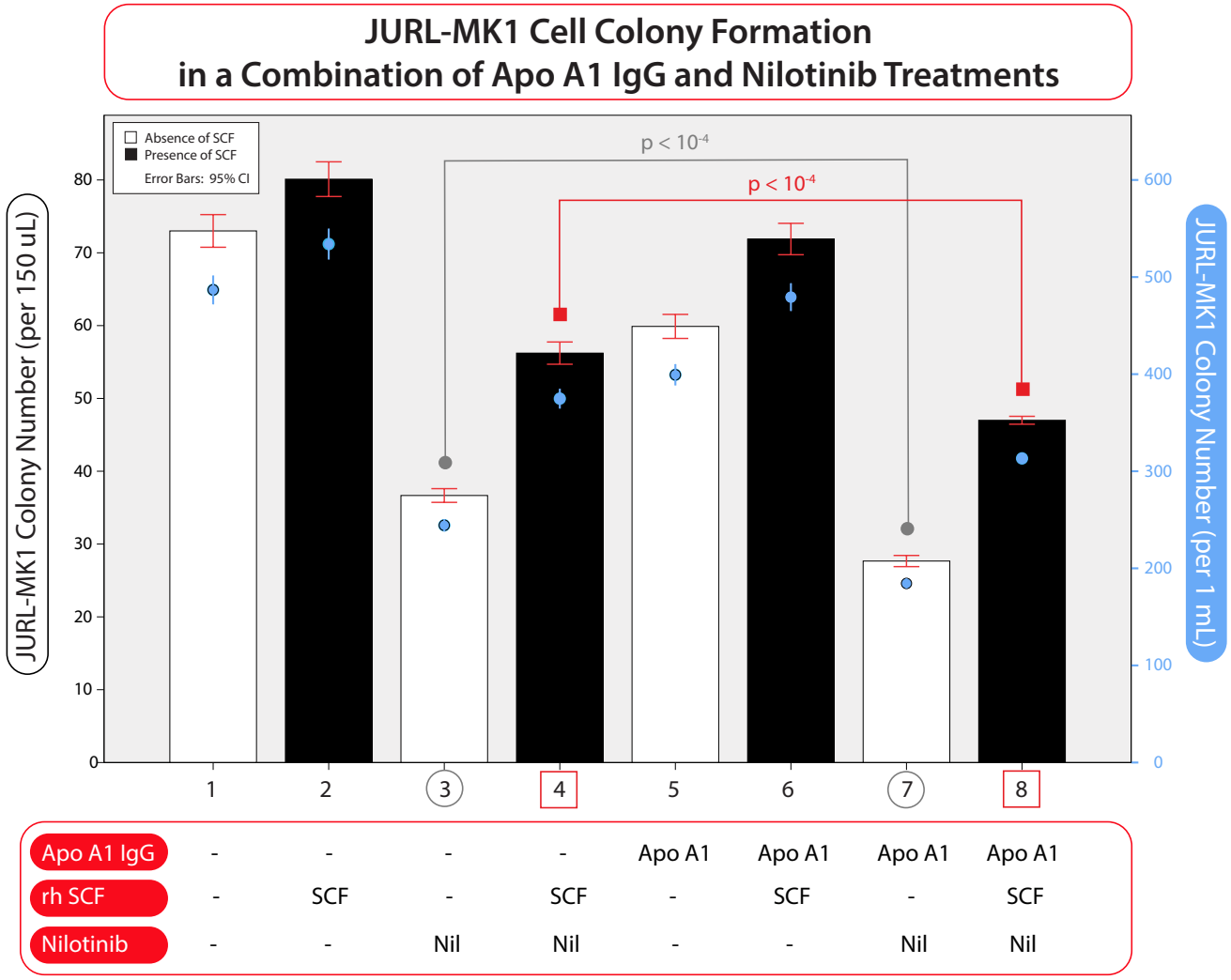

Figure 6.38: Colony Forming Cell Assay for JURL-MK1 Cells in a Combination of Apo A1 IgG and Nilotinib Treatments. The combinatorial treatment consists of 3 μg/mL Apo A1 IgG and 30 nM nilotinib (Nil), applied with 200 ng/mL recombinant human stem cell factor (rh SCF). Cells were first prepared in RPMI 1640 medium supplemented with 10% v/v FBS and 1% v/v penicillin-streptomycin solution, and maintained in a humidified incubator containing 5% CO_2 at 37° C for 48 hours before the CFC assay setup. Next, cells were then cultured in MethoCult™ H4434 methylcellulose medium, and maintained in a humidified incubator for 7-14 days. In the graph, white bars are used to specify an absence of SCF, whereas black shaded bars indicate a presence of SCF. P-values for colony number were calculated in the test pair labeled 3 and 7, and pair 4 and 8 to compare a combinatorial treatment versus one drug solution. In the treatment annotation table below the graph, a dash (-) stands for the absence of the corresponding treatment factor.

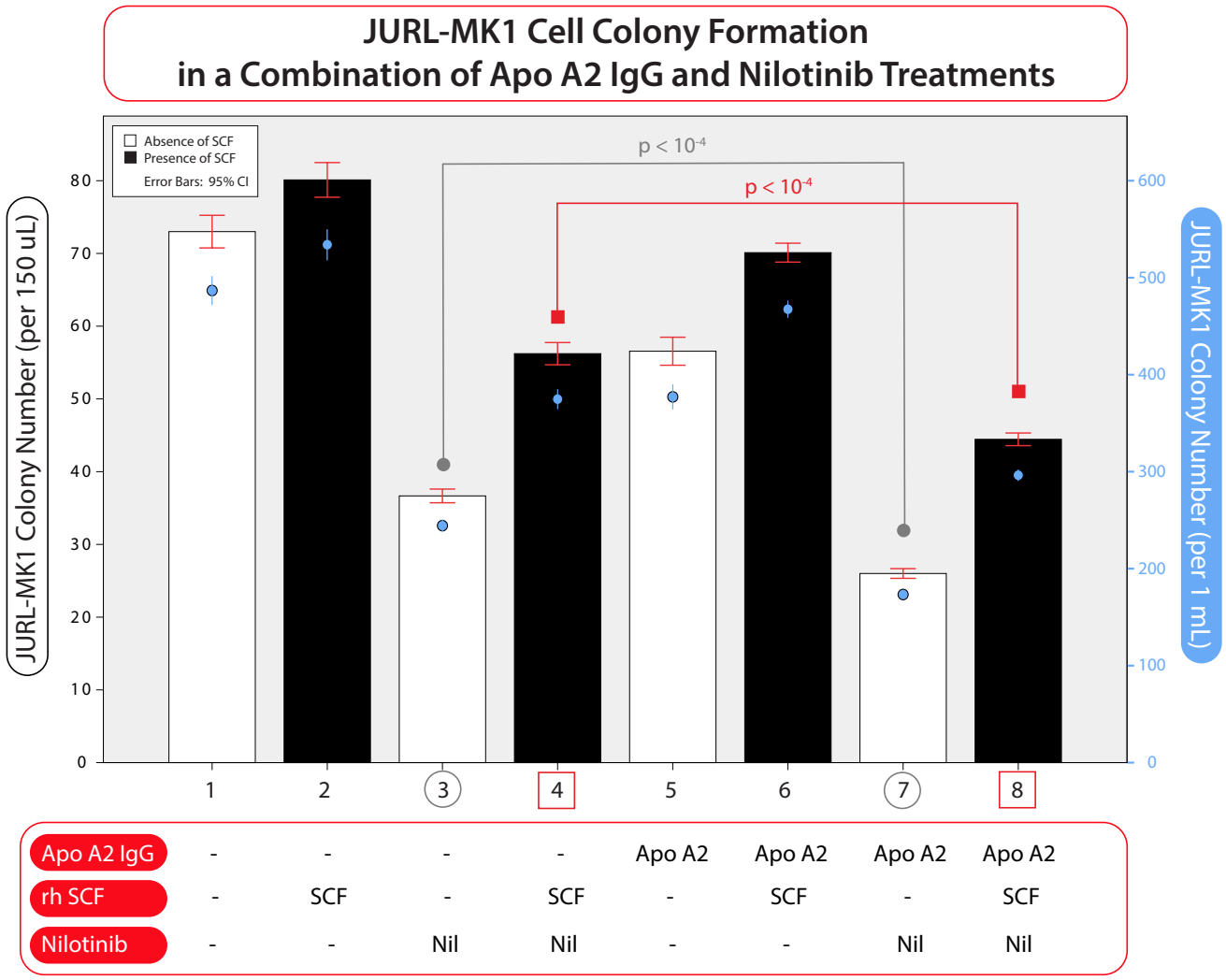

Figure 6.39: Colony Forming Cell Assay for JURL-MK1 Cells in a Combination of Apo A2 IgG and Nilotinib Treatments. The combinatorial treatment consists of 3 μg/mL Apo A2 IgG and 30 nM nilotinib (Nil), applied with 200 ng/mL recombinant human stem cell factor (rh SCF). Cells were first prepared in RPMI 1640 medium supplemented with 10% v/v FBS and 1% v/v penicillin-streptomycin solution, and maintained in a humidified incubator containing 5% CO_2 at 37° C for 48 hours before the CFC assay setup. Next, cells were then cultured in MethoCult™ H4434 methylcellulose medium, and maintained in a humidified incubator for 7-14 days. In the graph, white bars are used to specify an absence of SCF, whereas black shaded bars indicate a presence of SCF. P-values for colony number were calculated in the test pair labeled 3 and 7, and pair 4 and 8 to compare a combinatorial treatment versus one drug solution. In the treatment annotation table below the graph, a dash (-) stands for the absence of the corresponding treatment factor.

6.6.2 Data Analysis and Discussion: the Combinatorial Approach Has the Potential to Eliminate Progenitor Cells

A general observation reveals that, for all graphs, the number of colonies for all test scenarios significantly decreased when a combinatorial approach is applied. More specifically, this decrease is quantified by p-values less than 10^{-4} in a significance test between a combinatorial approach and the reference case of drug application alone (e.g., compare test pair labeled 3 and 7 or pair 4 and 8 in Figure 6.34, corresponding to KU-812 cells, in absence and presence of SCF). Therefore, a suitable drug combination has the potential to mitigate the progenitor effect. Furthermore, in all cases, the associated error bars are non-overlapping, reinforcing the count consistency for result reproducibility.

More specifically, focusing on more individual comparisons, it can be seen the decrease profiles do exhibit variations across different cell lines. For example, after treatment, a human CML cell line (e.g., KU-812) showed more differentiated clusters compared to a murine CML cell line (e.g., CJ). This implies that the progenitor cells respond differently to the cytokine stimulation, and have different susceptibility to therapy. But despite these varying responses under different operating conditions, the overall trend is maintained: for any particular cell line, relative to the control case with drug application alone, a combinatorial treatment leads to a decrease in colonies formed.

Taken together, the results obtained from CFC assays confirm that a properly designed combinatorial treatment has a promising potential to diminish the progenitor capacity, and that this potential may be realized for various operating conditions with different cell lines. And as previously noted, since progenitor cells are responsible for a number of hallmark characteristics in cancer — most notably drug resistance and relapse — the flexible approach of combinatorial treatment, which allows for attenuating the progenitor effect in various scenarios, represents indeed a promising and desirable paradigm for cancer therapy development.

7. Conclusion

This chapter summarizes the contributions and outline directions for future research.

7.1 Summary of Contributions and Main Results

In this thesis, the problem of innate resistance mediated by SCF signaling in CML is investigated. Specifically, the focus is on the disruption of nilotinib apoptotic activity due to the SCF/c-Kit signaling pathway, which protects the primitive population of CML cells implicated in innate resistance, i.e., the quiescent LSCs found in the bone marrow endosteal niche, where hematopoietic cytokines such as the ligand SCF are released.

To this end, a combinatorial strategy based on sABs is proposed to inhibit the receptor c-Kit, thus blocking the innate resistance and restoring nilotinib apoptotic activity. In particular, by exploiting the knowledge of c-Kit vulnerability, the sABs are designed based on antibody phage display technology to specifically target D1–D3 domains representing the SCF binding sites for pathway activation.

To assess the performance of the proposed strategy, a set of *in vitro* tests was conducted, focusing on performance behaviors such as cell binding, cell death, and the progenitor ability. Figure 7.1 provides an overall summary of the combinatorial treatment and main results. Notably, the obtained *in vitro* results demonstrate that:

- Based on cell binding tests, the sAB co-agents produced exhibit high affinity and strong binding specificity across various human and murine CML cell lines;
- Based on cell viability and apoptosis assays, the sAB co-agents have the potential to restore nilotinib induced apoptosis, resulting in significantly reduced cell viability.

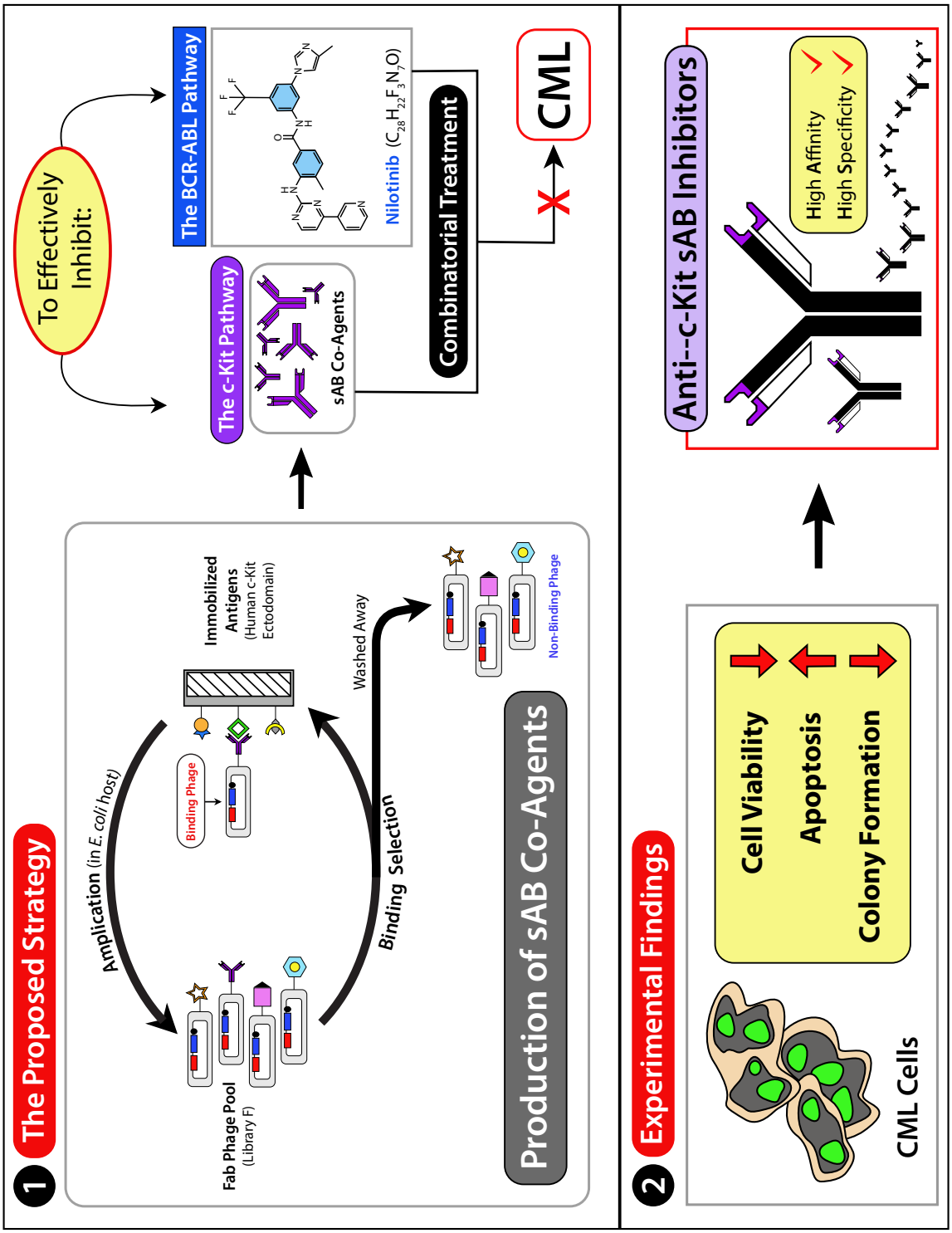

Figure 7.1: Overall Summary of the Combinatorial Treatment (Nilotinib and sABs) and Main Findings. 1) The proposed strategy: the sABs are designed using phage display technology to specifically target D1–D3 domains of the receptor c-Kit, with the goal of inhibiting the SCF/c-Kit pathway, in order to block the innate resistance and restore nilotinib activity; 2) Experimental findings: according to tissue culture assays, the sAB co-agents indeed have the potential to restore nilotinib induced apoptosis, and mitigate the proliferation and differentiation of hematopoietic progenitors.

- Based on the CFC assay, the sAB co-agents have the potential to mitigate the proliferation and differentiation of hematopoietic progenitors.

Altogether, these resulting research findings validate the hypothesis that a specifically designed combination of a BCR-ABL drug (i.e., Nilotinib) and an sAB co-agent (i.e., anti–c-Kit sAB) inhibiting the SCF/c-Kit pathway should be effective in mitigating the proliferating LSCs, thus providing a potential means to achieve a CML curative paradigm [5, 21].

7.2 Future Research Directions

In contemplating directions for potential future research, the following feasible methods and open problems may be considered in order to better illuminate and vindicate the proposed therapeutic strategy.

- So far, only *in vitro* testing has been performed in this thesis. For therapy development, the ultimate goal is to achieve clinically significant results in patients. To this end, *in vivo* testing should be pursued, which allows for investigating performance issues that may not be measurable using *in vitro* experiments within a lab environment. By extension, once *in vivo* testing produces promising results, patient testing would ensue.

- To improve the performance results, i.e., achieving higher efficiency, the methodology should be extended.

    1. If limited to a two-agent combination, it is possible to consider different BCR-ABL drugs (e.g., bosutinib or ponatinib with supposedly better performance) in conjunction with other possible sABs. Because different agents are utilized, this approach is expected to generate different performance; however, it is inherently constrained and not necessarily guaranteed to produce significant improvement.
    2. Alternatively, allowing for a multi-agent combination, it is feasible to further enhance synergy with multiple drugs and/or sABs. While this approach should offer more promising performance gains, there are also important caveats to heed, since the approach is actually contingent on a judicious selection of agents, which should be com-

plementary in order to realize the synergistic potential. In fact, if unapt agents, with antagonistic properties, are selected, the combinatorial approach may be invalidated.

- Almost serendipitously, in allowing for a multi-agent approach to initially enhance effectiveness, an additional benefit may be realized. Indeed, more interestingly, the approach also paves the way for addressing the multifactorial phenomenon of innate resistance, which may be due to multiple pathways [14]. This is because inhibition of a specific signaling pathway, e.g., c-Kit pathway, may be compensated by bone marrow cytokine stimulation of alternative and interacting pathways. For instance, alternative pathways may include cytokine pathways mediated by stromal factors such as interleukin-3 or insulin-like growth factor 1 [118–120]. In other words, while a panacea may not be practically attainable, at least this multi-agent solution should have the potential to address the different aspects of the multifactorial innate resistance, e.g., similar to the solution strategy proposed for the SCF-mediated innate resistance in this thesis, an sAB may be designed to specifically target a particular aspect of the multifactorial phenomenon. This in turn also implies future investigation of suitable domains for antibody binding in order to deactivate these different constituent pathways.

- Last but not least, with respect to long-term vision, the applicability of the proposed combinatorial therapy may be considered for other cancers and, by extension, for other diseases also. In particular, this vision should be germane to cancers driven by cancer stem cells, which exhibit the hallmarks of resiliency and mutability in resisting drug treatment [115]. Therefore, a suitable therapy platform should have sufficient versatility and diversity in order to counterattack this insidious challenge, i.e., similar to the versatile platform proposed in this thesis, in which a combinatorial strategy consisting of suitable co-agents demonstrates a significant potential to counteract the c-Kit pathway and mitigate the innate resistance.

References

[1] J. Cortes and M. Deininger, eds., *Chronic Myeloid Leukemia*. New York, NY: Informa Healthcare, 2007.

[2] B. A. Burke and M. Carroll, "BCR-ABL: a multi-faceted promoter of DNA mutation in chronic myelogeneous leukemia," *Leukemia*, vol. 24, pp. 1105–12, June 2010.

[3] N. C. P. Cross, G. Q. Daley, A. R. Green, T. P. Hughes, C. Jamieson, P. Manley, T. Mughal, D. Perrotti, J. Radich, R. Skoda, S. Soverini, W. Vainchenker, S. Verstovsek, J.-L. Villeval, and J. M. Goldman, "BCR-ABL1-positive CML and BCR-ABL1-negative chronic myeloproliferative disorders: some common and contrasting features," *Leukemia*, vol. 22, pp. 1975–89, Nov. 2008.

[4] A. S. Shet, B. N. Jahagirdar, and C. M. Verfaillie, "Chronic myelogenous leukemia: mechanisms underlying disease progression," *Leukemia*, vol. 16, pp. 1402–11, Aug. 2002.

[5] B. Clarkson, A. Strife, D. Wisniewski, C. L. Lambek, and C. Liu, "Chronic myelogenous leukemia as a paradigm of early cancer and possible curative strategies," *Leukemia*, vol. 17, pp. 1211–62, July 2003.

[6] R. Hehlmann, A. Hochhaus, and M. Baccarani, "Chronic myeloid leukaemia," *The Lancet*, vol. 370, pp. 342–350, Aug. 2007.

[7] D. Bixby and M. Talpaz, "Seeking the causes and solutions to imatinib-resistance in chronic myeloid leukemia," *Leukemia*, vol. 25, pp. 7–22, Jan. 2011.

[8] F. J. Giles, M. O'Dwyer, and R. Swords, "Class effects of tyrosine kinase inhibitors in the treatment of chronic myeloid leukemia," *Leukemia*, vol. 23, pp. 1698–707, Oct. 2009.

[9] P. J. Shami and M. Deininger, "Evolving treatment strategies for patients newly diagnosed with chronic myeloid leukemia: the role of second-generation BCR-ABL inhibitors as first-line therapy," *Leukemia*, vol. 26, pp. 214–24, Feb. 2012.

[10] N. P. Shah, F. Guilhot, J. E. Cortes, C. A. Schiffer, P. le Coutre, T. H. Brümmendorf, H. M. Kantarjian, A. Hochhaus, P. Rousselot, H. Mohamed, D. Healey, M. Cunningham, and G. Saglio, "Long-term outcome with dasatinib after imatinib failure in chronic-phase chronic myeloid leukemia: follow-up of phase 3 study," *Blood*, pp. 2317–2324, Feb. 2014.

[11] C. C. Smith and N. P. Shah, "Tyrosine kinase inhibitor therapy for chronic myeloid leukemia: approach to patients with treatment-naive or refractory chronic-phase disease," *Hematology / the Education Program of the American Society of Hematology. American Society of Hematology. Education Program*, vol. 2011, pp. 121–7, Jan. 2011.

[12] M. Breccia and G. Alimena, "Discontinuation of tyrosine kinase inhibitors and new approaches to target leukemic stem cells: Treatment-free remission as a new goal in chronic myeloid leukemia," *Cancer Letters*, vol. 347, no. 1, pp. 22–28, 2014.

[13] I. Sloma, X. Jiang, A. C. Eaves, and C. J. Eaves, "Insights into the stem cells of chronic myeloid leukemia," *Leukemia*, vol. 24, pp. 1823–33, Nov. 2010.

[14] E. Trela, S. Glowacki, and J. Blasiak, "Therapy of chronic myeloid leukemia: twilight of the imatinib era?," *International Scholarly Research Notices Oncology*, vol. 2014, pp. 1–9, Jan. 2014.

[15] S. Branford and T. Hughes, "Detection of BCR-ABL Mutations and Resistance to Imatinib Mesylate," *Methods in Molecular Medicine*, vol. 125, pp. 93–106, Jan. 2006.

[16] O. Frank, B. Brors, A. Fabarius, L. Li, M. Haak, S. Merk, U. Schwindel, C. Zheng, M. C. Muller, N. Gretz, R. Hehlmann, A. Hochhaus, and W. Seifarth, "Gene expression signature of primary imatinib-resistant chronic myeloid leukemia patients," *Leukemia*, vol. 20, pp. 1400–1407, May 2006.

[17] A. Hochhaus and P. La Rosée, "Imatinib therapy in chronic myelogenous leukemia: strategies to avoid and overcome resistance," *Leukemia*, vol. 18, pp. 1321–31, Aug. 2004.

[18] J. J. W. M. Janssen, W. Deenik, K. G. M. Smolders, B. J. Kuijk, W. Pouwels, A. Kelder, J. J. Cornelissen, G. J. Schuurhuis, and G. J. Ossenkoppele, "Residual normal stem cells can be

detected in newly diagnosed chronic myeloid leukemia patients by a new flow cytometric approach and predict for optimal response to imatinib," *Leukemia*, vol. 26, pp. 977–84, May 2012.

[19] D. M. Ross, T. P. Hughes, and J. V. Melo, "Do we have to kill the last CML cell?," *Leukemia*, vol. 25, pp. 193–200, Feb. 2011.

[20] R. Jones, "Strategies to Eliminate Cancer Stem Cells," *Cancer Stem Cells*, vol. 5, no. July, pp. 219–230, 2007.

[21] N. Misaghian, G. Ligresti, L. S. Steelman, F. E. Bertrand, J. Bäsecke, M. Libra, F. Nicoletti, F. Stivala, M. Milella, A. Tafuri, M. Cervello, A. M. Martelli, and J. A. McCubrey, "Targeting the leukemic stem cell: the Holy Grail of leukemia therapy," *Leukemia*, vol. 23, pp. 25–42, Jan. 2009.

[22] D. K. Hiwase, D. L. White, J. A. Powell, V. A. Saunders, S. A. Zrim, A. K. Frede, M. A. Guthridge, A. F. Lopez, R. J. D'Andrea, L. B. To, J. V. Melo, S. Kumar, and T. P. Hughes, "Blocking cytokine signaling along with intense Bcr-Abl kinase inhibition induces apoptosis in primary CML progenitors," *Leukemia*, vol. 24, pp. 771–8, Apr. 2010.

[23] Y. Chen, C. Peng, C. Sullivan, D. Li, and S. Li, "Critical molecular pathways in cancer stem cells of chronic myeloid leukemia," *Leukemia*, vol. 24, pp. 1545–54, Sept. 2010.

[24] K. Inokuchi and H. Yamaguchi, "Abnormality of c-kit oncoprotein in certain patients with chronic myelogenous leukemia-potential clinical significance," *Leukemia*, no. October 2001, pp. 170–177, 2002.

[25] L. K. Ashman, "The biology of stem cell factor and its receptor C-kit," *The International Journal of Biochemistry & Bell biology*, vol. 31, pp. 1037–51, Oct. 1999.

[26] F. Belloc, K. Airiau, M. Jeanneteau, M. Garcia, E. Guérin, E. Lippert, F. Moreau-Gaudry, F.-X. Mahon, and E. Guerin, "The stem cell factor-c-KIT pathway must be inhibited to enable apoptosis induced by BCR-ABL inhibitors in chronic myelogenous leukemia cells," *Leukemia*, vol. 23, pp. 679–685, Jan. 2009.

[27] K. Airiau, F.-X. Mahon, M. Josselin, M. Jeanneteau, and F. Belloc, "PI3K/mTOR pathway inhibitors sensitize chronic myeloid leukemia stem cells to nilotinib and restore the response of progenitors to nilotinib in the presence of stem cell factor," *Cell death & disease*, vol. 4, p. e827, Jan. 2013.

[28] J. Pande, M. M. Szewczyk, and A. K. Grover, "Phage display: concept, innovations, applications and future," *Biotechnology Advances*, vol. 28, no. 6, pp. 849–58, 2010.

[29] S. Miersch and S. S. Sidhu, "Synthetic antibodies: concepts, potential and practical considerations," *Methods*, vol. 57, pp. 486–98, Aug. 2012.

[30] S. S. Sidhu and F. A. Fellouse, "Synthetic therapeutic antibodies," *Nature Chemical Biology*, vol. 2, pp. 682–8, Dec. 2006.

[31] W. A. Schulz, *Molecular Biology of Human Cancers*. Dordrecht, The Netherlands: Springer, 2007.

[32] I. Bruns, A. Czibere, J. C. Fischer, F. Roels, R.-P. Cadeddu, S. Buest, D. Bruennert, A. N. Huenerlituerkoglu, N. H. Stoecklein, R. Singh, L. F. Zerbini, M. Jäger, G. Kobbe, N. Gattermann, R. Kronenwett, B. Brors, and R. Haas, "The hematopoietic stem cell in chronic phase CML is characterized by a transcriptional profile resembling normal myeloid progenitor cells and reflecting loss of quiescence," *Leukemia*, vol. 23, pp. 892–9, May 2009.

[33] E. Diaz-Blanco, I. Bruns, F. Neumann, J. C. Fischer, T. Graef, M. Rosskopf, B. Brors, S. Pechtel, S. Bork, A. Koch, A. Baer, U.-P. Rohr, G. Kobbe, A. von Haeseler, N. Gattermann, R. Haas, and R. Kronenwett, "Molecular signature of CD34(+) hematopoietic stem and progenitor cells of patients with CML in chronic phase," *Leukemia*, vol. 21, pp. 494–504, Mar. 2007.

[34] S. Faderl and H. Kantarjian, eds., *Leukemias: Principles and Practice of Therapy*. Chichester, West Sussex, UK: Wiley-Blackwell, 2011.

[35] A. Lakshmikuttyamma, N. Takahashi, E. Pastural, E. Torlakovic, H. M. Amin, G. Garcia-Manero, M. Voralia, M. Czader, J. F. DeCoteau, and C. R. Geyer, "RIZ1 is potential CML

tumor suppressor that is down-regulated during disease progression," *Journal of Hematology & Oncology*, vol. 2, p. 28, Jan. 2009.

[36] L. Galluzzi, L. Senovilla, L. Zitvogel, and G. Kroemer, "The secret ally: immunostimulation by anticancer drugs," *Nature Reviews Drug Discovery*, vol. 11, Feb. 2012.

[37] S. Neidle, ed., *Cancer drug design and discovery*. New York, NY: Academic Press, 2007.

[38] L. A. Kujawski and M. Talpaz, "The role of interferon-alpha in the treatment of chronic myeloid leukemia," *Cytokine & Growth Factor Reviews*, vol. 18, pp. 459–471, Oct. 2007.

[39] F. Guilhot, L. Roy, P.-J. Saulnier, and J. Guilhot, "Interferon in chronic myeloid leukaemia: past and future," *Best practice & research. Clinical haematology*, vol. 22, pp. 315–29, Sept. 2009.

[40] S. G. O'Brien and J. M. Goldman, "Diagnosis and Treatment of Chronic Myeloid Leukemia," in *Neoplastic Diseases of the Blood* (P. H. Wiernik, J. M. Goldman, J. P. Dutcher, and R. A. Kyle, eds.), New York, NY: Springer New York, 2013.

[41] M. Talpaz, R. Hehlmann, A. Quintás-Cardama, J. Mercer, and J. Cortes, "Re-emergence of interferon-α in the treatment of chronic myeloid leukemia," *Leukemia*, vol. 27, pp. 803–12, Apr. 2013.

[42] F. Bonifazi, A. de Vivo, G. Rosti, F. Guilhot, J. Guilhot, E. Trabacchi, R. Hehlmann, A. Hochhaus, P. C. A. Shepherd, J. L. Steegmann, H. C. Kluin-Nelemans, J. Thaler, B. Simonsson, A. Louwagie, J. Reiffers, F. X. Mahon, E. Montefusco, G. Alimena, J. Hasford, S. Richards, G. Saglio, N. Testoni, G. Martinelli, S. Tura, and M. Baccarani, "Chronic myeloid leukemia and interferon-α: a study of complete cytogenetic responders," *Blood*, vol. 98, pp. 3074–3081, Nov. 2001.

[43] T. Schindler, W. Bornmann, P. Pellicena, and W. T. Miller, "Structural Mechanism for STI-571 Inhibition of Abelson Tyrosine Kinase," *Science*, vol. 289, pp. 1938–1942, Sept. 2000.

[44] R. T. Paniagua and W. H. Robinson, "Imatinib for the treatment of rheumatic diseases," *Nature Clinical Practice Rheumatology*, vol. 3, no. 4, pp. 190–191, 2007.

[45] M. J. Mauro and B. J. Druker, "STI571: Targeting BCR-ABL as Therapy for CML," *The Oncologist*, vol. 6, pp. 233–238, June 2001.

[46] C. Gambacorti-Passerini and R. Gunby, "Molecular mechanisms of resistance to imatinib in Philadelphia-chromosome-positive leukaemias," *The Lancet Oncology*, vol. 4, no. February, pp. 75–85, 2003.

[47] A. Hochhaus, S. Kreil, A. S. Corbin, P. La Rosée, M. C. Müller, T. Lahaye, B. Hanfstein, C. Schoch, N. C. P. Cross, U. Berger, H. Gschaidmeier, B. J. Druker, and R. Hehlmann, "Molecular and chromosomal mechanisms of resistance to imatinib (STI571) therapy," *Leukemia*, vol. 16, pp. 2190–6, Dec. 2002.

[48] D. J. Barnes, D. Palaiologou, E. Panousopoulou, B. Schultheis, A. S. M. Yong, A. Wong, L. Pattacini, J. M. Goldman, and J. V. Melo, "Bcr-Abl expression levels determine the rate of development of resistance to imatinib mesylate in chronic myeloid leukemia," *Cancer Research*, vol. 65, pp. 8912–9, Oct. 2005.

[49] E. Buchdunger, C. L. Cioffi, N. Law, D. Stover, S. Ohno-jones, B. J. Druker, and N. B. Lydon, "Abl Protein-Tyrosine Kinase Inhibitor STI571 Inhibits In Vitro Signal Transduction Mediated by c-Kit and Platelet-Derived Growth Factor Receptors," *The Journal of Pharmacology and Experimental Therapeutics*, vol. 295, no. 1, pp. 139–145, 2000.

[50] T. J. Abrams, L. B. Lee, L. J. Murray, N. K. Pryer, and J. M. Cherrington, "SU11248 inhibits KIT and platelet-derived growth factor receptor beta in preclinical models of human small cell lung cancer," *Molecular Cancer Therapeutics*, vol. 2, no. May, pp. 471–478, 2003.

[51] Y. Minami, S. A. Stuart, T. Ikawa, Y. Jiang, A. Banno, I. C. Hunton, D. J. Young, T. Naoe, C. Murre, C. H. M. Jamieson, and J. Y. J. Wang, "BCR-ABL-transformed GMP as myeloid leukemic stem cells," *Proceedings of the National Academy of Sciences of the United States of America*, vol. 105, pp. 17967–72, Nov. 2008.

[52] E. Kavalerchik, D. Goff, and C. H. M. Jamieson, "Chronic myeloid leukemia stem cells," *Journal of Clinical Oncology*, vol. 26, pp. 2911–5, June 2008.

[53] M. Dean, T. Fojo, and S. Bates, "Tumour Stem Cells and Drug Resistance.," *Nature Reviews Cancer*, vol. 5, pp. 275–84, Apr. 2005.

[54] M. M. Gottesman, J. Ludwig, D. Xia, and G. Szakács, "Defeating drug resistance in cancer," *Discovery Medicine*, vol. 6, pp. 18–23, Mar. 2006.

[55] M. Gorre, M. Mohammed, and K. Ellwood, "Clinical resistance to STI-571 cancer therapy caused by BCR-ABL gene mutation or amplification," *Science*, vol. 293, no. August, pp. 876–880, 2001.

[56] N. J. Donato, J. Y. Wu, J. Stapley, G. Gallick, H. Lin, R. Arlinghaus, and M. Talpaz, "BCR-ABL independence and LYN kinase overexpression in chronic myelogenous leukemia cells selected for resistance to STI571," *Blood*, vol. 101, pp. 690–698, 2003.

[57] E. Jabbour, M. Deininger, and A. Hochhaus, "Management of adverse events associated with tyrosine kinase inhibitors in the treatment of chronic myeloid leukemia," *Leukemia*, vol. 25, pp. 201–10, Feb. 2011.

[58] F. Belloc, F. Moreau-Gaudry, M. Uhalde, L. Cazalis, M. Jeanneteau, F. Lacombe, V. Praloran, and F. Mahon, "Imatinib and nilotinib induce apoptosis of chronic myeloid leukemia cells through a Bim-dependant pathway modulated by cytokines," *Cancer biology & therapy*, vol. 6, pp. 912–9, June 2007.

[59] J. F. Apperley, J. E. Cortes, D.-W. Kim, L. Roy, G. J. Roboz, G. Rosti, E. O. Bullorsky, E. Abruzzese, A. Hochhaus, D. Heim, C. A. de Souza, R. A. Larson, J. H. Lipton, H. J. Khoury, H.-J. Kim, C. Sillaber, T. P. Hughes, P. Erben, J. Van Tornout, and R. M. Stone, "Dasatinib in the treatment of chronic myeloid leukemia in accelerated phase after imatinib failure: the START a trial," *Journal of Clinical Oncology*, vol. 27, pp. 3472–9, July 2009.

[60] J. Wehrle, H. L. Pahl, and N. V. Bubnoff, "Ponatinib: A Third-Generation Inhibitor for the Treatment of CML," in *Small Molecules in Oncology* (U. M. Martens, ed.), vol. 201 of *Recent Results in Cancer Research*, Berlin, Heidelberg: Springer Berlin Heidelberg, 2014.

[61] P. Bose, H. Park, J. Al-Khafaji, and S. Grant, "Strategies to circumvent the T315I gatekeeper

mutation in the Bcr-Abl tyrosine kinase," *Leukemia research reports*, vol. 2, pp. 18–20, Jan. 2013.

[62] N. P. Shah, D. W. Kim, H. Kantarjian, P. Rousselot, P. E. D. Llacer, A. Enrico, J. Vela-Ojeda, R. T. Silver, H. J. Khoury, M. C. Müller, A. Lambert, Y. Matloub, and A. Hochhaus, "Potent, transient inhibition of BCR-ABL with dasatinib 100 mg daily achieves rapid and durable cytogenetic responses and high transformation-free survival rates in chronic phase chronic myeloid leukemia patients with resistance, suboptimal response or int," *Haematologica*, vol. 95, no. 2, pp. 232–240, 2010.

[63] J. L. Snead, T. O'Hare, L. T. Adrian, C. A. Eide, T. Lange, B. J. Druker, and M. W. Deininger, "Acute dasatinib exposure commits Bcr-Abl-dependent cells to apoptosis," *Blood*, vol. 114, no. 16, pp. 3459–3463, 2009.

[64] E. Weisberg, P. W. Manley, W. Breitenstein, J. Brüggen, S. W. Cowan-Jacob, A. Ray, B. Huntly, D. Fabbro, G. Fendrich, E. Hall-Meyers, A. L. Kung, J. Mestan, G. Q. Daley, L. Callahan, L. Catley, C. Cavazza, M. Azam, A. Mohammed, D. Neuberg, R. D. Wright, D. G. Gilliland, and J. D. Griffin, "Characterization of AMN107, a selective inhibitor of native and mutant Bcr-Abl," *Cancer Cell*, vol. 7, pp. 129–41, Feb. 2005.

[65] E. Weisberg, P. W. Manley, S. W. Cowan-Jacob, A. Hochhaus, and J. D. Griffin, "Second generation inhibitors of BCR-ABL for the treatment of imatinib-resistant chronic myeloid leukaemia," *Cancer*, vol. 7, pp. 345–56, May 2007.

[66] T. O'Hare, M. S. Zabriskie, A. M. Eiring, and M. W. Deininger, "Pushing the limits of targeted therapy in chronic myeloid leukaemia," *Nature reviews. Cancer*, vol. 12, pp. 513–26, Aug. 2012.

[67] E. Weisberg, P. Manley, J. Mestan, S. Cowan-Jacob, A. Ray, and J. D. Griffin, "AMN107 (nilotinib): a novel and selective inhibitor of BCR-ABL," *British Journal of Cancer*, vol. 94, pp. 1765–9, June 2006.

[68] S. M. Graham, H. G. Jorgensen, E. Allan, and C. Pearson, "Primitive, quiescent,

Philadelphia-positive stem cells from patients with chronic myeloid leukemia are insensitive to STI571 in vitro," *Blood*, vol. 99, pp. 319–325, Jan. 2002.

[69] N. N. Bewry, R. R. Nair, M. F. Emmons, D. Boulware, J. Pinilla-Ibarz, and L. A. Hazlehurst, "Stat3 contributes to resistance toward BCR-ABL inhibitors in a bone marrow microenvironment model of drug resistance," *Molecular Cancer Therapeutics*, vol. 7, pp. 3169–75, Oct. 2008.

[70] E. Weisberg, R. D. Wright, D. W. McMillin, C. Mitsiades, A. Ray, R. Barrett, S. Adamia, R. Stone, I. Galinsky, A. L. Kung, and J. D. Griffin, "Stromal-mediated protection of tyrosine kinase inhibitor-treated BCR-ABL-expressing leukemia cells," *Molecular Cancer Therapeutics*, vol. 7, pp. 1121–9, May 2008.

[71] R. R. Nair, J. H. Tolentino, R. F. Argilagos, L. Zhang, J. Pinilla-Ibarz, and L. A. Hazlehurst, "Potentiation of Nilotinib-mediated cell death in the context of the bone marrow microenvironment requires a promiscuous JAK inhibitor in CML," *Leukemia Research*, vol. 36, pp. 756–63, June 2012.

[72] K. L. Sweet, L. A. Hazlehurst, and J. Pinilla-Ibarz, "The one-two punch: combination treatment in chronic myeloid leukemia," *Oncology Hematology*, vol. 88, pp. 667–79, Dec. 2013.

[73] C. T. Jordan, "The leukemic stem cell," *Best Practice and Research in Clinical Haematology*, vol. 20, no. 1, pp. 13–18, 2007.

[74] R. Di Noto, C. L. Lo Pardo, E. M. Schiavone, C. Manzo, and C. Vacca, "Stem cell factor receptor (c-kit, CD117) is expressed on blast cells from most immature types of acute myeloid malignancies but is also a characteristic of a subset of acute promyelocytic leukaemia," *British Journal of Haematology*, pp. 562–564, 1996.

[75] V. A. Dolgachev, M. R. Ullenbruch, N. W. Lukacs, and S. H. Phan, "Role of stem cell factor and bone marrow-derived fibroblasts in airway remodeling," *The American Journal of Pathology*, vol. 174, pp. 390–400, Mar. 2009.

[76] J. Lennartsson and L. Rönnstrand, "The stem cell factor receptor/c-Kit as a drug target in cancer," *Current cancer drug targets*, vol. 6, pp. 65–75, Feb. 2006.

[77] H. Liu, X. Chen, P. J. Focia, and X. He, "Structural basis for stem cell factor-KIT signaling and activation of class III receptor tyrosine kinases," *The EMBO journal*, vol. 26, pp. 891–901, Feb. 2007.

[78] L. Ronnstrand, "Signal transduction via the stem cell factor receptor/c-Kit," *Cellular and Molecular Life Sciences: CMLS*, vol. 61, pp. 2535–48, Oct. 2004.

[79] A. Q. Shen, N. M. Wilson, S. L. Gleason, and H. J. Khoury, "Bosutinib in the treatment of patients with Philadelphia chromosome-positive (Ph+) chronic myelogenous leukemia: an overview," *Therapeutic Advances in Hematology*, vol. 5, pp. 13–7, Mar. 2014.

[80] S. J. Neering, T. Bushnell, S. Sozer, J. Ashton, R. M. Rossi, P.-Y. Wang, D. R. Bell, D. Heinrich, A. Bottaro, and C. T. Jordan, "Leukemia stem cells in a genetically defined murine model of blast-crisis CML," *Blood*, vol. 110, pp. 2578–85, Oct. 2007.

[81] P. Besmer, J. E. Murphy, P. C. George, F. H. Qiu, P. J. Bergold, L. Lederman, H. W. Snyder, D. Brodeur, E. E. Zuckerman, and W. D. Hardy, "A new acute transforming feline retrovirus and relationship of its oncogene v-kit with the protein kinase gene family," *Nature*, vol. 320, pp. 415–21, 1986.

[82] R. Roskoski, "Signaling by Kit protein-tyrosine kinase - the stem cell factor receptor," *Biochemical and biophysical research communications*, vol. 337, pp. 1–13, 2005.

[83] S. Yuzawa, Y. Opatowsky, Z. Zhang, V. Mandiyan, I. Lax, and J. Schlessinger, "Structural basis for activation of the receptor tyrosine kinase KIT by stem cell factor," *Cell*, vol. 130, pp. 323–34, July 2007.

[84] F. Xiang, X. Lu, L. Hammoud, P. Zhu, P. Chidiac, J. Robbins, and Q. Feng, "Cardiomyocyte-specific overexpression of human stem cell factor improves cardiac function and survival after myocardial infarction in mice," *Circulation*, vol. 120, pp. 1065–74, 9 p following 1074, Sept. 2009.

[85] P. T. Went, S. Dirnhofer, M. Bundi, M. Mirlacher, P. Schraml, S. Mangialaio, S. Dimitrijevic, J. Kononen, A. Lugli, R. Simon, and G. Sauter, "Prevalence of KIT expression in human tumors," *Journal of Clinical Oncology*, vol. 22, pp. 4514–22, Nov. 2004.

[86] B. P. Rubin, S. Singer, C. Tsao, A. Duensing, M. L. Lux, R. Ruiz, M. K. Hibbard, C.-j. Chen, S. Xiao, D. A. Tuveson, G. D. Demetri, C. D. M. Fletcher, and J. A. Fletcher, "KIT Activation Is a Ubiquitous Feature of Gastrointestinal Stromal Tumors," *American Association for Cancer Research*, pp. 8118–8121, 2001.

[87] A. Beghini, L. Larizza, R. Cairoli, and E. Morra, "C-Kit Activating Mutations and Mast Cell Proliferation in Human Leukemia," *Blood*, vol. 92, pp. 701–2, July 1998.

[88] A. S. Corbin, T. O'Hare, Z. Gu, I. L. Kraft, A. M. Eiring, J. S. Khorashad, A. D. Pomicter, T. Y. Zhang, C. A. Eide, P. W. Manley, J. E. Cortes, B. J. Druker, and M. W. Deininger, "KIT signaling governs differential sensitivity of mature and primitive CML progenitors to tyrosine kinase inhibitors," *Cancer research*, vol. 73, pp. 5775–86, Sept. 2013.

[89] F. Nwajei and M. Konopleva, "The bone marrow microenvironment as niche retreats for hematopoietic and leukemic stem cells," *Advances in hematology*, pp. 1–8, Jan. 2013.

[90] E. A. Grimm, "Cytokines: Biology and Applications in Cancer Medicine," in *Holland-Frei Cancer Medicine* (R. C. Bast and J. F. Holland, eds.), Shelton, CT: PMPH USA, 8th ed., 2010.

[91] D. Kalderon, "Signaling Pathways in Cancer," in *Principles of Molecular Oncology* (M. H. Bronchud and E. al, eds.), ch. 8, pp. 153–188, Totowa, NJ: Humana Press, 2008.

[92] J. Liang, Y. Wu, B.-J. Chen, W. Zhang, Y. Tanaka, and H. Sugiyama, "The C-kit receptor-mediated signal transduction and tumor-related diseases," *International journal of biological sciences*, vol. 9, pp. 435–43, Jan. 2013.

[93] J. Schlessinger, "Cell Signaling by Receptor Tyrosine Kinases," *Cell*, vol. 103, pp. 211–225, 2000.

[94] M. A. Lemmon and J. Schlessinger, "Cell signaling by receptor tyrosine kinases.," *Cell*, vol. 141, pp. 1117–34, June 2010.

[95] C. V. Lee, W.-C. Liang, M. S. Dennis, C. Eigenbrot, S. S. Sidhu, and G. Fuh, "High-affinity human antibodies from phage-displayed synthetic Fab libraries with a single framework scaffold," *Journal of Molecular Biology*, vol. 340, pp. 1073–93, July 2004.

[96] R. K. Oldham and R. O. Dillman, "Monoclonal antibodies in cancer therapy: 25 years of progress," *Journal of Clinical Oncology*, vol. 26, pp. 1774–7, Apr. 2008.

[97] R. Kontermann, ed., *Bispecific Antibodies*. Heidelberg, Germany: Springer, 2011.

[98] I. Benhar, "Design of synthetic antibody libraries," *Expert Opinion on Biological Therapy*, vol. 7, no. 5, pp. 763–779, 2007.

[99] G. Hardiman, "Next-generation antibody discovery platforms," *Proceedings of the National Academy of Sciences of the United States of America*, vol. 109, pp. 18245–6, Nov. 2012.

[100] B. Nelson and S. S. Sidhu, "Synthetic Antibody Libraries," vol. 899, pp. 27–41, 2012.

[101] M. Silacci, S. Brack, G. Schirru, J. Marlind, A. Ettorre, A. Merlo, F. Viti, and D. Neri, "Design, construction, and characterization of a large synthetic human antibody phage display library," *Proteomics*, vol. 5, pp. 2340–2350, June 2005.

[102] F. A. Fellouse and S. S. Sidhu, "Synthetic Antibody Libraries," in *Phage Display in Drug Discovery and Biotechnology* (S. S. Sidhu, ed.), pp. 709–740, Boca Raton, FL: CRC Press, 2005.

[103] J. Krauss, "Application of recombinant antibodies in cancer patients," in *Recombinant antibodies for cancer therapy: methods and protocols* (M. Welschof and J. Krauss, eds.), vol. 207, ch. 2, pp. 4–27, Totowa, N.J: Humana Press Inc, 1st ed., 2003.

[104] C. R. Geyer, J. McCafferty, S. Dübel, A. R. M. Bradbury, and S. S. Sidhu, "Recombinant antibodies and in vitro selection technologies," in *Methods in molecular biology* (G. Proetzel and H. Ebersbach, eds.), vol. 901, ch. 2, pp. 11–32, Jan. 2012.

[105] S. M. Deyev and E. N. Lebedenko, "Modern Technologies for Creating Synthetic Antibodies for Clinical application," *Acta naturae*, vol. 1, pp. 32–50, Apr. 2009.

[106] M. S. Dennis, "Selection and screening strategies," in *Phage Display in Drug Discovery and Biotechnology* (S. S. Sidhu, ed.), ch. 4, pp. 143–161, Boca Raton, FL: CRC Press, 2005.

[107] ForteBIO, *Octet System - User's Guide*. ForteBIO, Inc., 2011.

[108] M. S. Silberberg, *Chemistry: the molecular nature of matter and change*. Boston, MA: McGraw-Hil, 6 ed., 2012.

[109] J. P. Landry, Y. Fei, and X. Zhu, "Simultaneous measurement of 10,000 protein-ligand affinity constants using microarray-based kinetic constant assays," *Assay and drug development technologies*, vol. 10, pp. 250–9, June 2012.

[110] Y. Sun, J. Landry, Y. Fei, X. Zhu, and J. Luo, "Effect of Fluorescently Labeling Protein Probes on Kinetics of Protein-Ligand Reactions," *Langmuir*, vol. 24, no. 23, pp. 13399–13405, 2008.

[111] J. Landry, Y. Fei, and X. Zhu, "High Throughput, Label-free Screening Small Molecule Compound Libraries for Protein-Ligands using Combination of Small Molecule Microarrays and a Special Ellipsometry-based Optical Scanner," *International Drug Discovery*, pp. 8–13, 2011.

[112] Y. S. Sun, J. P. Landry, Y. Fei, and X. Zhu, "an Oblique-Incidence Reflectivity Difference Study of the Dependence of Probe-Target Reaction Constants on Surface Target Density Using Streptavidin-Biotin Reactions As a Model," *Instrumentation Science & Technology*, vol. 41, pp. 535–544, Sept. 2013.

[113] G. Mor and A. Alvero, *Apoptosis and Cancer: Methods and Protocols*. Totowa, NJ: Humana Press, 2008.

[114] M. Sluyser, *Application of apoptosis to cancer treatment*. Dordrecht, The Netherlands: Springer, 2005.

[115] D. Hanahan and R. A. Weinberg, "Hallmarks of cancer: the next generation," *Cell*, vol. 144, pp. 646–74, Mar. 2011.

[116] R. A. Weinberg, *The Biology of Cancer*. New York: Garland Science, 2007.

[117] A. S. M. Yong, K. Keyvanfar, R. Eniafe, B. N. Savani, K. Rezvani, E. M. Sloand, J. M. Goldman, and a. J. Barrett, "Hematopoietic stem cells and progenitors of chronic myeloid leukemia express leukemia-associated antigens: implications for the graft-versus-leukemia

effect and peptide vaccine-based immunotherapy," *Leukemia*, vol. 22, pp. 1721–7, Sept. 2008.

[118] J. F. Dorsey, J. M. Cunnick, R. Lanehart, M. Huang, a. J. Kraker, K. N. Bhalla, R. Jove, and J. Wu, "Interleukin-3 protects Bcr-Abl-transformed hematopoietic progenitor cells from apoptosis induced by Bcr-Abl tyrosine kinase inhibitors," *Leukemia*, vol. 16, pp. 1589–95, Sept. 2002.

[119] A. Lakshmikuttyamma, E. Pastural, N. Takahashi, K. Sawada, D. P. Sheridan, J. F. DeCoteau, and C. R. Geyer, "Bcr-Abl induces autocrine IGF-1 signaling," *Oncogene*, vol. 27, pp. 3831–44, June 2008.

[120] R. G. Maki, "Small is beautiful: insulin-like growth factors and their role in growth, development, and cancer," *Journal of Clinical Oncology*, vol. 28, pp. 4985–95, Nov. 2010.